universität wien

DIPLOMARBEIT / DIPLOMA THESIS

Titel der Diplomarbeit / Title of the Diploma Thesis

„Interaction of the Ca^{2+}- Sensor Synaptotagmin with different types of membranes“

verfasst von / submitted by

Michael Derflinger

angestrebter akademischer Grad / in partial fulfilment of the requirements for the degree of

Magister der Pharmazie (Mag.pharm.)

Wien, 2017 / Vienna, 2017

Studienkennzahl lt. Studienblatt / degree programme code as it appears on the student record sheet:	A 449
Studienrichtung lt. Studienblatt / degree programme as it appears on the student record sheet:	Diplomstudium Pharmazie
Betreut von / Supervisor:	Ass.-Prof. Mag. Dr. Anna Weinzinger, Privatdoz.

Content

I. **Acknowledgement**

I would like to express my gratitude to Ass.-Prof. Dr. Anna Weinzinger, not only for giving me the chance to write my diploma thesis in this interesting field of study, but also for giving me a free hand in terms of development and time management.

My deepest appreciation goes to Dr. Eva-Maria Plessl. She was always willing to solve my problems or to answer my bumbling questions and spent countless hours giving me insightful comments and suggestions.

A big thank you goes to my mother for keeping faith in me over an exhaustingly long period of time and to Maximiliane for giving me motivation with every chuckle of hers.

Special thanks to Thomas for pushing me through the final part of this diploma thesis.

II. Abstract

The transmission of an electrical signal from one neuron to another is the fundamental process for communication of brain and muscle. This neurotransmission happens at the synapse, where an electrical signal is converted into a chemical signal to overcome the synaptic cleft. Neurotransmitters are held in vesicles and released into the synaptic cleft via exocytosis upon stimulation by an action potential. First, the arriving action potential causes voltage-gated Ca^{2+}-channels to open. The incoming Ca^{2+}- ions bind to the Ca^{2+}- sensor Synaptotagmin-1 (Syt-1), which facilitates membrane fusion between the vesicular and the presynaptic cell membrane. Syt-1 inserts into the presynaptic cell membrane and therefore causes the membrane to bend. The resulting curvature brings both membranes in close proximity and therefore helps to overcome the energy barrier for both membranes to fuse. A fusion pore opens up and the neurotransmitters move into the synaptic cleft via diffusion. (1, 11)

The interaction between Syt-1 and the membrane is believed to occur with its Ca^{2+}- binding loops orientated towards the presynaptic cell membrane and furthermore them inserting into the membrane. (11, 12, 22) Syt-1 also holds the polybasic lysine stretch (K324, K325, K326, K327) and two arginine amino acids (R398, R399), which have been reported to interact with membranes as well. (23) However, the exact molecular interface between the membranes, Syt-1 and the also participating SNARE-complex, has not been finally determined yet. (34)

Up to now, the exact compositions of vesicular and presynaptic cell membrane remain unknown. Therefore, the influence of different types of membrane lipids on the process of membrane fusion triggered by Syt-1 needs to be further investigated. Especially PIP2 and cholesterol are believed to have major influence on the likelihood of binding and therefore on the process of neurotransmission itself. (23, 51)

In this diploma thesis, we present multiple coarse-grained free molecular dynamics (MD) simulations with the Synaptotagmin-1 C2B-domain and different types of membranes. We aimed to generate unbiased simulations in order to catch the proteins most favoured interactions. Therefore, we placed the C2B-domain between two membranes of the same composition and ran simulations of 500ns each. We settled for seven systems with different membrane compositions and executed them with two different structures of the Syt-1 C2B-domain. Using these final systems, we performed a total of 46 runs per protein, which accounts for a total of 46,80 microseconds.

Interestingly, the membrane insertion of the Ca^{2+}-binding pockets was not observed. Instead, the most frequent interaction happened between the polybasic lysine stretch and PIP2. We showed a clear dependence on the membranes composition with regard to PIP2, as the likelihood of protein-

membrane interaction increased with higher PIP2-concentration. Also, the influence of Ca^{2+} on the membrane and therefore on the probability of interaction was disclosed.

Taken together, we found proof that the Syt-1 C2B-domain is able to interact with multiple parts of its structure, which are likely to play an additional role in membrane fusion next to loops-first membrane insertion.

III. Zusammenfassung

Die Übertragung eines elektrischen Signals von einem Neuron auf das Nächste ist ein grundlegender Prozess in der Kommunikation zwischen Gehirn und Muskel. Diese Signalübertragung geschieht an der Synapse, an welcher das elektrische in ein chemisches Signal umgewandelt werden muss, um den synaptischen Spalt passieren zu können. In Vesikeln sind Neurotransmitter gespeichert, welche nach Stimulation durch ein Aktionspotential via Exocytose in den synaptischen Spalt abgegeben werden. Als Erstes bewirkt das eintreffende Aktionspotential die Öffnung spannungsabhängiger Ca^{2+}-Kanäle. Das einströmende Ca^{2+} bindet an den Ca^{2+}- Sensor Synaptotagmin-1 (Syt-1), welches dann die Fusion zwischen den Membranen von Vesikel und präsynaptischer Zelle ermöglicht. Syt-1 dringt in die präsynaptische Zellmembran ein und verursacht dadurch eine Biegung der Membran. Diese Krümmung bringt die beiden Membranen in unmittelbare Nähe und hilft damit, die Energiebarriere für spontane Fusion der Membranen zu überwinden. Es öffnet sich eine Pore, durch welche die Neurotransmitter via Diffusion in den synaptischen Spalt entweichen können. (1, 11)

Es wird angenommen, dass Syt-1 mit den Ca^{2+}- Bindetaschen in Richtung der präsynaptischen Membran orientiert ist und in weiterer Folge in diese eintaucht. (11, 12, 22) Jedoch sind auch der polybasic lysine stretch (K324, K325, K326, K327) und die beiden aufeinanderfolgenden Arginine (R398, R399) Teil der Struktur von Syt-1 und auch mit diesen Teilen des Proteins wurden bereits Interaktionen zur Membran beobachtet. (23) Die exakte Schnittstelle auf molekularer Ebene zwischen Syt-1, dem ebenfalls beteiligten SNARE-complex und den Membranen konnte bisher aber noch nicht endgültig aufgeklärt werden. (34)

Mit aktuellem Stand der Wissenschaft verbleibt auch die exakte Zusammensetzung von vesikulärer und präsynaptischer Membran ungeklärt. Der Einfluss von unterschiedlichen Lipid-Typen auf die durch Syt-1 ermöglichte Fusion sollte daher näher untersucht werden. Vor allem PIP2 und Cholesterol könnten einen schwerwiegenden Einfluss auf die Interaktionswahrscheinlichkeit und damit auf den Prozess der Neurotransmission selbst haben. (23, 51)

In dieser Diplomarbeit präsentieren wir mehrere Moleküldynamiksimulationen mit der C2B-Domäne von Syt-1 und Membranen unterschiedlicher Zusammensetzung. Die Simulationen wurden als coarse-grained Model ausgeführt. Unser Ziel war, die Simulationen möglichst frei und unbeeinflusst zu gestalten, um die wahrscheinlichsten Interaktionen zwischen Protein und Membran beobachten zu können. Die C2B-Domäne wurde zwischen zwei Membranen gleicher Zusammensetzung platziert und anschließend mehrere Simulationen zu je 500ns durchgeführt. Wir beschränkten uns letztendlich auf sieben Systeme mit verschiedenen Membranzusammensetzungen und zwei verschiedene Strukturen

der Syt-1 C2B-Domäne. Mit dieser Konfiguration wurden insgesamt 46 Läufe pro Protein durchgeführt, was einer Gesamtsimulationszeit von 46,80 Mikrosekunden entspricht.

Interessanterweise konnten wir die erwartete Interaktion mit den in die Membran eindringenden Ca^{2+}- Bindungstaschen nicht beobachten. Stattdessen fand die häufigste Interaktion zwischen dem polybasic lysine stretch und PIP2 statt. Wir konnten eine klare Abhängigkeit zur PIP2-Konzentration in der Membran zeigen, wobei die Wahrscheinlichkeit der Interaktion mit steigender PIP2-Konzentration zunahm. Der Einfluss der Ca^{2+}- Konzentration auf die Interaktionswahrscheinlichkeit konnte ebenfalls offengelegt werden.

Insgesamt hat sich herausgestellt, dass die C2B-Domäne von Syt-1 mit mehreren Teilen zu Interaktionen mit der Membran fähig ist und es wahrscheinlich ist, dass auch andere Interaktionen als das Eintauchen der Ca^{2+}- Bindungstaschen eine Rolle beim Prozess der Membranfusion spielen.

1. Introduction

1.1 Neurotransmission

Neurotransmission is the communication of two neurons, where an electrical impulse is transferred from the presynaptic cell to the postsynaptic cell. These cells are separated by the synaptic cleft, which is about 20-40nm wide and filled with extracellular fluid. Therefore, the incoming electrical signal must be converted into a chemical signal to overcome this gap. When the action potential arrives, it activates voltage gated Ca^{2+}-channels and Ca^{2+}-ions start moving to the inside of the cell. Upon this influx, a Ca^{2+}-sensor detects the signal and triggers membrane fusion of the presynaptic cell membrane and vesicles, where neurotransmitters are being held. (see Figure 1) These neurotransmitters, such as acetylcholine, dopamine or norepinephrine serve as chemical signals and are released into the synaptic cleft. This process is called exocytosis. The freed neurotransmitters only move via diffusion, but eventually float across the cleft and reach the neighbouring cell. Receptors at the postsynaptic cell membrane are stimulated by these neurotransmitters and cause ion channels to open. In doing so, another electrical impulse is created and the transmission of the signal is complete. The neurotransmitters do not remain in the synaptic cleft; they are transported back into the presynaptic cell, where they are used again. (1, 2, 3)

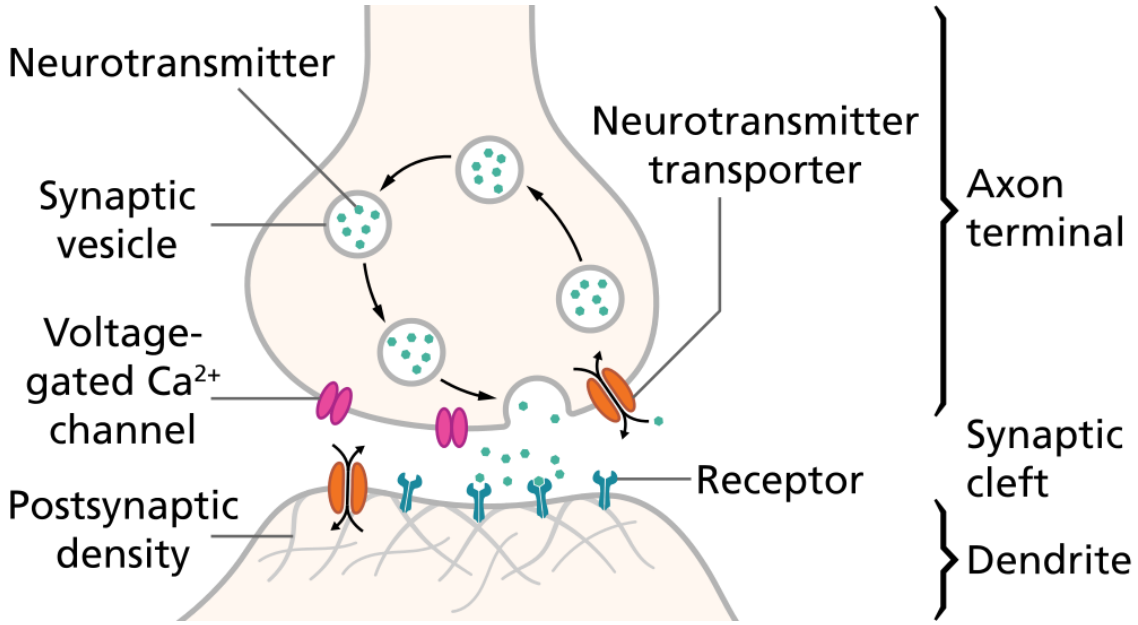

Figure 1: Overview of the synaptic neurotransmission;
Neurotransmitters are being packed in synaptic vesicles, released into the synaptic cleft upon Ca^{2+}-influx and then stimulate receptors at the postsynaptic cell to trigger a new action potential; simultaneously they are again transported back into the presynaptic cell again (reuptake)

This summary of neurotransmission is valid for the so called evoked synchronous synaptic neurotransmitter release. As the name already indicates, this kind of neurotransmission needs a cause, in this case the action potential, to take place. It is a Ca^{2+}-dependent release. Synchronous means that up to hundred vesicles per second fuse with the plasma membrane at the same time and free their neurotransmitters. (2, 4) This astounding speed and precision of neurotransmitter release is the reason why the mammalian reaction time is quite low, although the nerval impulse needs to pass many cells.

On the contrary, spontaneous neurotransmitter release also occurs, where only one vesicle every 60-90 seconds fuses. Although the probability of spontaneous release is low, a single vesicle fusing can be sufficient to trigger a postsynaptic action potential. It is believed, that this slow neurotransmission is something like a background activity, but also able to take over very high transmission rates if the fast system should fail. (see Figure 2) (2, 5, 6) Some studies even suggest that these two forms of release make use of different pools of vesicles. (2, 7, 8)

The synaptic vesicles are filled with neurotransmitters and assigned to certain pools. Usually, these pools are divided into the readily releasable pool, which is already docked at the plasma membrane active zone, the recycle pool of vesicles that have just been retrieved from the membrane, and the reserve pool. (2, 9)

All vesicles are acidified by proton pumps and therefore gain a pH gradient that drives neurotransmitter uptake. Some vesicles then move to the membrane and the "soluble N-ethylmaleimide-sensitive factor attachment protein receptor" (SNARE) complex forms itself, pulling the vesicles in close proximity to the membrane. This process is called priming. The vesicles gathered at the membrane active zone represent the readily releasable pool. Upon Ca^{2+}-influx and with the help of the Ca^{2+}-sensor Synaptotagmin 1, a fusion pore opens up and the neurotransmitters are being set free into the synaptic cleft. (5, 10) After being released, the vesicles are retrieved by endocytosis and the vesicle cycle starts again by acidifying the vesicles. (11)

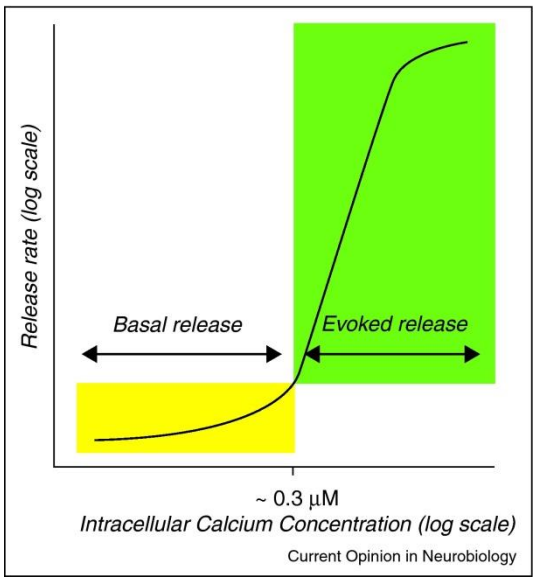

Figure 2: Spontaneous (basal) and evoked release in dependency on the Calcium concentration

Reprinted from Current Opinion in Neurobiology, Vol 21, Issue 2, Pages 275-282, Denise MO Ramirez, Ege T Kavalali, Differential regulation of spontaneous and evoked neurotransmitter release at central synapses, April 2011, with permission from Elsevier

Only one action potential arriving at the axon terminal of the presynaptic cell is enough to trigger the release of multiple vesicles, each filled with $10^4 – 10^5$ molecules of neurotransmitters. This non-linear dependence on calcium means that every signal is amplified and losses, due to transportation, can be prevented. This is one of the benefits of having to transfer the electrical signal to a chemical signal and back. (1)

The arriving action potential is based on calcium and triggers a release within a few hundred microseconds. Therefore, it is the fastest known fusing event of two membranes in the human body. (12) This very fast coupling of an action potential to transmitter release is essential for the amazing speed of neurotransmission itself. Synaptotagmin 1, a membrane protein located at the synaptic vesicle, mediates the speed and precision of this process. This is a major factor in order to process such a complex mechanism on the same timescale as the gating of an ion channel. (5)

1.2 Synaptotagmin

1.2.1 Structure, Sequence, Ca^{2+}- binding

Historically, the work of Bernard Katz first showed that neurotransmitter release via exocytosis is triggered by Ca^{2+}. (13) In 1981, *Matthew et al.* identified a protein anchored in the vesicular membrane of approximately 65-kDa. (14) It was not longer than until 1990, when *Perin et al.* reported a protein (at this time often called p65) with a homologous sequence as in protein kinase C. This newly identified protein was Synaptotagmin 1 (Syt-1) and already in 1991 its domain structure was described. (15, 16)

Transmembrane proteins are embedded in the lipid bilayer. Eventually, parts of the protein are exposed to both sides of the membrane. For example, the N-terminal end of the protein to the inside and the C-terminal end to the outside, as it happens to be the case with Syt-1. (17)

Syt-1 is a transmembrane protein in synaptic vesicles with a total of 422 amino acids. 57 of those amino acids are located inside the vesicle, forming the N-terminal end of the protein. 23 amino acids are spanning the vesicular membrane as a single alpha-helix and therefore represent the transmembrane domain. The biggest part of 342 amino acids is cytoplasmic. After a variable linker there is the first of two C2-domains, called C2A. Again following a connecting linker there is the C2B-domain, which also represents the C-terminal end of the protein. (see Figure 3) (11, 18, 19) The cytoplasmic part is not only the biggest, but also the part that interacts with the SNARE complex and the presynaptic plasma membrane. (11, 12, 18, 20)

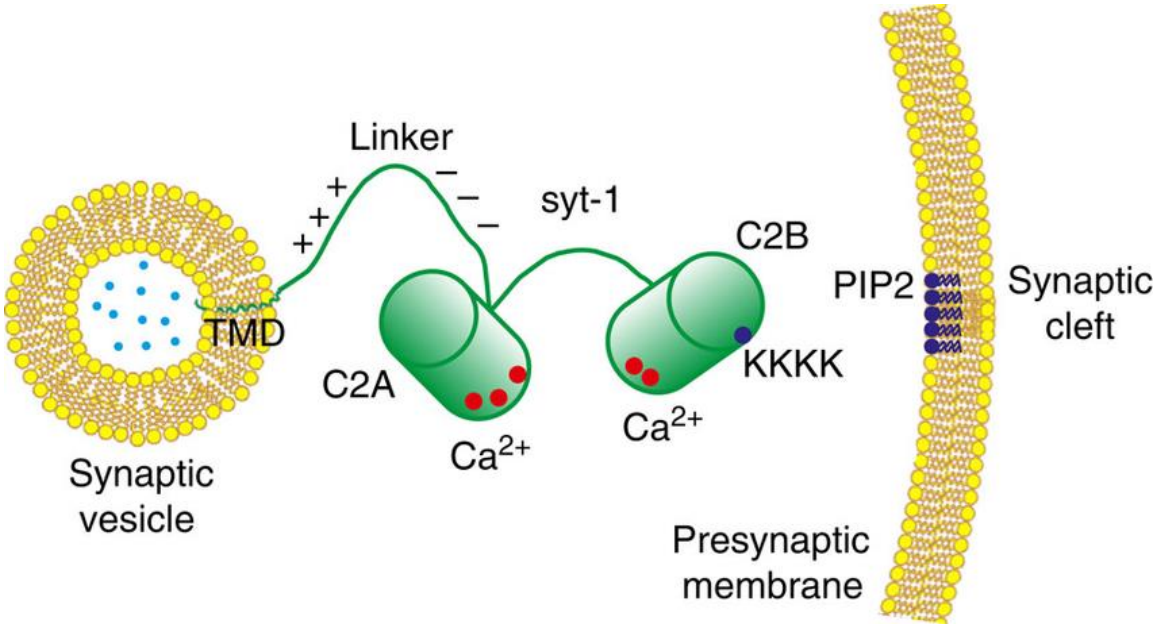

Figure 3: Synaptotagmin embedded in the vesicular membrane; whereas the C-terminal part is short, the part to the outside of the vesicle has two big Ca^{2+}-binding domains, named C2A and C2B, which are connected via a variable linker (green); also shown: 3 bound Ca^{2+}-ions in C2A and 2 in C2B (red); the polybasic lysine stretch (Lys 324-327) is marked as KKKK; the presynaptic membrane, which the domains need to interact with and its membrane lipids PIP2 (blue)

In this diploma thesis, **we focus on the C2-domains because of their importance in mediating membrane fusion**. Both domains together are also called the C2AB fragment, which comprises amino acids 141 – 422 of Syt-1.

The C2-domain is a highly conserved motif of about 140 amino acid residues and most proteins that contain this motif are known to bind Ca^{2+} and membranes. (11) The C2AB-domains are connected via a linker of about 14 amino acids length. In the absence of Ca^{2+}, the domains seem to be tightly coupled, whereas the Ca^{2+}-bound form of Syt-1 experiences an increase of flexibility. (21)

The domains structure is likewise but not equal. Both domains are built as stable beta-sandwiches with flexible loops emerging from top and bottom. (5) Both C2-domains are able to bind Ca^{2+}, which is obviously important for their role as a Ca^{2+}-sensor, but the exact architecture of binding is not yet fully understood. Two loops at the top form the Ca^{2+}-binding pocket, where aspartates ligate the ions. In C2A, five amino acid side chains (D172, D178, D230, D232 and D238) mediate the binding. The same goes for C2B (D303, D309, D363, D365 and D371). (11, 22) The membrane lipids such as POPS (1-palmitoyl-2-oleoyl-sn-glycero-3-phosphatidylserine) complete the ligation of Ca^{2+} or at least have a supportive character in this case. (23)

In most studies, there is consensus about the number of Ca^{2+}-ions bound to the C2-domains of Syt-1. *Chapman* (review, published in 2008) and also *Südhof* (essay, published in 2013) used models where three ions were bound at C2A and two at C2B. (11, 12) In studies using molecular dynamics simulations, variant findings have been published. Whereas *Bykhovskaia* found a total of four Ca^{2+}-ions bound to Syt-1 (two at both C2-domains) in her molecular dynamics (MD) simulations (21), *Wu and Schulten* (22) found three Ca^{2+}-ions chelated at the C2A- and also two chelated at the C2B-domain. In 2013, *Honigmann et al.* published their paper about the interactions of Syt-1, finding that even four Ca^{2+}-ions were bound at or near the loops in C2B. (23)
Compared to C2A, the C2B-domain seems to be the most essential part of Syt-1 for membrane fusion, making it our primary object of interest. (22)
The C2B-domain has an additional helix at its C-terminal end that could be important for membrane fusion. This helix is believed to undergo a conformational change upon Ca^{2+}-binding and furthermore act as some kind of anchor on the plasma membrane to stabilise the interaction of Syt-1 with the membrane lipids. (22)

The surface of the opposite end of C2B domain to its Ca^{2+}-binding loops has two arginine amino acids (R398, R399) located at the very edge. (see Figure 4) Their side-chains contain the functional group guanidine and therefore represent strong bases. In an environment where lots of anionic phospholipids are to be found, one can image that interactions between these groups are likely.
Another highly reactive part of the C2B-domain is the polybasic lysine stretch. A sequence of four lysine amino acids (K324, K325, K326 and K327) is in close proximity to two additional lysine amino acids (K313 and K321) and therefore is predestined to interact with anionic lipids such as PIP2. The four consecutive lysine amino acids are located on a beta-barrel and facing towards the side of the protein, compared to the binding loops and the arginine amino acids. *Honigmann et al.* report these lysine amino acids to be the motif by which Syt-1 binds to the SNARE complex. (23)

The plenty of possibilities to bind or interact are not yet fully understood, making the C2-domains a very exciting research object. There are several crystal structures of C2A, C2B or C2AB available, making a single domain the perfect research object for molecular dynamics simulations. The exact binding kinetics are not yet revealed thoroughly and so the role of Syt-1 in neurotransmitter release still needs to be studied.

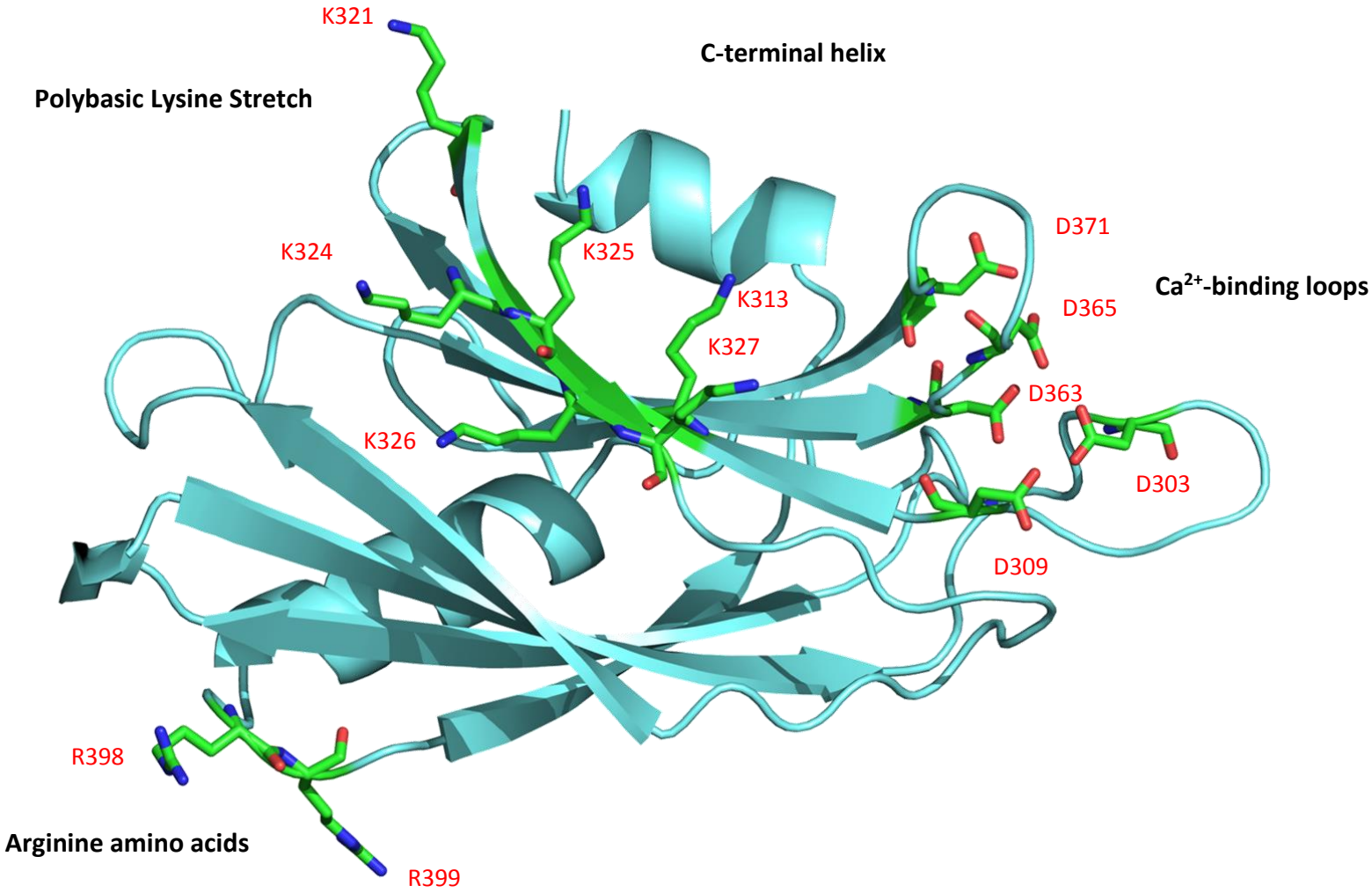

Figure 4: Synaptotagmin-1 C2B domain (taken from pdb 1tjx and truncated by a Val at the C-terminal end); sidechains shown: aspartates of the Ca^{2+}-binding loops (D303, D309, D363, D365, D371), arginines (R398, R399) and lysines of the polybasic lysine stretch (K324, K325, K326, K327) and nearby (K313, K321)

1.2.2 Function

While there is consensus about structure and sequence of Syt-1, the exact function and pathway of exocytosis upon Ca^{2+} influx remains unknown. The common opinion about Syt-1 is that it is inevitable as a Ca^{2+}-sensor for neurotransmission. Knockout studies of Syt-1 suppress fast synchronous neurotransmitter release and thereby support this finding. (12, 24)

To understand the role of Synaptotagmin 1 in neuronal transmission, it is important to know all involved parties. Membrane lipids are discussed in detail in Chapter 1.3. Alongside Syt-1, there are at least two other components necessary to mediate the merging of two membranes into a single bilayer. Particularly the SNARE complex and Complexin come to the fore; they are described in the following.

<u>The SNARE complex</u>

SNARE stands for soluble N-ethylmaleimide sensitive factor attachment protein receptor and plays a key role in neuronal exocytosis. The SNARE complex is formed by vesicle proteins and target membrane proteins. Its core is composed of 4 helices: two helices belong to SNAP-25, which is anchored in the plasma membrane; one helix is contributed by Syntaxin, which is also a target membrane protein and one helix belongs to Synaptobrevin, a vesicle protein (also referred to as VAMP, vesicle-associated membrane protein).

These SNARE proteins are also classified as t-SNAREs (target-SNAREs: SNAP-25 & Syntaxin) and v-SNAREs (vesicle-SNAREs: Synaptobrevin). (11)

First, the 3 helices of the t-SNAREs form a 3-helix bundle. When the vesicle comes in close range to the plasma membrane, the membrane proteins catch each other and form a 4-helix bundle. (see Figure 5) This bundle twists and thereby pulls the vesicle into close proximity of the membrane. This process is called SNARE zippering. (10, 25, 26) The complex is best known as the stable four-stranded coiled coil it becomes shortly before the membranes fuse. (25) The latest studies suggest that the SNARE complex is inevitable for neurotransmission but although it can bring the membranes into close proximity, it is not close enough to overcome the energy barrier for membrane fusion. (5, 27)

<u>Complexin</u>

Complexins are a family of small cytosolic proteins that interact with the SNARE-complex. They are believed to be a cofactor for Syt-1 because deletion of Complexin (Cpx) showed decrease of evoked neurotransmission. The complexin clamp model is a hypothesis in which Cpx works as a clamp on primed vesicles and disables them until the Ca^{2+}-trigger loosens the protein and the vesicles are free to fuse (5, 28, 29) Another possibility is that Syt-1 declamps and therefore frees the SNARE complex by kicking of Cpx. (25)

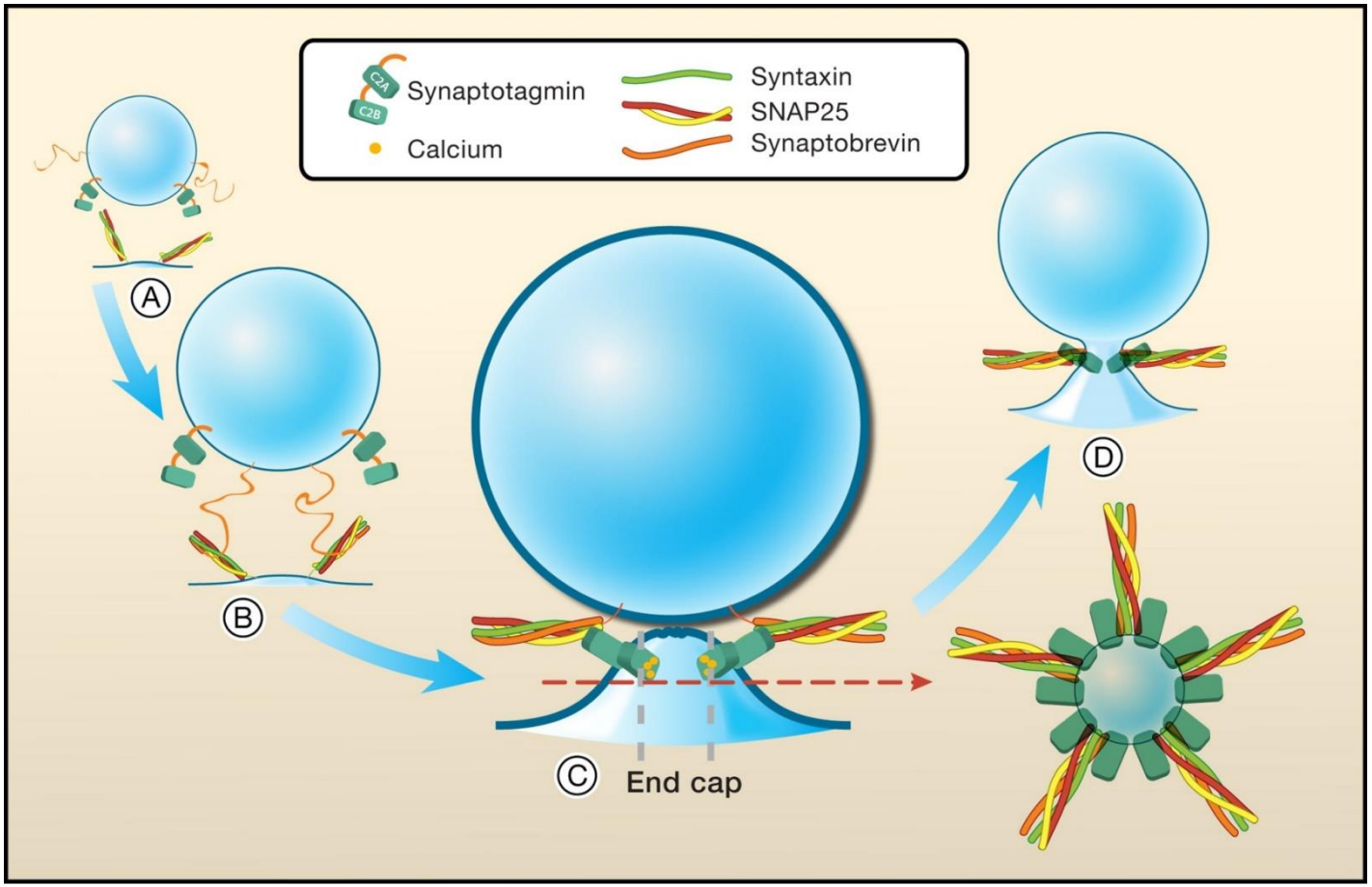

Figure 5: ***A:*** *the 3-helix-bundle made our of t-SNAREs is already formed;* ***B:*** *the vesicle (with v-SNAREs and Syt-1) approaches the membrane, the vesicular SNARE component binds to its SNARE counterparts on the target membrane,* ***C:*** *the SNARE -complex is assembled, the Ca^{2+}-bound C2B-domain of Syt-1 inserts into the presynaptic plasma membrane; the C2 domains of Syt-1 bind to the SNARE complex, potentially helping to complete their zippering into a continuous helix. This results in membrane buckling and an unstable membrane region optimally localized for fusion (jagged membrane in step C).* ***D:*** *the fusion pore opens*

The first big role of Syt-1 is to induce membrane curvature. After binding to Ca^{2+}, the C2B-domain penetrates the membrane and interacts with anionic phospholipids. (30) Syt-1 requires negatively charged phospholipids, with phosphatidyl-inositolphosphates as the most effective representatives. (12) *Honigmann et al.* suggest, that POPS completes the binding of Ca^{2+}, which also seems to be a major reason why Syt-1 does not interact with the plasma membrane until Ca^{2+}-binding. (23) Only after binding to Ca^{2+}, the negative net charge of the binding pocket is reversed and therefore interaction and membrane penetration is enabled. (26)

The tips of the Ca^{2+}-binding loops dip into the membrane up to a third of the lipid monolayer depth. This means that Syt-1 passes the hydrophilic heads and reaches the glycerol backbones. (26, 31) By inserting the presynaptic plasma membrane, Syt-1 induces disorder of the lipids in the proximal bilayer leaflet. This process generates tension amongst the phospholipids. The bulky tip of the C2B-domain pushes the headgroups aside, leaving a void below it. The fatty acid chains try to fill that gap by leaning sideways and therefore already evoking curvature. As a consequence, the lipids in the distal leaflet get stretched and ordered to keep in contact with the proximal leaflet and to fill otherwise empty space. As a result, the membrane bends and membrane curvature is achieved. (21, 22, 26) *Wu and Schulten* report that in their molecular dynamics simulations the C-terminal helix undergoes a conformational change after Ca^{2+}-binding to the C2B-domain. The helix shifts downwards, now looking in the same direction as the binding pocket and makes contact with the membrane. In this model, the helix is the part of the domain that causes disorder amongst the lipids and therefore is primarily responsible for membrane bending. (22)

This Ca^{2+}-dependent induction of membrane curvature is only a local event, but it has been shown that the effect of insertions is additive. In the molecular dynamics simulations of *Wu and Schulten*, two C2B-domains induced stronger membrane bending than only one C2B-domain. (22)

If there are enough C2B-domains causing membrane bending near to a vesicle, a buckle-like structure will form. This brings the plasma membrane into close proximity of the vesicle membrane and thereby dramatically reduces the energy barrier that needs to be overcome for membrane fusion. The lipids in this dimple are under stress and whilst membrane fusion this stress is relieved by rearranging the lipids. This also helps to reduce the energy cost of the fusion reaction. (26)

Furthermore, Syt-1 not only seems to be the main cause for fusion pore opening but also has a continuative role in fusion pore expansion. (26, 32)

While is it unquestioned that Syt-1 interacts with the plasma membrane, there is still little known about its binding to the SNARE complex and what other tasks it may fulfil in neurotransmission. (33) Besides membrane curvature, one of the most important tasks is to block the SNARE complex until the process of Ca^{2+}-binding. The SNARE complex keeps the synaptic vesicle and the presynaptic plasma

membrane in close range or rather connected generally. The four helix bundle core twists and thereby pulls the vesicle into close proximity of the plasma membrane. If the distance becomes too close, membrane fusion would occur in a Ca^{2+}-independent manner because of the lowered energy barrier for membrane fusion. Interestingly, Syt-1 is believed to have a dual mode of action and not only promote evoked synchronous release, but also prevent asynchronous release. This is achieved by functioning as a clamp on the SNARE-complex as well. Following this hypothesis, Syt-1 is a very effective regulator of neurotransmission by reversing its action upon binding to Ca^{2+}. (6, 12, 20, 34) There is also the possibility that not Syt-1 itself, but Cpx is blocking the SNARE complex upon Ca^{2+}-influx. In this model, the unbound form of Syt-1 would not 'attack' Cpx, whilst the Ca^{2+}-bound Syt-1 does and therefore knocks the Cpx-clamp off the SNARE complex. (25)
In December 2014, scientists of Max Planck Institute of Biophysical Chemistry, Munich published their view of things in a press release saying that the SNAREs catch each other like a zipper but are not able to completely close without increase of Ca^{2+}-concentration. They stop at a distance of 8nm and are not able to fuse the membranes. Syt-1 tethers the vesicle membrane from the presynaptic plasma membrane at this distance. It is still not close enough to overcome the energy barrier for spontaneous membrane fusion. Upon Ca^{2+} influx, Syt-1 pulls the vesicle even closer to a distance of 5nm, which is energetically attractive and close enough for the SNAREs to fuse the membranes and thereby release the neurotransmitters. (27)

The exact molecular mechanisms of Syt-1 binding to the SNARE complex have been studied extensively throughout the last years. In 2012, *Honigmann et al.* published their findings, in which Syt-1 binds to PIP2 in the membrane with its polybasic lysine stretch region and uses PIP2 as some kind of linker to also connect with Syntaxin-1 of the SNARE complex. (23) A very recent model of Syt-1, Cpx and the SNARE complex suggests that even two C2B-domains are involved simultaneously and interact with different regions of SNAREs. (34) This finding also supports the hypothesis of Syt-1 having a locking impact on the SNARE complex until Ca^{2+}-influx arises. (34)

The question about the involvement of C2A and C2B domains in the different tasks of Syt-1 remains unclear. While some studies suggest that C2A and C2B need to be linked to promote membrane fusion, others showed that membrane bending is achieved by the C2B-domain alone. (10, 22, 31)
Mutating the C2B-domains Ca^{2+} binding site showed similarity to complete Syt-1 knockout, which indicates that this domain is inevitable for neurotransmitter release. Similar mutations in the C2A-binding site showed a much less severe decline in release, whereas Ca^{2+}-titrations and blocking of the C2A Ca^{2+}-binding site showed a decrease of release. Even if C2A and C2B do not possess the same importance for neurotransmitter release, it is obvious that they work cooperatively. (5, 35)

1.2.3 Different Synaptotagmins and Isoforms

According to the HUGO Gene Nomenclature Committee there are 17 different genes known within the family of Synaptotagmins. (36)

The family characteristics are a short amino-terminal luminal sequence, followed by a transmembrane part and a variable linker connecting it to the two Ca^{2+}-binding domains, called C2A and C2B-domain. The C2B-domain forms the carboxy-terminal end of the protein. Whilst not all Syts actually bind Ca^{2+} (see Figure 6), science mostly focusses on the ones that do because of their importance as membrane-trafficking proteins. (5) Here is a short selection of Syts and their appearance: Syt-7 is to be found on secretory granules in neuroendocrine cells, whereas Syt-1, Syt-2, Syt-9 and Syt-12 are membrane proteins of the synaptic vesicle. Syt-10 is known to play a role in the secretion of IGF-1 and Syt-4 was localized to the trans-Golgi complex. Syt-1 is known to be the most important family member for neurotransmission, but a screen of other Synaptotagmins in a Syt-1 knockout phenotype showed, that only Syt-1, Syt-2 and Syt-9 could fulfil the role as a Ca^{2+}-sensor. (12, 23, 37, 38) More recent studies suggest, that Syt-2 and Syt-9 also play a role in evoked neurotransmitter release and Syt-7 is involved in the asynchronous release. (20, 25, 39, 40, 41)

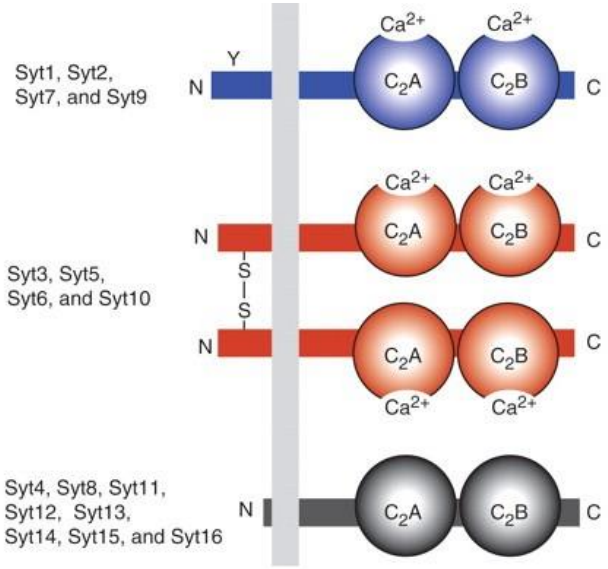

Figure 6: Different Isoforms of Syt: Syt-1, -2, -7 and -9 are the "classical" Syts, whereas Syt-3, -5, -6 and -10 are "double proteins" connected via disulphide bridge and Syt-4, -8, -11, -12, -13, -14, -15 and -16 do not even bind Ca^{2+}

Südhof TC. Calcium control of neurotransmitter release. Cold Spring Harb Perspect Biol (2012) 4(1):a011353.10.1101/cshperspect.a011353

Synaptotagmins are evolutionary conserved and most of the Ca^{2+}-regulated exocytosis in eukaryotic cells is based on the Synaptotagmin fusion-apparatus. The motif of the C2-domains as a Ca^{2+}-sensor is known to be highly conserved itself. The architecture of the binding pockets, using aspartic acids to ligate the Ca^{2+}-ion, stays the same. These C2-domains are not only found in Synaptotagmins but in a large number of membrane trafficking proteins. (5, 42)

1.3 Membrane lipids

The plasma membrane in mammalian cells is built as a phospholipid bilayer with additional cholesterol and glycolipids. The hydrophilic head groups point to the outside, whereas the lipophilic tails are oriented towards each other in the middle. This setting of lipids is seen in the plasma membrane of the presynaptic cell as well as it is in the vesicles that carry the neurotransmitters. (1)

If the right amount of lipids was put into an environment of water, they spontaneously assemble to the bilayer structure we call membrane. (43)

Membranes fulfil a very important role as a barrier and are impermeable for water-soluble molecules. The fluidity of the membrane, and therefore also its ability to bend, is determined by its composition and its temperature. As we work with constant temperature in Molecular Dynamics, we focus on the composition. (43) For example, the composition of the human erythrocyte plasma membrane is already identified: Phosphatidylcholine 20%, Phosphatidylethanolamine 18%, Phosphatidylserine 7%, Phosphatidylinositol 3%, Sphingomyelin 18%, Glycolipids 3%, Cholesterol 20%, others 11%. (44)

The exact composition of the neuron plasma membrane or the synaptic vesicle is yet unknown, but the importance of anionic phospholipids being present in the plasma membrane is out of the question. Syt-1 is a vesicular membrane protein and needs these anionic phospholipids for interaction and membrane fusion, subsequently. (23)

Here is an excerpt of the most important membrane lipids for this diploma thesis, subsequently:

<u>POPC</u> (1-palmitoyl-2-oleoyl-sn-glycero-3-phosphocholine)

The head group of POPC is choline, with a charge of +1. Together with the negative charge of the phosphate group, the total charge of this lipid is zero.

For the membranes built for this diploma thesis, POPC is the standard lipid used, with a concentration of a minimum of 45% (and up to 70% in the non-cholesterol-membranes).

<u>POPE</u> (1-palmitoyl-2-oleoyl-sn-glycero-3-phosphoethanolamine)

Like POPC, POPE has a head group with a charge of +1: ethanolamine. Therefore, its total charge is also zero. In all membranes, which were used in this diploma thesis, the average concentration of POPE is 15%.

<u>POPS</u> (1-palmitoyl-2-oleoyl-sn-glycero-3-phosphatidylserine)

With its head group serine, POPS has a total net charge of -1. This is a major difference to the other lipids discussed so far, which are electrically neutral at physiological pH. Therefore POPS is expected to interact with the protein, respectively its positively charged amino acids lysine or arginine.

Honigman et al. even report that POPS binds directly to the Ca^{2+} binding site of Syt-1 and thereby completes the Ca^{2+}-binding in its pocket. (23) A concentration of 10% was used in all membranes.

PIP2 (1-palmitoyl-2-oleoyl-*sn*-glycero-phosphatidylinositol-4,5-bisphosphate)

In POPI (phosphatidylinositol) the head group is inositol, which is not charged. Therefore this membrane lipid has a total net charge of -1.

PIP2 has the same head group. Different to the other membrane lipids, PIP2 has not only one phosphate group connecting fatty acid chains and head group, but two additional phosphate groups in position 4 and 5 of the inositol head group. This feature is the reason why PIP2 has a total charge of -3 or -4, making it the most negatively charged lipid used in this diploma thesis.

PIP2 is known to be a major regulating membrane lipid, serving as ligand that activates proteins, as substrate for the generation of second messengers and also regulating cell migration. (45, 46)

In 1990, *Emberhard et al.* showed that PIP2 is necessary for exocytosis. (47) Given that Syt-1 and its role in neurotransmitter exocytosis is the main focus of this diploma thesis, we put emphasis on the role of PIP2 and its interactions with Syt-1 as well. We used PIP2 in a concentration of 1%, respectively 5% in our so called “high PIP2 membranes”.

Cholesterol

Cholesterol contains a hydroxyl group which is oriented outside, analogue to the other hydrophilic head groups. The hydrophobic part of cholesterol contains a very rigid steroid ring system, which stiffens the membrane. Plasma membranes with high concentrations of cholesterol therefore tend to be less flexible than membranes with lower cholesterol levels. At very low temperatures, cholesterol maintains membrane fluidity by preventing the membrane from freezing and therefore stiffening. The finding that cholesterol is able move from one bilayer to the other within milliseconds also indicates its role in preventing the integrity and functionality of the membrane. (48) Also, cholesterol (as well as sphingolipids) is known to cluster in so called rafts, a small microdomain in the lipid bilayer with higher concentrations of certain lipids. These rafts tend to interact with specific membrane proteins and play a role in exo- or endocytosis. (17, 43)

In this diploma thesis membrane bending is an important consideration. This is why cholesterol and its fluidity influencing characteristics are attached great importance. Therefore we used membranes with a cholesterol concentration of 25% as well as membranes without any cholesterol at all.

1.4 Cholesterol influence on neurotransmission

Anionic membrane phospholipids are inevitable for the interaction with Syt-1 and furthermore membrane fusion. POPS for example is believed to coordinate the Ca^{2+} in synergy with the C2AB-domains of Syt-1. (20, 23) The role of cholesterol however, is not yet completely understood.

Cholesterol is not only an essential membrane component, but also essential for the exocytosis apparatus. The cholesterol to phospholipid ratio is estimated to be between 0.5 and 1, which is in common range of plasma membranes. However, the distribution of cholesterol amongst the bilayer leaflets in synaptic membranes is different to other known membranes. The inner leaflet contains up to eight-fold more cholesterol than the outer leaflet does. (49, 50) Cholesterol gathers in so called rafts, a cholesterol-rich part of the membrane and it is believed that this high concentration of cholesterol is needed to organize signalling proteins such as SNAREs. (51) Further studies showed that Syntaxin is concentrated in 200nm large cholesterol-dependent clusters and also SNAP-25 tends to cluster in rafts, partially overlapping the syntaxin-clusters. (51) According to the assumption that a sufficient number of SNARE complexes is needed to mediate membrane fusion at a local site, it seems plausible that they gather in hot spots or active zones. Later on, vesicles dock and fuse in a highly preferential number at these rafts, which indicates the crucial role of cholesterol in neurotransmission. (49, 51) This is also supported by some cholesterol depletion studies: removal of cholesterol leads to dispersion of the rafts, meaning that also the rate of neurotransmitter release is reduced dramatically. Studies showed that a cholesterol-removal of 40% leads to a decrease of dopamine release by 60%. (51)

Interestingly, only evoked synchronous release was impaired by cholesterol depletion, whereas an augmentation of spontaneous release was revealed under the same conditions. This finding implicates a balancing role of cholesterol, preventing the synapses from spontaneous release or in other words “being leaky”. On the other hand, cholesterol appears to be another factor in regulation of the amazingly precise synchronous release, evoked by an action potential. (4, 52)

2. Methods

2.1 Molecular dynamics simulations

The most complex chemical systems can be found in living organisms. Although there are numerous ways to study them and their function, it is rather difficult to take a look on separated structures, such as proteins, when it comes to a more detailed perspective. (53) Whereas X-ray crystallography or NMR spectroscopy give us a fair view on the structures, it has remained hard to picture dynamic systems.
Molecular dynamics (MD) is a computational method to simulate the movement and interaction of atoms and molecules in a defined system for a specified period of time (typically ns to µs). By solving Newton's equations of motion for every particle in the system it is possible to describe their trajectories. To calculate these equations, the forces that take effect on every atom must be known. These forces are described by a force field that holds the information for bonded (e.g. bond-stretching, angels, dihedrals) and non-bonded (e.g. Coulomb, Lennard-Jones or electrostatic) interactions. (54)

Molecular dynamics is thereby a computational but non-invasive method that enables the description of biomolecular systems with all-atomic detail. For example, different conformations of a molecule or a complex can be tested on thermal accessibility. It is possible to check, if a modelled protein structure is stable and therefore the model is energetically reasonable. Recently, also protein folding has become a field of study where MD simulations are used. (55)

The first molecular dynamics simulation of a protein was reported in 1977, but computational power was limited back then, allowing only simple and short models. (56) More recently, increasing computational capacities make simulations of bigger systems and longer simulation times feasible. As of today, molecular dynamics offer the chance to take on complex systems like transmembrane channels. Without doubt, molecular dynamics have become a widely acknowledged way to investigate proteins, lipids and other biomolecules. (55)

2.2 Corse-grained MDs

Although there are big steps made every day to increase computational power, the usability of molecular dynamics simulations is limited regarding simulation length and size of the system. Even in smaller systems, a simulation length of over 100ns is associated with major efforts. The problem is simple: with every additional atom in the system, the computational effort grows. Also, many physiological processes take more time than available with state-of-the-art computers. (57)

Coarse-Graining is one of the possible ways to extend simulation length. The system is represented in a simplified way by a reduced number of degrees of freedom. Basically, there are many shades of simplification. The all-atomistic model is the most realistic model, but also consumes the most time and capacities. In the united-atom model, pseudo-atoms are created. For example, a methylene group is represented as only one pseudo-atom and the hydrogens are not calculated separately. In other words, the degrees of freedom that belong to the hydrogen atoms are saved and thereby the computational effort is eased. (58)

Even more simplified are coarse-grained models. In this presentation, atoms are summarized as one pseudo-atom, for example one amino acid side chain can be pictured as only one or two pseudo-atoms. (see Figure 7) (53, 59) This allows the simulations to go much faster than if the same system was represented all-atomistic and thereby extends the possible total length of the simulation. Systems too large to be studied in atomistic detail get a new chance to be looked at using coarse-grained simulations, albeit at lower resolution.
The three-dimensional structure of a protein is not only determined by its backbone, but also by the different sidechains of the amino acids. Therefore, it is important to carefully design coarse-grained models, so that the integrity of the model is ensured and the model thereby is reliable. (53)
It is always a balancing act to choose between the computationally more effective simplified model and a more realistic model that requires higher effort.

Today, coarse-grained models are widely used for modelling and the simulation of bigger systems. The Nobel Prize Committee awarded Michael Levitt, Ariel Warshel and Martin Karplus for their work in 2013. Their research included coarse-grained modelling of proteins. (53) It is safe to say that coarse-grained molecular dynamics simulations have become a standard tool in biochemical research.

With regard to the wide use of coarse-graining and the extensive MD simulations planned for this diploma thesis, we decided to run all simulations using coarse grained models. To get an impression of what coarse-graining means in our case, the coarse-grained C2B-domain of *1tjx_trunc* is shown in Figure 8 in comparison to an all-atomistic model.

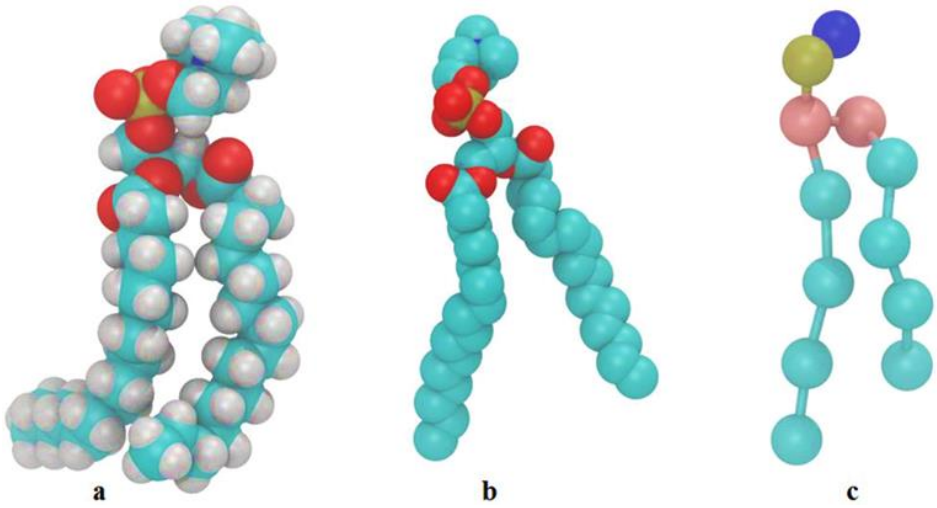

Figure 7: Representation of 1,2-dipalmitoyl-sn-glycero-3-phosphocholine (DPPC) with (a) atomistic (all-atom; AT), (b) united-atom (UA), and (c) coarse-grain (CG) force fields as van der Waals spheres

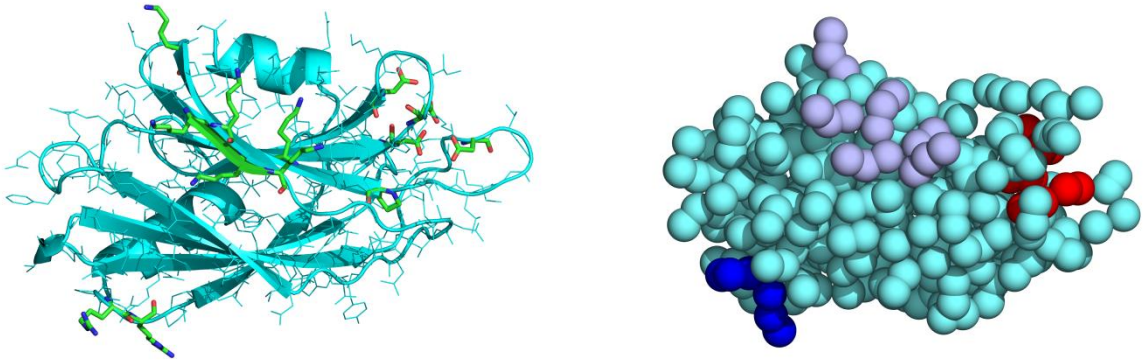

a) *b)*

Figure 8: Synaptotagmin-1 C2B domain (1tjx_trunc) ***(a)*** *all-atomistic model without hydrogens; for better orientation, cartoon-representation is also depicted; Arginines (R398 & R399), Polybasic Lysine Stretch and Ca^{2+}- binding pocket are shown as sticks* ***(b)*** *coarse-grained model, rendered with VMD. Aspartates in the binding pocket are coloured red, Lysine amino acids of the polybasic lysine stretch are coloured iceblue and arginine amino acids are coloured blue*

2.3 Description of used programs

Here is a list of programs we used to set up, run and evaluate molecular dynamics simulations in alphabetical order:

2.3.1 Gromacs

Gromacs is a software package designed for running molecular dynamics simulations. Simply put, it solves Newtonian equations of a set up system. It was first developed at the department of Biophysical Chemistry at the University of Groningen, Netherlands. It was released in 1991 and the name stands for Groningen Machine for Chemical Simulation.

Gromacs is very fast and user-friendly, therefore it is (besides NAMD) one of the most commonly used programs. (60) The speed is founded on the separation of calculating bonded and non-bonded interactions. (see Chapter 3.3) Calculating the non-bonded interactions is usually the bottleneck in MD simulations. (55) Gromacs assigns bonded interactions to the CPU and non-bonded interactions to the GPU, which allows the program to perform fast and efficient. It is mostly used for simulating proteins, lipids and nucleic acids; it supports many different force fields and is free of charge. (61, 62) The latest version of Gromacs is 5.1.4, but due to practicability reasons, version 4.6.7 was used for this diploma thesis. Being the most important program for running MD simulations, a little more detailed description is given in the following.

2.3.1.1 Gromacs file formats

There are numerous file formats which are used by the Gromacs software package. Every command and every process needs specific file formats as input. Here is a list of the most common file formats used for this diploma thesis in alphabetical order:

- **.gro*: structure file; this file contains information about the molecular structure of the protein, lipid or system in Gromos87 format and is comparable with *.pdb files.
- **.itp*: topology file; itp stands for include topology. Force-fields are written in this file format.
- **.mdp*: parameter file; includes data like temperature, step-size, pressure and simulation time
- **.ndx*: index file; contains information about different groups in the system, for example protein, lipids, solvent. It is mostly used if special groups are necessary, i.e. for analysis.
- **.pdb*: structure file like *.gro, but using the protein data bank format. Basically, these files contain the coordinates of every atom.
- **.top*: topology file; data content like number of solvent ions or number of lipids is found in this file. It is needed by the pre-processor command *grompp* to create a run input file.
- **.tpr*: run input file; this file is the output file of the *grompp* pre-processor command and includes the information about the starting structure, the molecular topology and all

simulation details. It is the only file format needed to start a molecular dynamics simulation via the *mdrun* command.

- **.xtc*: trajectory file; is one of the output files of the *mdrun* command and contains the complete trajectory of the simulation.
- **.xvg*: output file of gromacs analysis tools; it can be used as an input file for Grace (see Chapter 2.3.8) to create graphs.

There are more file formats involved, please see the official Gromacs manual for a complete list and more detailed information (63).

2.3.1.2 Gromacs commands

Gromacs commands are the basis of the whole program. Given the fact that this software package works without graphical interface, each command is typed into the terminal at the local computer. Every command requires different files as input to handle and process them as desired. The following list represents the most common commands that have been used for this diploma thesis in alphabetical order. A short description of each command is given to illustrate its functionality. The official Gromacs manual and the Gromacs tutorial by Justin Lemkuhl were used as source of information. (63, 64)

- *editconf*: converts generic structure files, e.g. a *.pdb file to a *.gro file. This command was heavily used, because it is also needed to change the coordinates of a structure or to rotate it. That was of great importance for generating the systems and the correct placement of membranes and protein.
- *genbox*: solvates the simulation box. Van der Waals radii can be assigned manually and the topology-file will be updated automatically.
- *genion*: randomly replaces solvate molecules with ions. This command needs a *.tpr file as input, so the *grompp*-command needs to be used first. It is possible to replace exactly as many solvent molecules as needed to get a total zero net charge by adding *-neutral*. Besides, it is also possible to set a concentration by typing *-conc* and the desired concentration.
- g_mindist: measures the distance between two index groups over the time of the simulation. For example, it was used to show that Syt-1 was in a Ca^{2+}-bound state at all times.
- *grompp*: is a pre-processor that creates a *.tpr-file. The molecular topology file is read and information needed for a free energy simulation is packed into the output-tpr-file. As input, the following file formats are needed: *.pdb/*.gro, *.mdp, *.top, *.ndx (optional)
- *make_ndx*: creates an index for a structure file. With the index editor it is possible to create different index groups, for example a group for the residues located at the binding pocket of

Syt-1. Having created a special group, it is possible to address only this group with other commands.

- *mdrun*: performs MD simulations and represents the main computational chemistry engine of Gromacs. It can also be used for energy minimization and equilibration. The trajectory file *.xtc is one of the most important output files.
- *pdb2gmx*: reads a *.pdb or *.gro file, generates coordinates in Gromacs and creates a topology file (*.top). This is usually the starting command after retrieving a protein structure file from the Protein Data Bank (PDB). It also determines the force field. In this diploma thesis, a perl-script was used that already includes this command.
- *tpbconv*: can extend a completed simulation. This command was used for simulations, where an interaction was about to take place or already happened at the end of the simulation.
- *trjconv*: converts a trajectory file. Offers the opportunity to create a *.gro file at any time of the trajectory.

For further commands and information, please see the official Gromacs manual. (63)

2.3.1.3 Gromacs Flow Chart

A typical work flow is shown in Figure 9. This flow chart is based on the official Gromacs flow chart and the *Introduction to protein simulation* by Bert de Groot. (63, 65)

Usually, the starting file is retrieved from the Protein Data Bank (PDB). (66) This starting file contains information about the structural conditions of the protein (primary, secondary and tertiary structure) and is normally solved by X-ray crystallography, Cryo-EM or NMR spectroscopy. This file (usually the file format is *.pdb) is evaluated with special regard to the resolution.

This structure is now – if necessary – set up to a system, for example a membrane is added or in case of a membrane protein it needs to be embedded in the membrane. The positioning can be checked via VMD or PyMol (see Chapter 2.3.2 / 2.3.6). A topology file is created via the *pdb2gmx* command and a simulation box is set up. Once the simulation box is determined, it is filled with solvent. In the last step of the setup, ions are added in the desired concentration, using the *genion* command. In-between these steps, energy minimisation runs are recommended to relax the system.

The actual simulation is preceded by the pre-processor step using the *grompp*-command. After the most time-consuming step, the simulation itself, is finished, numerous sorts of analysis and evaluation can be done.

A more detailed description of the preparation, setup, simulation and analysis we have done throughout this diploma thesis can be found in Chapter 3.

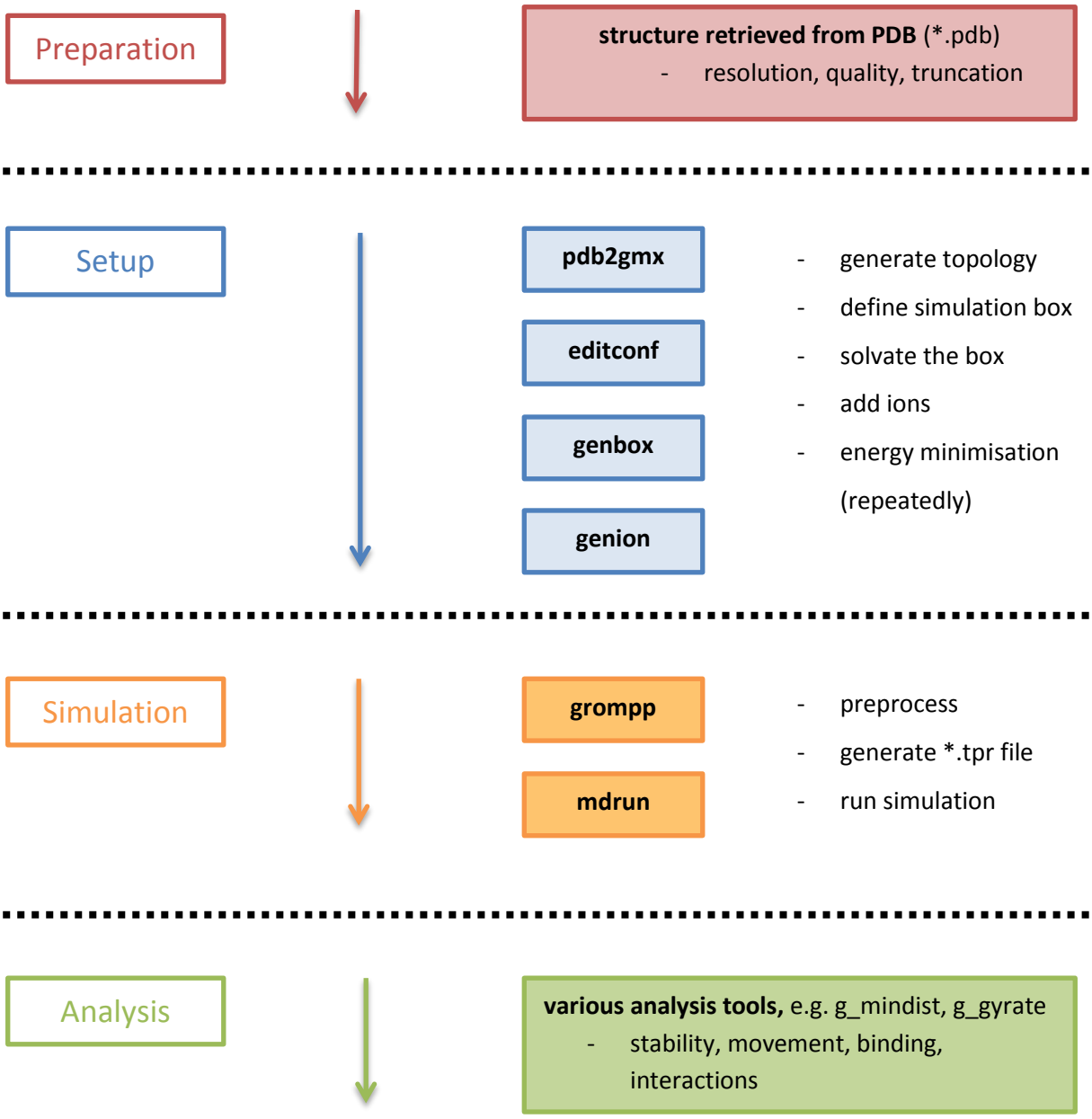

Figure 9: Gromacs Flow Chart; Preparation: structure file (.pdb) is retrieved and conditioned; Setup: topology file is generated (using pdb2gmx), the system is adjusted and the simulation box defined, the box is solvated and ions are added; Simulation: after preprocessing (generation of a *.tpr file) the simulation is executed with the mdrun command; Analysis: there are many different tools for all sorts of analysis, for example g_mindist (measures the distance between groups over the simulation time or g_gyrate (computes the radius of gyration)*

based on: Practical 2: Introduction to protein simulation; Available from: http://www3.mpibpc.mpg.de/groups/de_groot/compbio1/p2/

2.3.2 PyMol

PyMol is open source graphics software currently commercialised by *Schrödinger, Inc.* It is perfectly suitable for visualization of small molecules and bigger biomolecules, such as proteins. It can produce high resolution images and is highly user-friendly due to an intuitive interface. In this diploma thesis, it was heavily used for structural analysis, allocation of groups, creation of figures and the elimination of too much water in the membrane. (67)

2.3.3 Python

Python is a programming language that was used for scripting and to ease the process of analysis. (68)

2.3.4 Swiss Pdb-Viewer / Deep View

Swiss Pdb Viewer is a graphics program that has been developed in 1994 by Nicolas Guex at the Swiss Institute of Bioinformatics (SIB) in Basel, Switzerland. It is primarily used to analyse structures such as proteins. Also, it allows comparing different structures at the same time by superimposing them in the graphical interface. Furthermore, it provides modelling tools, for example residues can be mutated and side-chains rotated. (69)

Amongst other things, the program was used to mutate the quintuple mutant *5ccj* of the protein data bank back to wild type.

2.3.5 Vi

Vi is a text editor that can be used within the terminal of linux. It was used for scripting commands that had to be entered repeatedly and thereby saved a lot of time. (70)

2.3.6 VMD

VMD stands for Visual Molecular Dynamics and is a graphics program for larger biomolecular structures. For example, a large system containing membranes and proteins can be visualised and analysed. Furthermore, the program can animate the trajectory of a MD simulation and thereby offers the possibility to analyse not only a structure, but a system in motion. The numerous possibilities to shape, hide or colour different lipids or residues come in handy for displaying certain interactions. (71)

VMD is the main tool to view the results of molecular dynamics simulations. It was used, inter alia, for a first visual analysis of finished MD runs and to specify the seen interactions between protein and membrane throughout the work on this diploma thesis.

2.3.7 xxdiff

The graphical file comparator xxdiff allows comparing and merging of up to three files. It is a small program that can proof very useful working with large text files, because it highlights and thereby easily reveals little deviations. (72)

2.3.8 Xmgrace/Grace

Grace is a program that creates two-dimensional graphs and plots for the X Window System. It is free of charge and its name stands for Graphing, Advanced Computation and Exploration of data. The data received from various analysing tools is shown as a 2D-graph for better comprehensibleness and clearness. (73)

All graphs in this diploma thesis (see Chapter 6) have been created with Grace or a python script.

3. Results

3.1 Aim

With reference to the multiple possibilities of membrane-interaction (see Chapter 1.2.2), the C2B-domain of Syt-1 is the main focus of this diploma thesis. Whereas other studies only examined the Ca^{2+}-binding pocket and its possible insertion into the membrane bilayer, the importance of the polybasic lysine stretch and the arginine amino acids (R398, R399) remain unclear. (21, 22) These assumptive interaction-hot-spots are not as well understood as the Ca^{2+}-binding site. A 2013 study found, that Syt-1 uses PIP2 as bridge for interaction with the SNARE complex, binding with its polybasic lysine stretch. (13) This study also raises the question, if the C2B-domain could be oriented the other way around, interacting with the vesicular membrane as well. These possible orientations are described as parallel (C2B interacts with the presynaptic plasma membrane via the Ca^{2+}-binding site) and perpendicular (the Ca^{2+}-binding site interacts with the vesicular membrane). (13) A more recent study suggests that more Syt-1 proteins are necessary for membrane fusion and at least one of these binds to the vesicular membrane. (34) This is important with regard to the assumption, that the membrane composition of vesicle and presynaptic plasma membrane differs. (43, 44)

These findings bring up the question, if a special membrane composition is needed to interact with Syt-1. It is known that negatively charged phospholipids are needed to ligate the bound Ca^{2+}, but little is known about the role of cholesterol and other possibly involved lipids. (4, 31, 23)

So far, MD simulations on this matter mostly looked into conformational changes of Syt-1 or tried to facilitate membrane bending. (21, 22) *Schulten et al.* chose to place the isolated C2B (or C2A) domain only 5 Å (Ångstrom) above the membrane, with the Ca^{2+}-binding site already pointing towards the membrane, therefore making it easier to bind in the desired orientation. (22)

We decided to go for a completely unbiased approach with respect to interaction of the C2B-domain and the membrane. The C2B-domain is placed near a membrane or between two membranes, without any restraints or orientation setups. (see Chapter 3.3 and 3.8) Our goal was to observe the expected interactions at the Ca^{2+}-binding site and also every other possible interaction, with a special focus on the polybasic lysine stretch and the two arginine amino acids (R398, R399).

3.2 Process, Implementation

Lipids are computationally very costly to perform. This is why all-atom simulations with a membrane large enough to bend are still a major effort in molecular dynamics. *Schulten et al.* used the highly mobile membrane mimetic model (HMMM), which allows keeping specific head group interactions, but greatly accelerates lipid redistribution and therefore simulation speed. (22) It was clear, that using this al-atomistic model would take an enormous amount of simulation time to observe as many

interactions as possible. Our next goal was to explore the interactions with different membrane compositions. To produce a significant amount of simulation time for multiple membrane systems is an even bigger effort and encouraged our considerations to simplify the system. Based on our goal to generate multiple microseconds of simulation time and the availability of computational capacities, we decided to perform all simulations with coarse-grained models of every participating molecule.

3.3 Simulation details

One of the first and most important decisions when setting up a MD simulation is the choice of the force field. A force field is a mathematical expression holding the information for energy terms (e.g. bonds, angles, dihedrals). (74) It describes the dependence of the systems energy on the coordinates of its particles. (see Chapter 2.1) (75) The parameterisation of force fields needs to fit the desired system as good as possible in terms of system size, boundary conditions and treatment of longer range electrostatic interactions. For example, periodic boundary conditions (PBC) ensure that the system does not end abruptly. Simply put, if a particle leaves the simulation box on one side, it re-enters the box from the other side. This elegantly prevents sudden borders to a vacuum. (55) Also, temperature and pressure need to be set and hold constant for all simulations. For example, it has been found, that with the pressure, hydrogen-bonding patterns change drastically. (76)

There are several widely used force fields for all-atomistic simulations (CHARMM, OPLS-AA, GROMOS). (77) These force-fields have been optimised in terms of parameters for alkanes throughout the last years. (55) Therefore the results of the same simulation can vary, if performed with different force fields and furthermore influence the outcome significantly. This gives an idea, how important the choice of a fitting force field is in regard to the findings of the MD simulations.

We planned to perform coarse-grained simulations and therefore used a force field especially suitable for simulating coarse-grained biomolecules.

We chose to go with the Martini force field, which uses a four-to-one mapping. This means, that a single interaction centre represents an average of four heavy atoms and their associated hydrogens. (78) Interaction centres are also cut down to four main types: polar, non-polar, apolar and charged. Different subtypes ensure the atomistic structure is represented accurately. (78)

Another choice was to let the MD simulations run completely free. We did not use any position restraints or forces to accelerate interactions. We were willing to risk that plenty of our precious simulation time was without an outcome, because the protein had to “find” the membrane by itself. Most kindly, my supervisor, Ass.-Prof. Mag. Dr. Anna Weinzinger provided new workstations so we could run our simulations almost twenty-four hours a day, seven days a week.

Therefore, the biggest part of all molecular dynamics simulations was calculated at the local workstation at The Department of Pharmacology, University of Vienna. For this purpose, we had multiple computers with the following specifications: CPU: Intel Core i7-6900K, 8x3.4GHz; 64gb random access memory and NVIDIA Geforce GTX 1080 graphic board with CUDA support. CUDA stands for Compute Unified Device Architecture and allows additional computing capacity via the GPU. (79) It is mostly used in scientific calculations, where parallel processes are a benefit as it is the case with Gromacs. The working load is being split between CPU and GPU. Whereas the CPU mostly calculates the bonded interactions, the GPU carries the load of the non-bonded interactions. This is one of the main reasons Gromacs is known as a very fast program for molecular dynamics simulations. (61)
Although the local workstation did a fine job processing the simulations, we decided to outsource some of them as the number of systems became bigger. We used the group owned HPC (high performance computer), which is a CPU only cluster and located at the VSC (Vienna Scientific Cluster) building. We had access to 5 nodes with 32 CPUs (AMD Opteron Processor 6220) each.

The defined time between two calculated steps was in our focus rather soon. It was our goal to find the perfect time per step, which was small enough to allow stable simulations, but also big enough to generate long simulation times. We started out with 20 femtoseconds (fs) per step, but faced multiple crashed simulations due to exceedance of the maximum cut-off length. After reducing the time-step, simulations became more stable and we finally settled with 10fs. The only exception is the *Standard 895* system with *1tjx_trunc*, in which we performed runs with a time-step of 12fs.

As shown in Table 1, we performed a total of 87,85 microseconds of MD simulations. As discussed in Chapter 3.7 and following, we tried various different approaches and therefore generated numerous simulations that are not included in our final analysis. Starting with scripted simulations where the membrane needed to assemble itself, we found, that only a pre-assembled membrane could represent the physiological conditions correctly. It took some time to figure out the best system setup for our purposes, but eventually we came up with a standard setup for all tested membranes. The final systems (see Chapter 3.10) accounted for 46,80 microseconds, which is still a big computational effort and took several months to execute.

		1tjx_trunc [ns]	5ccj_WT [ns]	Total [ns]
Scripted Membrane Assembling with Protein		4.950	1.800	6.750
Membrane Assembling	850			850
Test Runs, Crashed Simulations		14.150	19.300	33.450
Final Systems Runs		23.800	23.000	46.800
Total	850	42.900	44.100	87.850

Table 1: Summary of runtimes (in ns);

3.4 Syt-1 C2B 1tjx_trunc and 5ccj_WT

The protein files used in this diploma thesis have been downloaded from the Protein Data Bank. (66) There are not only numerous structures of Syt-1 available, but also many other members of the Synaptotagmin family. Even a structure of Syt-1 with the SNARE complex has been released (PDB code 2N1T). With regard to the multiple binding possibilities of the C2B-domain, we decided to run our simulations with only this domain, disregarding the role of C2A. To back up our findings, we chose two different structures of the C2B domain and ran the same simulations with each of them.

The first structure is *1tjx*. (80) It was released in 2004 and has an excellent resolution of 1.04 Å. We used the Swiss Pdb Viewer (see Chapter 2.3.4) to edit the structure. Originally, *1tjx* had 159 residues, but the pdb-file held no complete information for V419, K420 and K421. We truncated the protein and called it *1tjx_trunc* further on. (see Figure 10) Therefore, the used structure has 156 residues and the last amino acid residue is Alanine (A418).

The second structure is *5ccj*, which is a quintuple mutant (R281A, E295A, Y338W, R398A, R399A). (20) This more recent crystal structure was published in 2015 and has a resolution of 1.65 Å. To make the two structures comparable, we used the Swiss Pdb Viewer to mutate *5ccj* back to wild type and further refer to it as *5ccj_WT*. (see Figure 11)

The main difference between the two structures is the length of the linker to C2A. In *5ccj*, the domain starts with S270, whereas in *1tjx*, it starts with S263, followed by five Glycine amino acids which belong to the linker. (see Table 7) We did not expected the elongated linker in *1tjx_trunc* compared to *5ccj_WT* to make any major differences in our MD simulations as the expected interaction sites with the membrane are not in immediate proximity of the linker. The sequences of *1tjx_trunc* and *5ccj_WT* are shown in Table 7.

A sequence alignment of *1tjx* and *5ccj* is provided in Chapter 6.1 – Supplements as well as a sequence alignment of the processed and finally used structures *1tjx_trunc* and *5ccj_WT*. (20, 80) The used structures have also been compared via structure alignment (see Chapter 6.3).

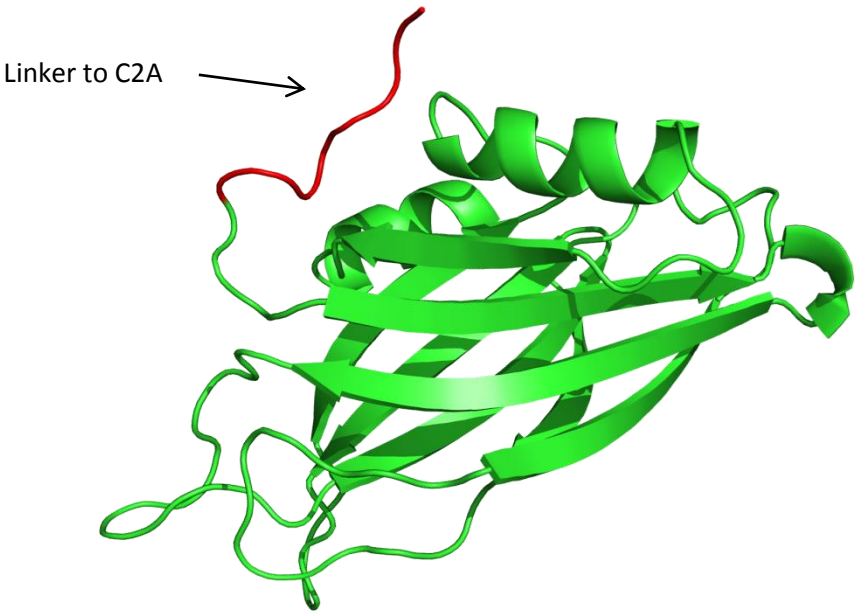

Figure 10: Cartoon illustration of 1tjx_trunc; the linker to C2A is elongated, compared to 5ccj_WT – the part, that includes amino acid residues not existent in 5ccj_WT is coloured red (S263, G264, G265, G266, G267, G268, I269)

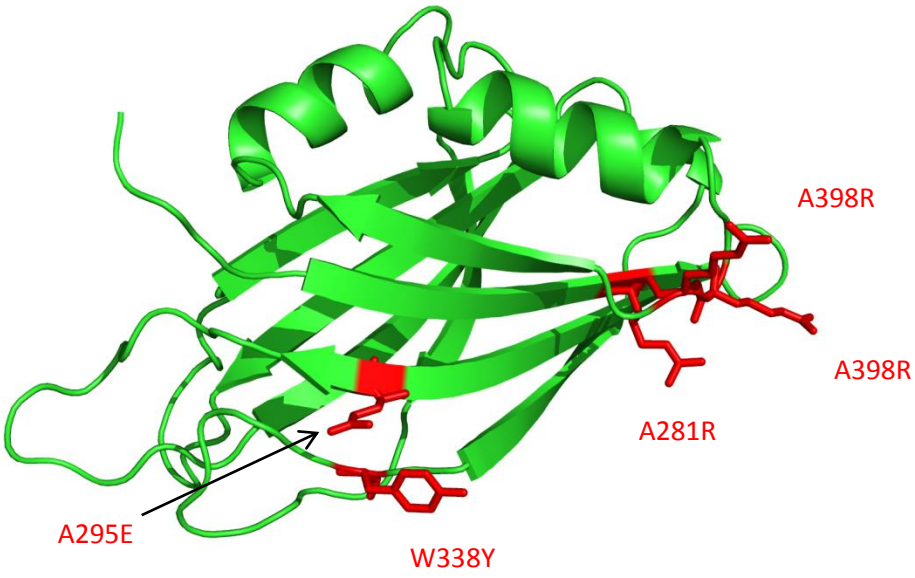

Figure 11: Cartoon illustration of 5ccj_WT; the amino acid residues, which have been mutated back to wild type are coloured red and shown as sticks (A281R, A295E, W338Y, A398R, A399R)

3.5 Membrane Composition

Our goal was to build a membrane that represents the presynaptic plasma membrane, because many studies confirm interaction between Syt-1 and this membrane. (5, 11, 12) A recent study also suggests interaction between the C2AB domains of Syt-1 and the vesicular membrane. (34) Unfortunately, the exact membrane compositions of presynaptic plasma membrane and especially the vesicular membrane are still unknown. (43, 44) (see Chapter 1.3) This is why we decided to generate multiple different membrane types to run MD simulations with. The goal was to find out, if any of the tested membranes stood out in terms of interaction with C2B. The used membrane lipids are described in Chapter 1.3. We used different concentrations of these lipids, especially of the anionic phospholipids. A special focus on cholesterol was also a main interest, because of its importance to membrane fusion. (see Chapter 1.4)

Our collaboration partner at the *Izmir International Biomedicine and Genome Institute (iBG-izmir)* in Turkey, Yongsoo Park, Ph.D. studies the regulation of Syt-1 induced membrane deformation regulated by cholesterol. He asked my supervisor, Ass.-Prof. Mag. Dr. Anna Weinzinger to support his work with some molecular dynamics simulations. In order to execute the simulations according to his specifications, he gave us the exact membrane composition to start with. We called this membrane "*Standard 895*". (see Chapter 3.10.1)

3.6 All-atomistic to coarse-grained

Before we started to generate the different systems, we needed to convert our structures *1tjx_trunc* and *5ccj_WT* from all-atomistic to coarse-grained using a perl-script. For example, the used Gromacs command for the *5ccj_WT* structure was `> perl make-cg-martini.pl 1tjx_trunc.pdb <` .
The coarse-grained membrane lipids have also been received from Dr. Plessl, ensuring a functional system by using already proven and tested lipids and saving the time to parameterise them.

3.7 Membrane Assembling

3.7.1 Membrane Assembling with Protein

The first idea was, in accordance to our unbiased approach, to let the membrane assemble itself in presence of the protein. Membrane assembling only takes a few ns. This allowed us to guarantee random placement of lipids, but in addition also to perform only one simulation in which the lipids assemble and the possible interaction with the protein could take place after that.
For this purpose, we used a perl-script, defined the box size and specified the number of different lipids we wanted in the simulation box. A typical command line for this task was:

> perl add-lipids.pl 20 12 15 5 popc 436 pope 135 pops 90 chol 225 pip2 9 <

In this example, “20” stands for the x- and y-axis size of the box in nm, whereas “12 15” defines the z-axis to be in the range of 12-15 nanometres (nm). The following “5” determines how many different lipid-types should be packed into the system. After that, the lipids are defined by name and number (for example “436 popc” means 436 single popc-lipids are to be used). The perl-script also contains commands to add water and ions to the system and defines the simulation itself by including the .mdp-file.

After the lipids are packed, it is of paramount importance to check the topology file to verify the correct number of lipids. The lipids have different sizes and volumes and if the box size was chosen too small, not all the lipids would fit into the simulation box. This was the first problem we needed to overcome, when the desired number of lipids would not fit exactly into the box, even when we tried multiple different system sizes. We decided to approach the favoured membrane composition as close as possible, but not to persist on exact lipid numbers.

The second, but unfortunately much bigger problem was the interaction of the protein with the membrane during the process of membrane assembling. We found that the protein immediately started to interact with free lipids, before they could assemble in the membrane. This resulted in a delay of membrane assembling. Also, after the membrane was formed, the protein was already bound to it. In some runs, the protein was already stuck in the middle of the membrane much deeper than any other studies believed to be possible. (22) We stopped scripted runs after approximately 6.750ns and decided to go step-by-step to avoid such errors from then on.

3.7.2 Membrane Assembling without Protein

To generate an uninfluenced membrane, we replaced the protein with a dipeptide consisting of Serine and Aspartic acid. This was necessary in order to fulfil the requirements of the script we used. Both are polar amino acids, with Aspartate even being acidic. This ensures that no interaction with the membrane takes place during a simulation and therefore the assembled membrane stays uninfluenced. The process as described in Chapter 3.7.1 remained the same. After finishing the simulation, the position of the dipeptide was reviewed to be as far away from the membrane as possible to rule out unexpected interactions. The membrane information in the resulting .gro-file was used for further simulations. All membranes generated for this diploma thesis have been generated using this method.

The simulations with one membrane and the protein in a box using periodic boundary conditions started promising. The defined time-step of 10fs was computational very time consuming and in some

simulations, the protein did not come into contact with the membrane. Our conclusion was that we had to generate a system that facilitates contact or increases the likelihood of contact, respectively.

3.8 Two-Membrane System

An additional second membrane in the simulation box offered the possibility to "trap" the protein in-between two membranes. The protein would come in close contact with the membrane more often than with just one membrane and if this bumping happens with the protein being orientated in the right direction, we expected to see interaction. The second membrane was generated by simple copy and paste of the data of the .gro-file. Afterwards, the membranes were placed at distance using the *editconf* command. The protein (*1tjx_trunc* or *5ccj_WT*) was then added into the simulation box and placed in-between the two membranes. The distance between the two membranes was of great importance. If too small, the protein would be "caught" by the membranes instantaneously, preventing it from rotating freely and therefore biasing the simulation. If the membranes were placed too far away from each other, the computational effort would rise because of the increasing box size. The first runs looked promising in regard to system setup. The probability of a contact between the protein and the membrane was higher with two membranes, as expected.

We expected interaction mainly with PIP2, which concentrated in clusters in some membranes. If these clusters are in the outer leaflet of the membrane, they are not accessible to the protein. If the membrane holds only nine molecules PIP2, there is a high chance that they are all clustered at the outer leaflet, making them inaccessible. Cholesterol for example is known to flip-flop, which means a position change to the other membrane bilayer leaflet. (48) This quality has not been shown for PIP2 and we could not observe it in our simulations either. This finding reduced some of the benefits of the two-membrane-system and led to a membrane with high PIP2-concentration. (see Chapter 3.10.3)

Nevertheless, the two-membrane-system was our final choice in regard to system setup. All 46.800ns of simulations have been carried out using this setup in a box that averaged a size of 16,27nm x 25,64nm. (see Table 1)

A system including two different membrane types was planned as well. Simply put, this system could show which membrane is favoured by the tested C2B-domain. It turned out, that using our method of setup, this system is technically not feasible, because the box size is determined by the membrane type and different types of membranes therefore result in an unstable simulation box.

3.9 System Setup

Setting up a system was carried out by following standardised workflow. The sequence of the procedure is shown in the following listing:

- The membrane information was retrieved as described in Chapter 3.7.2. At this point, the .gro-file only includes information about the membrane. Water, ions and the dipeptide have been erased.
- The files of two distant membranes of the same composition and the particular protein are reviewed using VMD. If necessary, the membranes and the protein are placed at a distance, where no interactions from the very beginning are expected. This is achieved by using the *editconf* command. Via –translate, the protein is moved on the x-, y- or z-axis (in nm).
  A typical command line would be:

  > editconf -f protein.gro -o protein_translated.gro -translate 0 0 2 <

  After the coordinates are settled, the files are merged into one file.
- The box size is adjusted via text editor and checked for correctness using VMD.
- The system is solvated using the *genbox* command. Van der Waals radii are set and the result is analysed visually. Here is a typical command line:

  > genbox -cp sys.gro -cs wat.pdb -vdwd 0,23 -o sys_solv.gro <

- If the box is not filled equally with water, the Van der Waals radii need to be adjusted. We faced the problem of too much water in the membranes. We decided to cut out the relevant water using PyMol. The correct number of water molecules needs to be updated in the topology file.
- The now solvated system undergoes the first energy minimisation. Technically, this is a short MD simulation. This is why it needs the pre-processor command *grompp*:

  > grompp -f em.mdp -c sys_solv.gro -o sys_solv_em.tpr -p topol.top -maxwarn 8 <

  Afterwards, the actual energy minimisation is carried out:

  > mdrun -s sys_solv_em.tpr -deffnm sys_solv_em -v <

- The *genion* command adds ions to the system by exchanging water molecules with ions. The option "- neutral" adds as many ions as needed, to balance the system to a total zero net charge. This command needs to be pre-processed using grompp and the typical command line looks like this:

  > grompp -f em.mdp -c sys_solv_em.gro -o sys_solv_em_ions.tpr -p topol.top -maxwarn 8 <

  > genion -s sys_solv_ions.tpr -p topol.top -o sys_solv_em_ions.gro -neutral -pname CA <

  After the ions have been added to the system, we ran an energy minimisation as described above.

- Very important for the following evaluation is the index file. (see Chapter 2.3.1.1) This file can be adjusted later in the process and is generated by using this command:

  > make_ndx -f sys_solv_em_ions_em.gro -o index.ndx <

- After these steps, the system is ready for the actual free MD simulation. The details of the simulation itself (runtime, time-per-step) are hold in the .mdp file, which is why it has to be pre-processed again.

  > grompp -f md500ns.mdp -c sys_solv_em_ions_em.gro -p topol.top -n index.ndx -o testrun1.tpr -maxwarn 8 <

  > mdrun -f testrun1.tpr -deffnm testrun1 -v <

The resulting files are ready to be reviewed with VMD or alternative software. The following evaluation is discussed in Chapter 3.12.

3.10 Seven Different Systems (membrane compositions)

We started with the Standard 895, for which we received the composition from our collaboration partner (see Chapter 3.5). One of the main tasks of this diploma thesis was to investigate the role of cholesterol, for which we generated a membrane without any cholesterol to compare to. The other membrane types are validation or cross-check decisions. When our simulations showed that the concentration of PIP2 is of major importance, the logical decision was to create a membrane with a high concentration of PIP2 and a membrane without any PIP2 at all. With regard to our focus on cholesterol, we generated a membrane without cholesterol, but with high PIP2 as well: "*NCHP*". Two more membranes (*High PIP2 Low Ca^{2+}* and *No Chol Low Ca^{2+}*) have been created in view of the Ca^{2+}-concentration, which is discussed in Chapter 3.11.

Many more membrane compositions and system variations looked interesting, but we decided to limit our simulations to the following seven systems (also see Table 2):

3.10.1 Standard 895

This system is composed – as every other system – of two membranes, each containing the following lipids: 436 POPC, 135 POPE, 90 POPS, 225 CHOL and 9 PIP2.

It is named *Standard 895*, because of the 895 lipids in each membrane. Because of the low concentration of PIP2, interactions with Syt-1 are very unlikely. PIP2 tends to cluster and if this clustering happened to be on the outer layer of the membrane, it was just not accessible for Syt-1. This reduced the probability of protein-membrane interaction.

We performed eight runs with both proteins using this system. (see Table 3) With *1tjx_trunc,* this is the only system, in which we performed MD simulations with a time-step of 12 fs. The number of

steps remained at 50 million, which resulted in a total run-time of 600ns, different to the 500ns in every other system.

3.10.2 No PIP2

The difference to the standard-membrane is that there is no PIP2 in this membrane. The PIP2 was replaced by POPC, which requires less space. To keep the box size approximately the same, we used exactly 900 lipids per membrane:

452 POPC, 135 POPE, 90 POPS, 225 CHOL

As we did not expect many interactions due to the absence of highly reactive PIP2, we performed five runs each.

3.10.3 High PIP2

As many test-runs confirmed, we found that most interactions between Syt-1 and the membrane happened with PIP2, so we came up with a system with an increased PIP2 concentration. The simulations with the Standard 895 membrane showed us, that a concentration of only 1% PIP2 results in a longer running idle, before the protein finds a PIP2 molecule. The new membrane has an elevated PIP2-concentration of 5%.

405 POPC, 135 POPE, 90 POPS, 225 CHOL, 45 PIP2

Eight runs have been carried out with each protein using this system configuration.

3.10.4 High PIP2 Low Ca^{2+}

Due to the finding that high Ca^{2+}- concentration saturates the negatively charged membrane lipids and therefore prohibits interactions with Syt-1, we created some kind of super-reactive system. (see Chapter 3.10) First, we placed a Ca^{2+}-ion into its binding pocket to ensure the correct confirmation of Syt-1. This remained to be the only Ca^{2+}-ion in the system, because we balanced the systems net charge to a neutral equilibrium with K^{+}-ions instead. We also used the already known “high PIP2 membrane” to ensure best external preconditions for interaction and performed six runs each.

405 POPC, 135 POPE, 90 POPS, 225 CHOL, 45 PIP2

3.10.5 No Chol

As already discussed, cholesterol is believed to play a major role in the ability of membranes to bend and therefore their likelihood to facilitate membrane fusion (see Chapter 1.4). This is why we decided to create a cholesterol-free system and compare its protein interaction to the usual cholesterol-rich membranes.

For the first system without cholesterol, the amount of PIP2, POPE and POPS stayed the same as in the 895 Standard membranes. The cholesterol-part was replaced by POPC, which resulted in a membrane of 899 lipids:

665 POPC, 135 POPE, 90 POPS, 9 PIP2

This system was simulated in five runs with each protein.

3.10.6 No Chol Low Ca^{2+}

In this system we used the NoChol-membrane, but did not alter the Ca^{2+}-concentration to a higher level. We used Ca^{2+}-ions to settle the charge of the negatively charged membrane lipids, so the system had a total zero net charge. We still had only 9 PIP2, but with this system we achieved direct comparison concerning Ca^{2+} levels.

665 POPC, 135 POPE, 90 POPS, 9 PIP2

As Ca^{2+}- concentration being the only difference to the *No Chol* system, we decided to perform six runs with each protein.

3.10.7 NCHP

NCHP stands for "no cholesterol high PIP2". We felt it would be a good addition to create a system in which we increased the probability of interaction by adding more PIP2 and also focused on the aspect of missing cholesterol. A total of sixteen runs (eight runs each with *1tjx_trunc* and *5ccj_WT*) were performed.

626 POPC, 135 POPE, 90 POPS, 45 PIP2

Standard 895	No PIP2	High PIP2	High PIP2 Low Ca	No Chol	No Chol Low Ca	NCHP
436 POPC	450 POPC	405 POPC	405 POPC	665 POPC	665 POPC	626 POPC
135 POPE	135 POPE	135 POPE	135 POPE	135 POPE	135 POPE	135 POPE
90 POPS	90 POPS	90 POPS	90 POPS	90 POPS	90 POPS	90 POPS
225 CHOL	225 CHOL	225 CHOL	225 CHOL			
9 PIP2		45 PIP2	45 PIP2	9 PIP2	9 PIP2	45 PIP2

Table 2: Overview of the seven systems membrane compositions

Reruns	Standard 895	No PIP2	High PIP2	High PIP2 Low Ca	No Chol	No Chol Low Ca	NCHP
1tjx_trunc	8	5	8	6	5	6	8
5ccj_WT	8	5	8	6	5	6	8

Table 3: Reruns; every rerun has a total runtime of 500ns (only 1tjx_trunc with Standard 895 has reruns with a total runtime of 600ns each)

3.11 Ca^{2+}- concentration

Syt-1 is a known Ca^{2+}-sensor, because it takes action only after binding to Ca^{2+}. Therefore, the Ca^{2+}-concentration in the simulated system is of major importance.

In previous studies, two different approaches have been made to ensure binding of Ca^{2+} to the C2AB domains. Either, Ca^{2+} is placed directly into the binding pocket before the simulation starts, or the Ca^{2+}-concentration in the simulated system is altered to a level, where the likelihood of binding is very high. (21, 22) We decided to go with the latter case in order to stay unbiased, except for *High PIP2 Low CA.*

The Ca^{2+}-concentrations as seen in Tables 4 and 5 are above physiological level to ensure binding to the C2B-domain of Syt-1. To verify the bound state of the protein, we checked the minimum distance between Ca^{2+} and the five Aspartic acids (D303, D309, D363, D365, D371) in the binding pocket of *1tjx_trunc* and *5ccj_WT*. (see Chapter 3.12.4.1; see Supplements Chapter 6.4 – 6.17)

Unfortunately, PIP2, as a negatively charged membrane lipid, can also interact with Ca^{2+}. High Ca^{2+} concentrations may lead to saturation of the membrane and the reactive membrane lipids, respectively. Figures 12 and 13 show screenshots of membranes with Ca^{2+}- ions located around the membrane in higher concentration. This saturation of membrane lipids could cause a lower reactivity concerning the protein, which would lead to less interaction results. We took this into account by generating two systems with low Ca^{2+}-concentration. In the *No Chol Low Ca* system, the addition of Ca^{2+}- ions is limited to a total zero net charge of the whole system. That means that only as much Ca^{2+} was added, as was needed to balance the negatively charged membrane lipids. In the *High PIP2 Low Ca* system, we decided to place one Ca^{2+}- ion into the binding pocket of the protein. Interestingly, a system with only one Ca^{2+}- ion results in a concentration, which meets the physiological extracellular Ca^{2+}- concentration. With currently available computing capacities, it is not constructive to set the system to the physiological concentration and wait for the only existing Ca^{2+}- ion to find the binding pocket of the C2B-domain.

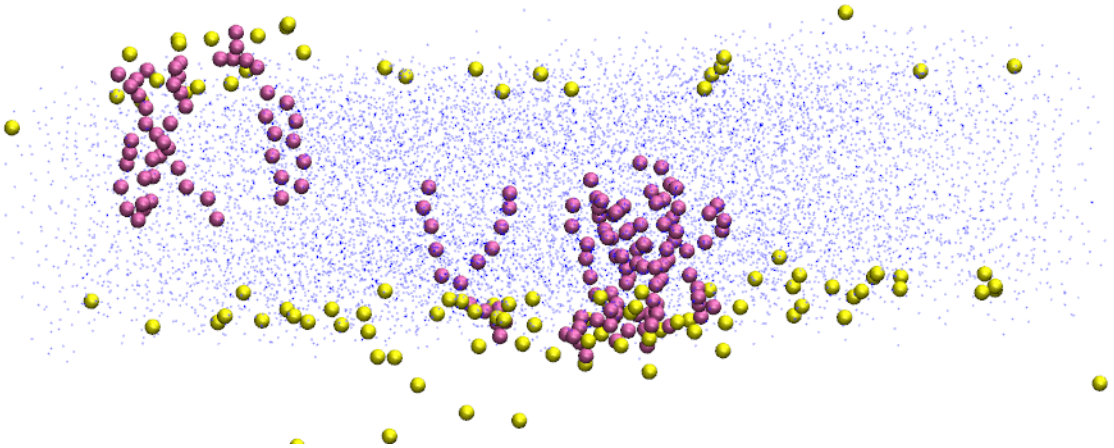

Figure 12: Membrane pictured with blue dots; PIP2 pictured with purple spheres; Ca^{2+}- ions pictured with yellow spheres; a local rise of Ca^{2+}-concentration near PIP2 can be observed

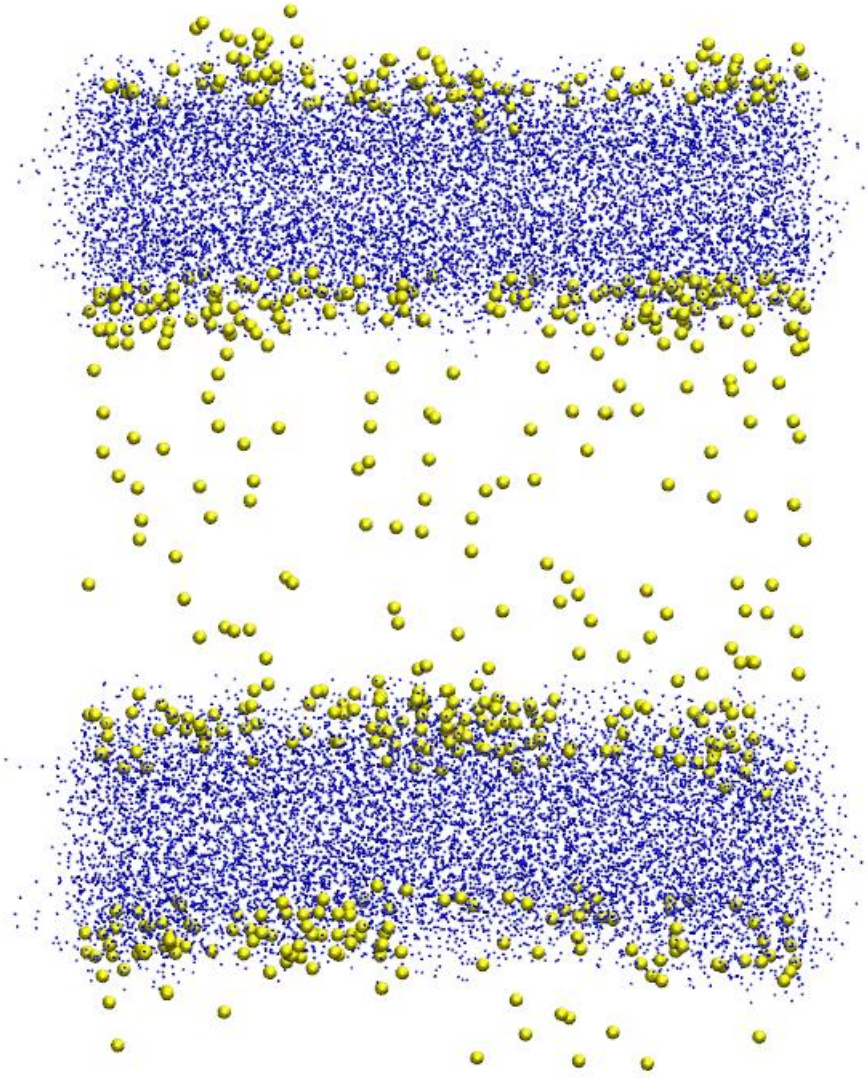

Figure 13: Two membranes pictured with blue dots; Ca^{2+}- ions pictured with yellow spheres; whereas PIP2 is not highlighted in this figure, a local rise of Ca^{2+}-ions near the membrane can be observed

1tjx_trunc	Standard 895	No PIP2	High PIP2	High PIP2 Low Ca	No Chol	No Chol Low Ca	NCHP
H_2O Molecules	22.447	24.611	28.356	24.909	28.588	28.719	32.183
Ca2+ Ions	265	175	625	1	265	133	625
Ca2+ Concentration	0,655 mol/l	0,395 mol/l	1,223 mol/l	0,002 mol/l	0,515 mol/l	0,257 mol/l	1,078 mol/l

Table 4: Concentration of Ca^{2+}- ions in the seven different membrane systems with 1tjx_trunc; the number of H_2O-molecules and the number of Ca^{2+}- ions is shown in the first two lines; the system "No Chol Low Ca" has a total zero net charge, resulting in a low number of Ca^{2+}- ions; the system "High PIP2 Low Ca" has only 1 Ca^{2+}- ion, which was placed in the binding pocket. This system was balanced to total zero net charge with K^{+}- ions.

5ccj_WT	Standard 895	No PIP2	High PIP2	High PIP2 Low Ca	No Chol	No Chol Low Ca	NCHP
H_2O Molecules	22.931	23.279	23.424	23.542	26.569	31.863	25.142
Ca2+ Ions	263	173	623	1	263	132	623
Ca2+ Concentration	0,637 mol/l	0,413 mol/l	1,476 mol/l	0,002 mol/l	0,549 mol/l	0,229 mol/l	1,375 mol/l

Table 5: Concentration of Ca^{2+}- ions in the seven different membrane systems with 5ccj_WT; the number of H_2O-molecules and the number of Ca^{2+}- ions is shown in the first two lines; the system "No Chol Low Ca" has a total zero net charge, resulting in a low number of Ca^{2+}- ions; the system "High PIP2 Low Ca" has only 1 Ca^{2+}- ion, which was placed in the binding pocket. This system was balanced to total zero net charge with K^{+}- ions.

3.12 Evaluation

3.12.1 Likelihood of Interaction

Our main interest was to observe interactions between the membranes and the protein. The first and most important question for evaluation was: is there any interaction at all? An interaction was defined as close contact to the membrane that lasts longer than 100ns. This condition was set in order to ignore simple bounce-offs, where the protein got into contact with the membrane without establishing a real interaction. Every run was analysed visually and, in case of an interaction, verified with the *g_mindist* command. (see Chapter 2.3.1.2) If a run had one or more interactions, that fulfilled the definition, our focus was on the part of the protein that interacted with the membrane. (see Chapter 3.12.3) We evaluated the runs of the seven final systems, making it a total of 46.800ns.

3.12.2 Visual analysis

Visual analysis was performed using VMD (see Chapter 2.3.6). Looking at the trajectory of a complete run gives a very good first impression of what the protein does and if there are any interactions with the membrane.

We checked the binding pocket for Ca^{2+} at multiple points of every run, finding that the C2B-domains were in a bound state most of the time. According to recent literature, we expected to find two or three Ca^{2+}- ions bound in or at the binding pocket. (11, 12, 22) Visual analysis only shows one Ca^{2+}- ion bound, which could be a result of using a coarse-grained model. All runs with high Ca^{2+}-concentration show the C2B-domain in a Ca^{2+}-bound state throughout the entire simulation. (For detailed information see Chapter 3.12.4.1). In the *High PIP2 Low Ca* system, the placed Ca^{2+}- ion exits the pocket in all six runs with *1tjx_trunc*. The time of detachment varies within the first 120ns of simulation time. With *5ccj_WT*, the ion exits the pocket in four out of six runs, but stays inside the pocket at all times in rerun 1 and rerun 4. (see Chapter 3.12.4.1)

The visual analysis with respect to the interaction of protein and membrane shows multiple contacts in each rerun. The self-imposed definition of an interaction is to last for a minimum of 100ns. Taking this into consideration, a different picture appears. (see Table 6)

The *Standard 895* membrane shows only one interaction in eight reruns with *1ttjx_trunc* and also one interaction in eight reruns with *5ccj_WT*. As expected, due to the absence of PIP2, no interaction is found with the *No PIP2* membrane. The *High PIP2* membrane contains 5% PIP2, instead of 1% in the *Standard 895*. For this reason, we expected to see more interactions with the protein. Visual analysis shows two runs with interactions with *1tjx_trunc* and one run with *5ccj_WT* in the *High PIP2* system with high Ca^{2+}-concentration. Also, multiple runs have short interactions of about 20ns, which do not fulfil the conditions.

In the *High PIP2 Low CA* system, we set a low Ca^{2+}-concentration, but the same membrane is used as in the *High PIP2* system, making it an interesting comparison. Visual analysis reveals that every single run has an interaction. In most runs the interaction lasts all 500ns and in every run the interaction is still stable at the end of the simulation. The *No Chol* system shows only one interaction in five reruns with *1tjx_trunc* and none with *5ccj_WT*. The same membrane with lower Ca^{2+}-concentration is used in the system *No Chol Low CA*. In six reruns, we found five interactions with *1tjx_trunc*. Those do not proof to be as stable as the interactions in the *High PIP2 Low CA* system, as three out of five dissolve before the simulation is over. With *5ccj_WT* in the same system, the interactions are even shorter, falling below 100ns and therefore dropping out of the interaction picture. Being a matter of definition, we report that we found four contacts, which last about 30ns. The *NCHP* membrane shows two interactions with *1tjx_trunc*. Both last about 100ns and dissolve before the end of the simulation. With *5ccj_WT*, only one contact of about 60ns was found.

	Standard 895	**No PIP2**	**High PIP2**	**High PIP2 Low CA**	**No Chol**	**No Chol Low CA**	**NCHP**
1tjx_trunc – Run 1	Run 1	Run 1	Run 1d	Run 1	Run 1	Run 1	Run 1
1tjx_trunc – Run 2	Run 2	Run 5	Run 2	Run 2	Run 3	Run 2	Run 2
1tjx_trunc – Run 3	Run 3	Run 6	Run 3	Run 3	Run 4	Run 3	Run 3
1tjx_trunc – Run 4	Run 4	Run 7	Run 4	Run 4	Run 7	Run 4	Run 4a
1tjx_trunc – Run 5	Run 5	Runsc 1	Run 5	Run 5	Run 8	Run 5	Run 5
1tjx_trunc – Run 6	Runsc 1		Run 6	Run 6		Run 6	Run 6
1tjx_trunc – Run 7	Runsc 2		Run 7				Run 7
1tjx_trunc – Run 8	Runsc 3		Run 8				Run 8
5ccj_WT – Run 1	Run 1	Run 1	Run 1	Run 1	Run 1	Run 1	Run 1
5ccj_WT – Run 2	Run 2	Run 2	Run 2	Run 2	Run 7	Run 2	Run 2
5ccj_WT – Run 3	Run 3	Run 3	Run 3	Run 3	Run 8	Run 3	Run 3
5ccj_WT – Run 4	Run 4	Run 5	Run 5	Run 4	Runsc 1	Run 4	Run 4
5ccj_WT – Run 5	Run 5	Run 8	Run 6	Run 5	Runsc 2	Run 5	Run 5
5ccj_WT – Run 6	Run 6		Run 7	Run 6		Run 6	Run 6
5ccj_WT – Run 7	Run 7		Run 8				Run 7
5ccj_WT – Run 8	Run 8		Run 9				Run 8

Table 6: Listing of every performed run with regard to protein-membrane interaction; red coloured runs do not show any interactions between membrane and protein; orange coloured runs show contact, but the length of the interaction is not long enough to comply with the definition of an interaction to last at least 100ns; green coloured runs show at least one membrane-protein interaction that lasts longer than 100ns

3.12.3 Groups

To correctly assess the interaction sites of the protein with the membrane seen in the trajectories, the two proteins were divided into groups. After studying the surface of the proteins we decided to apportion every single amino acid to a total of eight different groups *(see Table 7 and Figure 14).*

Allocation has been carried out on a visual basis, using PyMol. We examined the surface of both proteins and distributed every single amino acid to a group. This is why the amino acid portfolio of the groups of *1tjx_trunc* and *5ccj_WT* do not exactly match each other.

The group "Loops" contains the binding pocket of the C2B-domain and therefore the amino acids D303, D309, D363, D365 and D371, which are essential for Ca^{2+}-binding. (11) The "Linker" group represents the N-terminus and is longer by seven amino acids in *1tjx_trunc*. This allows the linker to move more freely.

Given that we truncated the *1tjx* protein, the "Lateral2" group is longer by 3 amino acids (VKK) in *5ccj_WT*. The remaining groups are mostly identical with small discrepancies, since the apportionment was based on visual findings. The group "ARG" contains the two essential arginine amino acids (R398 and R399). The polybasic lysine stretch (K324, K325, K326, K327) is found in the group "lysinestretch", which also holds K313 and K321.

	1tjx_trunc			5ccj_WT	
1	Ser263	Linker			
2	Gly264	Linker			
3	Gly265	Linker			
4	Gly266	Linker			
5	Gly267	Linker			
6	Gly268	Linker			
7	Ile269	Linker			
8	Leu270	Linker	1	Ser270	Linker
9	Glu271	Linker	2	Glu271	Linker
10	Lys272	Linker	3	Lys272	Linker
11	Leu273	Linker	4	Leu273	Linker
12	Gly274	Linker	5	Gly274	Linker
13	Asp275	Linker	6	Asp275	Linker
14	Ile276	Rest	7	Ile276	Rest
15	Cys277	Rest	8	Cys277	Rest
16	Phe278	Rest	9	Phe278	Rest
17	Ser279	lateral1	10	Ser279	lateral1
18	Leu280	lateral1	11	Leu280	lateral1
19	Arg281	lateral1	12	Arg281	lateral1
20	Tyr282	Rest	13	Tyr282	Rest
21	Val283	oppARG	14	Val283	oppARG
22	Pro284	oppARG	15	Pro284	oppARG
23	Thr285	oppARG	16	Thr285	oppARG
24	Ala286	oppARG	17	Ala286	oppARG

25	Gly287	oppARG	18	Gly287	oppARG
26	Lys288	oppARG	19	Lys288	oppARG
27	Leu289	Rest	20	Leu289	Rest
28	Thr290	Rest	21	Thr290	Rest
29	Val291	Rest	22	Val291	Rest
30	Val292	Rest	23	Val292	Rest
31	Ile293	Rest	24	Tle293	Rest
32	Leu294	Rest	25	Leu294	Rest
33	Glu295	Rest	26	Glu295	Rest
34	Ala296	Rest	27	Ala296	Rest
35	Lys297	Rest	28	Lys297	Rest
36	Asn298	Rest	29	Asn298	Rest
37	Leu299	Rest	30	Leu299	Rest
38	Lys300	Loops	31	Lys300	Loops
39	Lys301	Loops	32	Lys301	Loops
40	Met302	Loops	33	Met302	Loops
41	Asp303	Loops	34	Asp303	Loops
42	Val304	Loops	35	Val304	Loops
43	Gly305	Loops	36	Gly305	Loops
44	Gly306	Loops	37	Gly306	Loops
45	Leu307	Loops	38	Leu307	Loops
46	Ser308	Loops	39	Ser308	Loops
47	Asp309	Loops	40	Asp309	Loops
48	Pro310	Rest	41	Pro310	Rest
49	Tyr311	Rest	42	Tyr311	Rest
50	Val312	Rest	43	Val312	Rest
51	Lys313	lysinestretch	44	Lys313	lysinestretch
52	Ile314	lysinestretch	45	Ile314	lysinestretch
53	His315	lysinestretch	46	His315	lysinestretch
54	Leu316	lysinestretch	47	Leu316	lysinestretch
55	Met317	lysinestretch	48	Met317	lysinestretch
56	Gln318	lysinestretch	49	Gln318	lysinestretch
57	Asn319	lysinestretch	50	Asn319	lysinestretch
58	Gly320	lysinestretch	51	Gly320	lysinestretch
59	Lys321	lysinestretch	52	Lys321	lysinestretch
60	Arg322	lysinestretch	53	Arg322	lysinestretch
61	Leu323	lysinestretch	54	Leu323	lysinestretch
62	Lys324	lysinestretch	55	Lys324	lysinestretch
63	Lys325	lysinestretch	56	Lys325	lysinestretch
64	Lys326	lysinestretch	57	Lys326	lysinestretch
65	Lys327	lysinestretch	58	Lys327	lysinestretch
66	Thr328	Rest	59	Thr328	lysinestretch
67	Thr329	Rest	60	Thr329	lysinestretch
68	Ile330	Rest	61	Ile330	lysinestretch
69	Lys331	Loops	62	Lys331	Loops
70	Lys332	Loops	63	Lys332	Loops
71	Asn333	Loops	64	Asn333	Loops
72	Thr334	Loops	65	Thr334	Loops
73	Leu335	Loops	66	Leu335	Loops
74	Asn336	Loops	67	Asn336	Loops
75	Pro337	Loops	68	Pro337	Loops
76	Tyr338	lateral1	69	Tyr338	lateral1
77	Tyr339	lateral1	70	Tyr339	lateral1
78	Asn340	lateral1	71	Asn340	lateral1

79	Glu341	lateral1	72	Glu341	lateral1
80	Ser342	lateral1	73	Ser342	lateral1
81	Phe343	Rest	74	Phe343	lateral1
82	Ser344	oppARG	75	Ser344	lateral1
83	Phe345	oppARG	76	Phe345	lateral1
84	Glu346	oppARG	77	Glu346	oppARG
85	Val347	oppARG	78	Val347	oppARG
86	Pro348	oppARG	79	Pro348	oppARG
87	Phe349	oppARG	80	Phe349	oppARG
88	Glu350	oppARG	81	Glu350	oppARG
89	Gln351	oppARG	82	Gln351	oppARG
90	Ile352	oppARG	83	Ile352	oppARG
91	Gln353	oppARG	84	Gln353	oppARG
92	Lys354	oppARG	85	Lys354	oppARG
93	Val355	Rest	86	Val355	Rest
94	Gln356	Rest	87	Gln356	Rest
95	Val357	Rest	88	Val357	Rest
96	Val358	Rest	89	Val358	Rest
97	Val359	Rest	90	Val359	Rest
98	Thr360	Rest	91	Thr360	Rest
99	Val361	Rest	92	Val361	Rest
100	Leu362	Rest	93	Leu362	Rest
101	Asp363	Loops	94	Asp363	Loops
102	Tyr364	Loops	95	Tyr364	Loops
103	Asp365	Loops	96	Asp365	Loops
104	Lys366	Loops	97	Lys366	Loops
105	Ile367	Loops	98	Ile367	Loops
106	Gly368	Loops	99	Gly368	Loops
107	Lys369	Loops	100	Lys369	Loops
108	Asn370	Loops	101	Asn370	Loops
109	Asp371	Loops	102	Asp371	Loops
110	Ala372	Rest	103	Ala372	Loops
111	Ile373	Rest	104	Ile373	Rest
112	Gly374	Rest	105	Gly374	Rest
113	Lys375	Rest	106	Lys375	Rest
114	Val376	Rest	107	Val376	Rest
115	Phe377	lateral2	108	Phe377	Rest
116	Val378	lateral2	109	Val378	lateral2
117	Gly379	lateral2	110	Gly379	lateral2
118	Tyr380	lateral2	111	Tyr380	lateral2
119	Asn381	lateral2	112	Asn381	lateral2
120	Ser382	lateral2	113	Ser382	lateral2
121	Thr383	lateral2	114	Thr383	ARG
122	Gly384	lateral2	115	Gly384	ARG
123	Ala385	Rest	116	Ala385	ARG
124	Glu386	Rest	117	Glu386	ARG
125	Leu387	Rest	118	Leu387	ARG
126	Arg388	ARG	119	Arg388	ARG
127	His389	ARG	120	His389	ARG
128	Trp390	ARG	121	Trp390	ARG
129	Ser391	ARG	122	Ser391	ARG
130	Asp392	ARG	123	Asp392	ARG
131	Met393	ARG	124	Met393	ARG
132	Leu394	ARG	125	Leu394	ARG

133	Ala395	ARG	126	Ala395	ARG
134	Asn396	ARG	127	Asn396	ARG
135	Pro397	ARG	128	Pro397	ARG
136	Arg398	ARG	129	Arg398	ARG
137	Arg399	ARG	130	Arg399	ARG
138	Pro400	Rest	131	Pro400	ARG
139	Ile401	Rest	132	Ile401	Rest
140	Ala402	Rest	133	Ala402	Rest
141	Gln403	Rest	134	Gln403	Rest
142	Trp404	Rest	135	Trp404	Rest
143	His405	Rest	136	His405	Rest
144	Thr406	Rest	137	Thr406	Rest
145	Leu407	Rest	138	Leu407	Rest
146	Gln408	Rest	139	Gln408	lateral2
147	Val409	Rest	140	Val409	lateral2
148	Glu410	lateral2	141	Glu410	lateral2
149	Glu411	lateral2	142	Glu411	lateral2
150	Glu412	lateral2	143	Glu412	lateral2
151	Val413	lateral2	144	Val413	lateral2
152	Asp414	lateral2	145	Asp414	lateral2
153	Ala415	lateral2	146	Ala415	lateral2
154	Met416	lateral2	147	Met416	lateral2
155	Leu417	lateral2	148	Leu417	lateral2
156	Ala418	lateral2	149	Ala418	lateral2
			150	Val419	lateral2
			151	Lys420	lateral2
			152	Lys421	lateral2

*Table 7: Comparison of amino acid group allocation in 1tjx_trunc and 5ccj_WT; Groups and colouring: Pink: **Linker**, Light Green: **Lateral 1**, Green: **Lateral 2**, Blue: **ARG**, Cyan: **oppARG**, Purple: **Lysinestretch**, Red: **Loops** and Grey: **Rest***

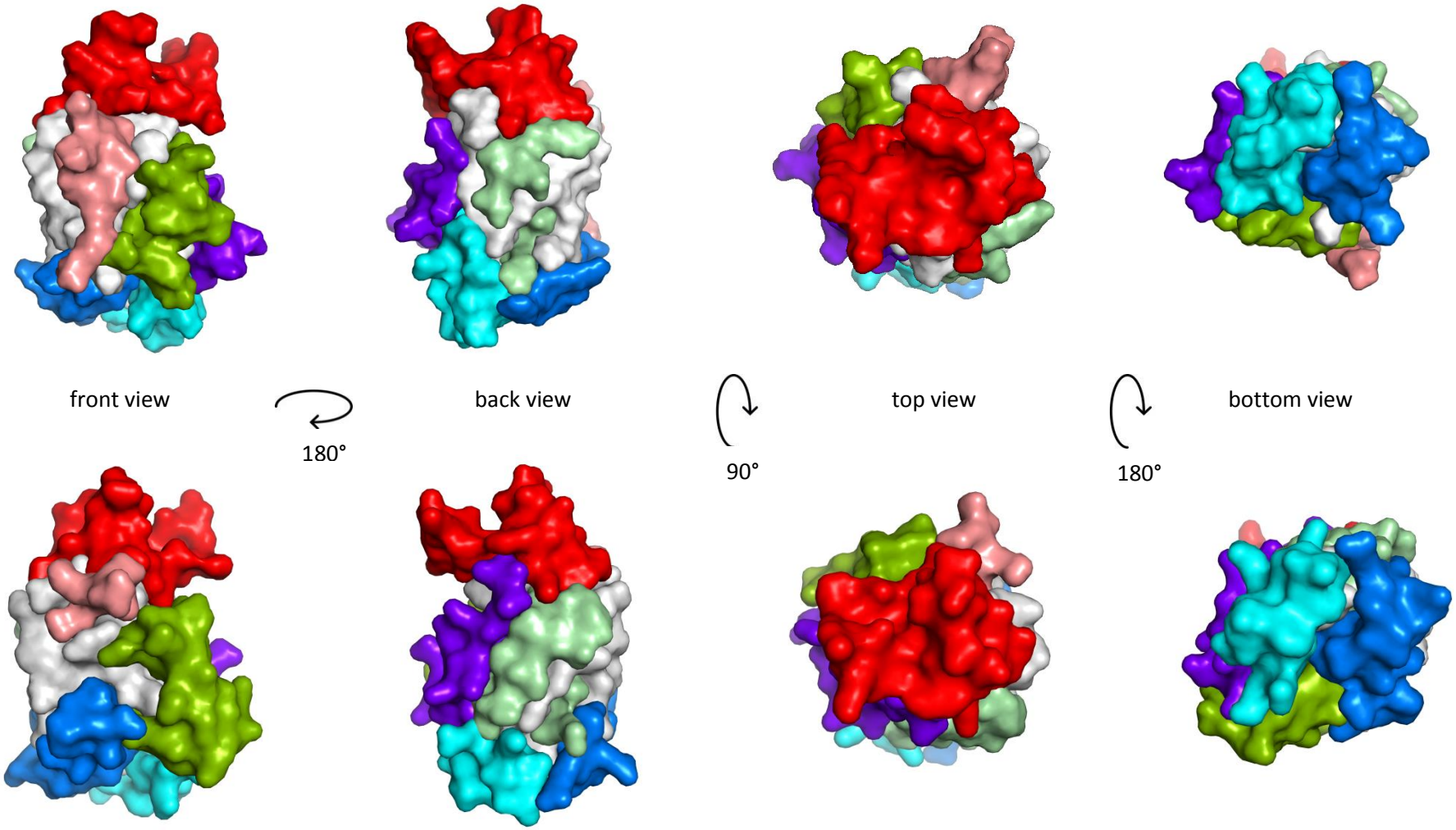

Figure 14: C2B-domain of Synaptotagmin 1 (1tjx_trunc in the top row and 5ccj_WT in the bottom row) divided into different groups and depicted in different views for analysis purposes; Groups by colour: ***Red:*** *Loops;* ***Pink:*** *Linker (the elongated linker of 1tjx_trunc is well shown in the back view);* ***Purple:*** *Lysinestretch;* ***Blue:*** *ARG;* ***Cyan:*** *oppARG;* ***Light Green:*** *Lateral1;* ***Green:*** *Lateral2;* ***White:*** *Rest*

3.12.4 Distance Evaluations

To verify the findings of the visual analysis, we performed multiple distance measurements using the *g_mindist* command. The first goal was to determine the distance between Ca^{2+} and the five aspartic amino acids in the binding pocket of the C2B-domain. We defined, that if the distance is held to a maximum of four Ångstrom, the domain can be considered to be in a bound state, which is the requirement for membrane insertion of the loops. (26)

The second goal was to determine the exact binding situation, as this cannot be sufficiently achieved by visual analysis. The assumption was that the closest group to the membrane is also the interacting group.

3.12.4.1 Ca^{2+} - Aspartic acids of the binding pocket

To perform this evaluation, we created an index group that includes only the five aspartic amino acids of the binding pocket (D303, D309, D363, D365, D371). We ran this index group against all Ca^{2+}- ions in the system using the *g_mindist* command. (see Supplements Chapter 6.4 – 6.17)

Except *High PIP2 Low CA,* the high Ca^{2+}-concentration leads to a bound state in every simulation system. In these systems, the distance never exceeds four Ångstrom, with *No Chol Low CA* being the system with the highest mean distance between Ca^{2+} and the five aspartic amino acids. Although the Ca^{2+}-concentration was set at a lower level in *No Chol Low CA*, the C2B-domain can be considered to be in a bound state at all times.

In *High PIP2 Low CA,* only one Ca^{2+}- ion was placed in the binding pocket at the start of the simulations. This ion exits the pocket in all six runs with *1tjx_trunc*. Whereas it vacates the pocket after only a few ns in rerun 3, it takes a maximum of 120ns in rerun 2 to detach. The same system with *5ccj_WT* shows a similar picture in the reruns 2, 3, 5 and 6. The ion exits the pocket after a minimum of 50ns and a maximum of 130ns, respectively. In the reruns 1 and 4 however, the Ca^{2+} stays bound to the pocket at all times of the simulation.

3.12.4.2 Groups – Membrane Lipids

Every run that shows interaction between protein and membrane was checked using the *g_mindist* command to identify the involved groups. Also, a total of ten runs with interactions shorter than the defined 100ns were evaluated. (see Table 6) The graphs are shown in Chapter 6.18 – 6.36 (*1tjx_trunc*) and 6.37 – 6.52 (*5ccj_WT*).

For *1tjx_trunc*, interactions are presented subsequently:

- 1tjx_trunc / Standard 895 Runsc2: the interacting groups are *ARG* and *oppARG*. These groups are located on the opposing end of the Ca^{2+}-binding pockets. (see Figure 14) The interaction

starts at approximately 250ns and lasts for a total of 350ns until the end of the simulation. (see Chapter 6.18)

- 1tjx_trunc / High PIP2 Run3: the graph shows minimal distance with the group *Lysinestretch*. The protein rotates slightly during interaction and it is assumed that *Lateral2* is also involved. The interaction lasts for about 230ns, with only 80ns of definitive binding to the *Lysinestretch* group. Visual analysis shows PIP2 is involved. (see Chapter 6.19)
- 1tjx_trunc / High PIP2 Run4: the interaction is too short to meet the definition, but there is definite contact with the *Loops* for about 70ns. (see Chapter 6.20)
- 1tjx_trunc / High PIP2 Run5: in this run an insertion to the membrane was detected. Interestingly, the interaction takes place with *Linker*, *ARG*, *Lateral2* and *Rest*, which can be summarized to be located at the opposite end of the domain compared to the loops. Insertion starts at about 130ns into the run and is stable for 370ns until the end of the run. (see Chapter 6.21)
- 1tjx_trunc / High PIP2 Low Ca Run1: the first run of the so called super-reactive system meets the expectation as it shows insertion and a strong interaction, lasting for nearly 500ns, which is the whole runtime. The graph shows a flat line for *Lysinestretch*, *oppARG* and *Rest*, with *Lateral2* being also involved. A constant minimal distance in multiple groups confirms the visual analysis finding of membrane insertion taking place. Interestingly, Ca^{2+} exits the pocket after about 40ns runtime, which does not affect the interaction. Every run in the High PIP2 Low Ca system shows involvement of PIP2. (see Chapter 6.22)
- 1tjx_trunc / High PIP2 Low Ca Run2: the result is similar to run 1, whereas interaction starts only after 230ns. In this run, Ca^{2+} vacates the pocket after 120ns, which is also before interaction takes place. Involved are the groups *Linker, Lysinestretch, Lateral2, oppARG* and *Rest*. (see Chapter 6.23)
- 1tjx_trunc / High PIP2 Low Ca Run3: this run also shows an interaction that lasts until the end of the simulation time. Other than in the previous runs, interaction starts at 40ns with *Lateral1* and *ARG*. After 90ns, *oppARG* and *Rest* also show a constant minimum distance of approximately 4nm. With 110ns into the run, the graph shows a flat line for the group *Lysinestretch* as well. This corresponds to the slow insertion into the membrane, seen in visual analysis. During the entire run the protein has an empty pocket, as Ca^{2+} exits it at the very beginning. (see Chapter 6.24)
- 1tjx_trunc / High PIP2 Low Ca Run4: The graph shows a constant minimum distance for the *Lysinestretch* in this run, with *Loops* and *Rest* also involved. Being the first run in which the *Loops* group is also part of the interaction, it is important to say that the protein is not inserting

into the membrane loops-first. The centre of interaction to PIP2 is located between *Lysinestretch* and *Loops*, which is not the expected orientation for membrane insertion of the loops. A Ca^{2+}-ion can be found in the pocket until 110ns simulation time. (see Chapter 6.25)

- 1tjx_trunc / High PIP2 Low Ca Run5: run 5 shows a slight insertion of the protein. The graph shows flat lines for *Lateral1, Lysinestretch, ARG, oppARG* and *Rest*, whereas *ARG* seems to be the first group to interact with PIP2, starting at 70ns. The interaction is stable until the end of the run and Ca^{2+} leaving the binding pocket at 110ns does not affect insertion. (see Chapter 6.26)
- 1tjx_trunc / High PIP2 Low Ca Run6: the final run of this system shows interaction start at 40ns, which is approximately the time that Ca^{2+} vacates the binding pocket. Constant minimum distance is found for *Linker, Loops* and *Rest*, which is a new combination of groups, indication another centre of interaction. Still, no loops-first insertion can be found. (see Chapter 6.27)
- 1tjx_trunc / No Chol Run4: this is the only run in the *NoChol* system that shows an interaction. It starts at 340ns and is stable until the end. *Linker, Lateral2* and *Rest* are involved, in which *Linker* starts and *Rest* is getting close only at 400ns. Visual analysis shows that PIP2 interacts with the flexible linker region of C2B, most likely with SER263 being the primarily responsible amino acid residue. (see Chapter 6.28)
- 1tjx_trunc / No Chol Low Ca Run1: this system has, in comparison with the other systems, a low Ca^{2+}-concentration. The *Loops* group is the only group in this run that gets really close, whereas the orientation is again not right for the expected loops-first membrane insertion which has been shown in a recent study. (22) Contact stays superficial and lasts for approximately 180ns, starting with 300ns into the run. (see Chapter 6.29)
- 1tjx_trunc / No Chol Low Ca Run2: the C2B-domain inserts into the membrane a little, with *ARG, oppARG, Rest, Lateral2* and *Linker* involved. Whereas the graph shows flat lines for *ARG* and *oppARG* from 70ns on till the end, *Lateral2, Rest* and especially *Linker* slightly depart from the membrane after 250ns. (see Chapter 6.30)
- 1tjx_trunc / No Chol Low Ca Run4: accordingly to run 1, there is also an interaction between the *Loops* group and the membrane. Contact is made at 200ns and lasts for 120ns. Additionally, there is a short interaction with the *Lysinestretch* for about 50ns at the end of the run. (see Chapter 6.31)
- 1tjx_trunc / No Chol Low Ca Run5: there is a relatively short interaction between the *Linker* group and the membrane, with *Lateral2* also getting close. Interaction most likely occurs between SER263 and PIP2. (see Chapter 6.32)

- 1tjx_trunc / No Chol Low Ca Run6: the graph for the *Loops* group shows a constant minimum distance starting at 60ns. The long-lasting interaction is stable until the end of simulation time. As seen in other runs with this system, there is no membrane insertion, although the *Loops* are involved. (see Chapter 6.33)
- 1tjx_trunc / NCHP Run3: the first interaction in this system is seen between the *Linker* and the membrane. Interaction takes place from 140 to 240ns of simulation time. All interactions found with this system (see runs 6 and 7) happen with the *Linker*, which tends to be a result of the longer and more flexible linker chain in *1tjx_trunc*. (see Chapter 6.34)
- 1tjx_trunc / NCHP Run6: this run shows a similar scenario as run 3. There is an interaction between the *Linker* and the membrane, starting at 60ns and lasting for 100ns. (see Chapter 6.35)
- 1tjx_trunc / NCHP Run7: distance evaluation shows, that the *Linker* group comes very close, but does not establish a real interaction longer than 20ns. (see Chapter 6.36)

For 5ccj_WT, only eight interactions longer than 100ns are seen in distance evaluations. Additionally, eight contacts shorter than 100ns have been evaluated as well.

- 5ccj_WT / Standard 895 Run2: only one run with an interaction can be found with the *Standard 895* system. In return, it is a very strong and long contact with PIP2 of the membrane. *Lysinestretch* and *Lateral2* show constant minimum distance in the graph over a time stretch of 490ns. After 80ns, *oppARG* also has constant minimum distance and all three groups stay this close until the end. (see Chapter 6.37)
- 5ccj_WT / High PIP2 Run1: the longest interaction of *5ccj_WT* with the membrane can be found in this run. *ARG* and *oppARG* are the two groups closest to the membrane. In this case, interaction seems to take place with POPS instead of PIP2. First contact is made at 350ns and is still stable at simulation end. (see Chapter 6.38)
- 5ccj_WT / High PIP2 Run3: only a short contact of about 70ns is made at the end of this run with *ARG, oppARG* and *Lateral2*. The interacting membrane lipid is POPS, similar to run 1. (see Chapter 6.39)
- 5ccj_WT / High PIP2 Run5: a very short contact at 100ns is made with the Loops group. It lasts only 20ns and therefore does not meet the criteria for interaction. (see Chapter 6.40)
- 5ccj_WT / High PIP2 Run8: two short contacts of 15ns can be found in this run. The first contact starts at 140ns and has the *Rest* group involved, the second contact starts at 485ns and involves *ARG, Lateral2* and *oppARG*. Even combined, both contacts are too short to be defined as an interaction. (see Chapter 6.41)

- 5ccj_WT / High PIP2 Low Ca Run1: comparable to *1tjx_trunc*, every run in the High PIP2 Low Ca system showed interaction with *5ccj_WT*. Run 1 has a strong and long-lasting interaction with multiple groups involved, which indicates a slight membrane insertion. The graph shows completely flat lines for *Linker, Lateral1, ARG, Loops* and *Rest*. The remaining groups *oppARG*, *Lysinestretch* and *Lateral2* also get close to the membrane. The interaction is stable almost from the beginning until the end of simulation time. (see Chapter 6.42)
- 5ccj_WT / High PIP2 Low Ca Run2: similar to run 1, there is an interaction that lasts nearly 500ns. *ARG* and *oppARG* are closest to the membrane, with *Lateral1, Lateral2* and *Lysinestretch* also heavily involved. Visual analysis shows slight membrane insertion and contact with PIP2. (see Chapter 6.43)
- 5ccj_WT / High PIP2 Low Ca Run3: the distance evaluation brings up an interaction mainly with *Lysinestretch* that starts at 30ns and lasts for the remaining 470ns. The interaction centre is located between *Lysinestretch* and *Loops*, as the latter is also at constant minimum distance to the membrane. (see Chapter 6.44)
- 5ccj_WT / High PIP2 Low Ca Run4: visual analysis shows multiple groups involved in interaction to the membrane. Distance evaluations confirm this finding, showing close contact starting at 50ns with *ARG*. *Lateral1, Loops*, *Rest* get to constant minimum distance at approximately 75ns and the groups *Linker* and *oppARG* make contact around 125ns. (see Chapter 6.45)
- 5ccj_WT / High PIP2 Low Ca Run5: in this run, two interactions, independently of one another are found. *ARG* makes contact with PIP2 for approximately 100ns, starting at 20ns. After departing from the membrane, the C2B domain makes contact once again, starting at 160ns. This time, *Lysinestretch* and *Loops* are involved and the interaction is stable until the simulation ends. (see Chapter 6.46)
- 5ccj_WT / High PIP2 Low Ca Run6: starting at 25ns, a stable interaction can be found between PIP2 and *Lysinestretch*. Also involved are *oppARG, Lateral1, Lateral2, ARG* and *Rest*, which indicates a strong interaction with slight insertion. The interaction is stable until the end. (see Chapter 6.47)
- 5ccj_WT / No Chol Low Ca Run1: in contrast to *1tjx_trunc*, no interaction >100ns is found in this system. There are some short contacts, however. In this run, there is a short contact between *Lysinestretch, Lateral2* and *PIP2*. It starts at 230ns and lasts for about 30ns. (see Chapter 6.48)

- 5ccj_WT / No Chol Low Ca Run2: similar to run 1, there is only a short contact. In this run, the Loops group comes closest to the membrane, where the contact is stable for 45ns. (see Chapter 6.49)
- 5ccj_WT / No Chol Low Ca Run3: starting at 30ns, the group Lysinestretch makes contact with the membrane for approximately 30ns. (see Chapter 6.50)
- 5ccj_WT / No Chol Low Ca Run4: similar to run 3, it is also the group Lysinestretch, that makes contact with the membrane. Again, it is a short touch of 30ns, this time starting at 100ns. (see Chapter 6.51)
- 5ccj_WT / NCHP Run5: there is no real interaction to be found in this system, but a contact involving oppARG and ARG exists at the end of the simulation. The groups make contact with the membrane at 415ns and hold it stable until the simulation ends. (see Chapter 6.52)

4. Conclusion, Discussion, Outlook

The simulations performed with the final seven systems show that interactions mostly happen with PIP2 involved. There is a clear dependence on the concentration of PIP2 with *1tjx_trunc* as well as with *5ccj_WT*. Without PIP2 in the membrane we found no interaction at all, whereas the *High PIP2* systems showed multiple interactions. Given the fact, that PIP2 is the membrane lipid that provides the most negative charges of all used membrane lipids, this is not surprising. In literature, there is consensus about the importance of PIP2 for exocytosis. (5, 47) The results of our simulations are in agreement with these findings.

The second determining parameter seems to be the Ca^{2+}- concentration. We found interactions in both systems with High PIP2 levels, but the system with low Ca^{2+}- concentration proofed to facilitate protein-membrane interaction efficiently. As shown in Figures 12 and 13, Ca^{2+} locally concentrates around PIP2. We believe that membrane saturation causes PIP2 to lose potential reactivity and therefore oppresses otherwise possible interactions. This can lead to falsified results in MD simulations carried out with Ca^{2+}- concentration levels high above the physiological standard. Whereas it is still a widespread technique to elevate Ca^{2+}- levels in order to ensure Ca^{2+} binding, membrane saturation has to be taken into account or we advise to work with already bound structures instead. (21, 22) At least coarse-grained simulations, where parameterisation of Ca^{2+} is still not precise enough, should be carried out in a biased, but rather significant way.

The role of cholesterol however, is not sufficiently clarified. In membranes with a PIP2 concentration of 1%, the results of the membrane without cholesterol are similar to the *Standard 895* membrane. Also, the likelihood of interaction in *NCHP* and *High PIP2* is very much alike. The increase of interactions in *No Chol Low Ca* could also be a matter of Ca^{2+}- concentration within the system. The fact that there are interactions with membranes exclusive of cholesterol at least indicates that protein-membrane interaction is still possible. However, no conclusion can be made concerning the loops-first membrane insertion, which is supposed by most studies. (11, 12, 22)
Also, further distance evaluations are necessary. To clarify the dependence on cholesterol, every interaction found has to be examined on whether cholesterol is anywhere near the centre of interaction and thereby plays a role. As to the composition of the presynaptic plasma membrane in human cells, a significant concentration of PIP2 can be assumed and it seems likely that this is the case with cholesterol as well.

The expected loops-first membrane insertion was not observed in any of the performed runs. This may be a result of the unbiased placement of Syt-1 and completely free MD simulations. The SNARE complex plays a key role in membrane fusion and has multiple interfaces with Syt-1. (34) Therefore, the positioning and orientation of Syt-1 can also be influenced by the SNARE complex. It is possible that the SNARE complex is responsible for the correct orientation that facilitates membrane insertion of the Ca^{2+}- binding loops.

Whereas most studies show two Ca^{2+}- ions bound in the binding pocket of the C2B-domain, our coarse-grained models only show one ion bound at a time. (11, 12, 21, 22) It is possible, that the conformational flexibility increase, described by *Bykhovskaia,* is not to be seen in a coarse-grained model. (21) Also, the Ca^{2+}- induced conformational transition, as described by *Wu and Schulten*, is maybe not precisely reflected in a coarse-grained model. (22) This would also explain, why we could not observe any change in binding probability after Ca^{2+} exits its pocket in the *High PIP2 Low Ca* system. In these runs, Ca^{2+} did not seem to make any difference. *Honigmann et al.* also found that if the PIP2 concentration is high enough, the protein is able to bind in a Ca^{2+}- independent manner. (23) Our simulation results support these findings. In addition, the structures retrieved from the PDB (*1tjx* & *5ccj*) have been crystallized in a bound state. Therefore, it is possible that this state still lasts after detachment of Ca^{2+}. This conformation could also be the existing state at all times of the simulation, even without Ca^{2+} anywhere near the protein. This assumption presents a plausible explanation, as we are looking at a ns-timescale, which could be a time frame too short for conformational changes in coarse-grained models.

In runs with *1tjx_trunc*, a total of 17 interactions (interaction time > 100ns) occur, whereas the runs with *5ccj_WT* only show 8 interactions. However, this is probably due to the fact, that the elongated linker in *1tjx_trunc* is involved in interaction, as seen in particular in the *No Chol Low Ca* system. In the same system with *5ccj_WT* we also observed contacts, which proved to be too short to meet our definition of an interaction. Every other membrane composition with *1tjx_trunc* was comparable to the same membranes with *5ccj_WT,* with regard to the probability of interaction. Therefore, the choice of the used C2B-domain structures can be recommended for further simulations.

With increasing computational power, simulations unthinkable to perform a few years ago are now possible. It would be of importance to run similar simulations as presented in this diploma thesis with an all-atomistic model. The detailed molecular interaction between PIP2 and Syt-1 would be very interesting to investigate in addition to the already existing studies on membrane insertion of the Ca^{2+}-binding loops. (21, 22) Further knowledge of the physiological membrane composition of the

presynaptic cell membrane and the vesicular membrane would also open the possibility to investigate those using MD simulations. Therefore, the likelihood of C2B to bind to each of these membranes could be determined and furthermore help to understand the exact binding kinetics of Syt-1.

The focus on loops-first membrane insertion may cause a limited view on membrane fusion itself, as other interactions seem likely as well. (23, 34) Especially, the possibility of the C2AB-domains to bind simultaneously to the presynaptic and the vesicular membranes, as described by *Honigmann et al.,* requires an additional type of interaction to take place. (23)

If made possible by increased computational power, it would also be advantageous to run simulations with both C2-domains and the SNARE complex. The interaction between C2AB and the SNARE complex in a system with one or two membranes could reveal the orientation of Syt-1 and therefore its interactions with the membranes. The overall goal is to perform MD simulations in which membrane fusion itself can be observed, even if this sounds like a vision of the future at present day.

5. List of Figures and Tables

6. Supplements

```
1TJX:A|PDBID|CH..          1   SGGGGGILEKLGDICFSLRYVPTAGKLTVVILEAKNLKKMDVGGLSDPYVKIHLMQNGKR        60
5CCJ:A|PDBID|CH..          1   -------SEKLGDICFSLAYVPTAGKLTVVILAAKNLKKMDVGGLSDPYVKIHLMQNGKR        53
                                      ********** ************* ****************************

1TJX:A|PDBID|CH..         61   LKKKKTTIKKNTLNPYYNESFSFEVPFEQIQKVQVVVTVLDYDKIGKNDAIGKVFVGYNS       120
5CCJ:A|PDBID|CH..         54   LKKKKTTIKKNTLNPWYNESFSFEVPFEQIQKVQVVVTVLDYDKIGKNDAIGKVFVGYNS       113
                               ***************:********************************************

1TJX:A|PDBID|CH..        121   TGAELRHWSDMLANPRRPIAQWHTLQVEEEVDAMLAVKK                           159
5CCJ:A|PDBID|CH..        114   TGAELRHWSDMLANPAAPIAQWHTLQVEEEVDAMLAVKK                           152
                               ***************  **********************
```

6.1 Sequence Alignment of pdb structures 1tjx and 5ccj; the 5ccj-structure is a quintuple mutant (R281A, E295A, Y338W, R398A, R399A); the linker to the C2A-domain is longer by seven amino acid residues in 1tjx;

structures aligned with the Uniprot alignment tool; available from: http://www.uniprot.org/help/sequence-alignments

```
1TJX_trunc:A|PD..          1   SGGGGGILEKLGDICFSLRYVPTAGKLTVVILEAKNLKKMDVGGLSDPYVKIHLMQNGKR        60
5CCJ_WT:A|PDBID..          1   -------SEKLGDICFSLRYVPTAGKLTVVILEAKNLKKMDVGGLSDPYVKIHLMQNGKR        53
                                      **************************************************

1TJX_trunc:A|PD..         61   LKKKKTTIKKNTLNPYYNESFSFEVPFEQIQKVQVVVTVLDYDKIGKNDAIGKVFVGYNS       120
5CCJ_WT:A|PDBID..         54   LKKKKTTIKKNTLNPYYNESFSFEVPFEQIQKVQVVVTVLDYDKIGKNDAIGKVFVGYNS       113
                               ************************************************************

1TJX_trunc:A|PD..        121   TGAELRHWSDMLANPRRPIAQWHTLQVEEEVDAMLA---                           156
5CCJ_WT:A|PDBID..        114   TGAELRHWSDMLANPRRPIAQWHTLQVEEEVDAMLAVKK                           152
                               **********************************
```

6.2 *Sequence Alignment of arranged structures 1tjx_trunc and 5ccj_WT; in 1tjx_trunc, the linker to the C2A-domain is longer by seven amino acid residues, the last three amino acid residues are truncated*

structures aligned with the Uniprot alignment tool; available from: http://www.uniprot.org/help/sequence-alignments

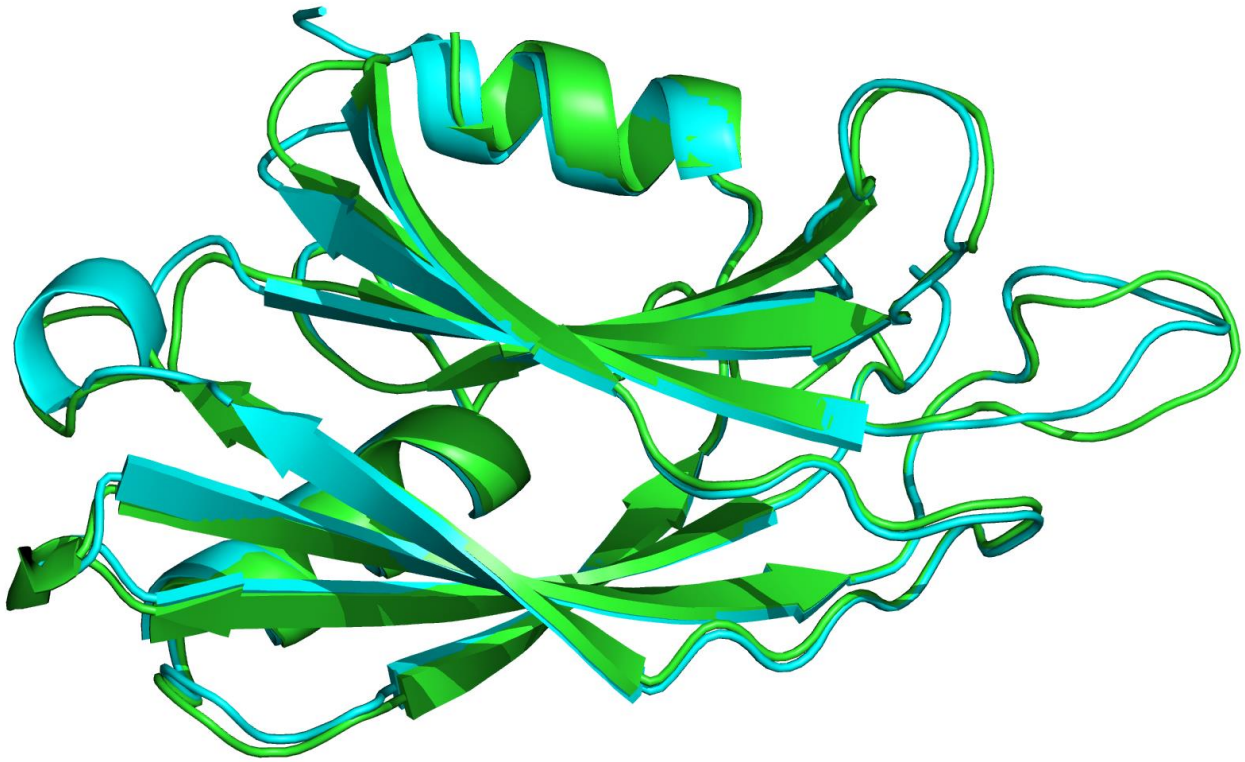

6.3 Structure Alignment of arranged structures 1tjx_trunc and 5ccj_WT;
Both structures shown as cartoon model, 1tjx_trunc coloured green, 5ccj_WT coloured cyan; structures aligned via Swiss pdb-Viewer; the backbone-RMSD for Glu271 – Ala418 = 0,78nm

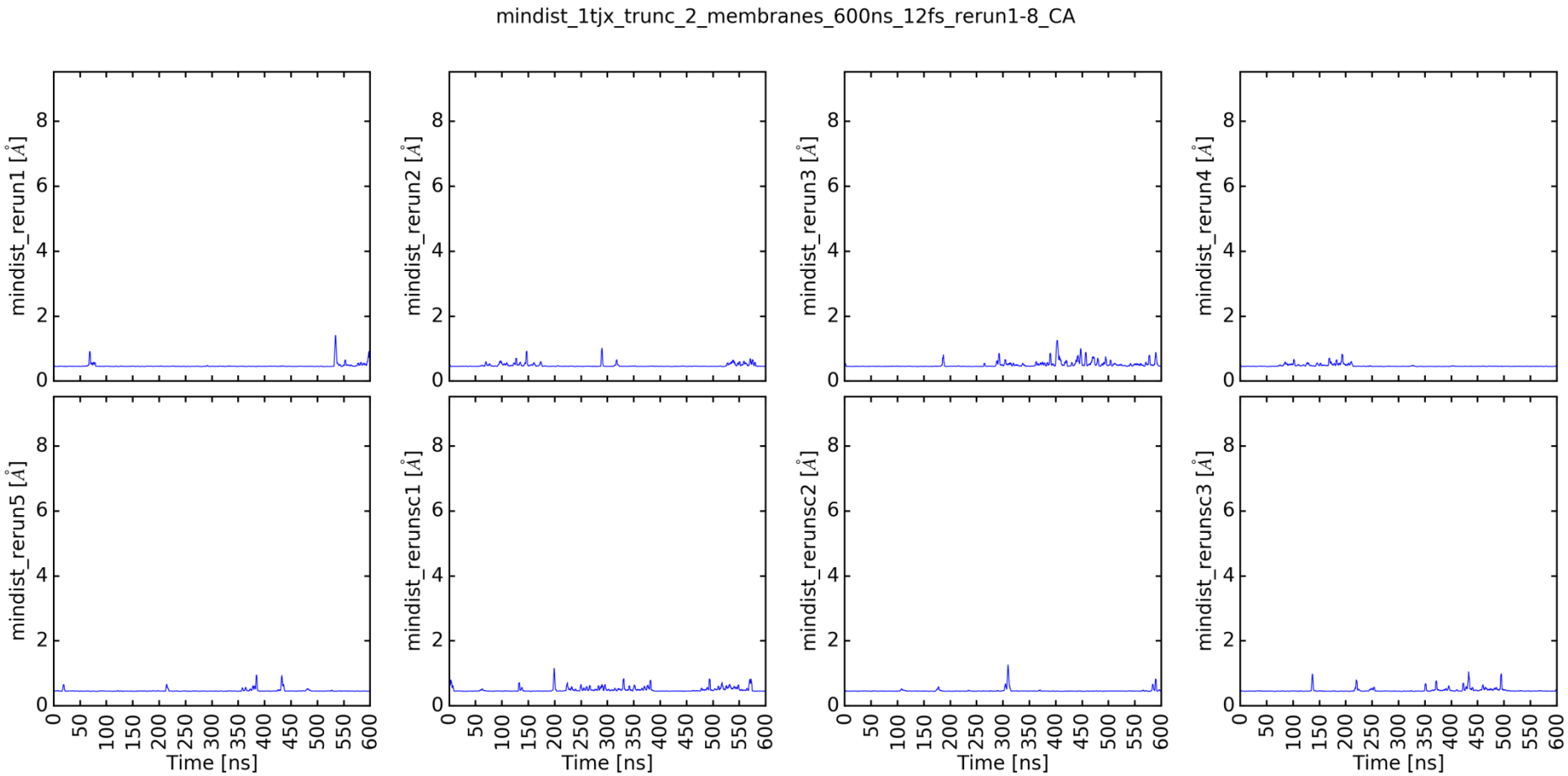

6.4 Distance between Ca^{2+} and the five Aspartic acids (D303, D309, D363, D365, D371) in the binding pocket of 1tjx_trunc over the runtime of 600ns in system Standard 895 (eight runs), calculated with g_mindist (see Chapter 2.3.1.2)

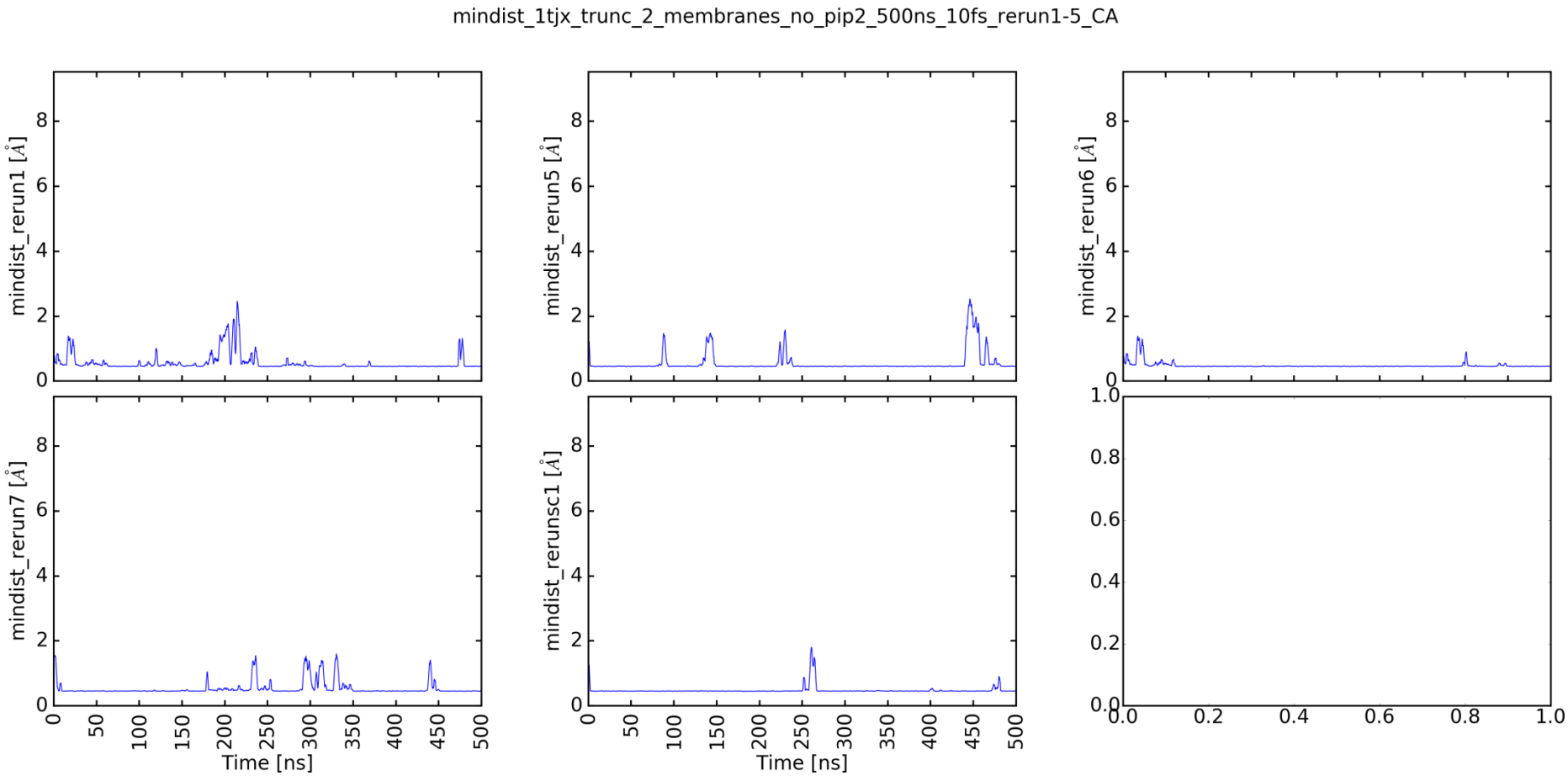

6.5 Distance between Ca^{2+} and the five Aspartic acids (D303, D309, D363, D365, D371) in the binding pocket of 1tjx_trunc over the runtime of 500ns in system No PIP2 (five runs), calculated with g_mindist (see Chapter 2.3.1.2)

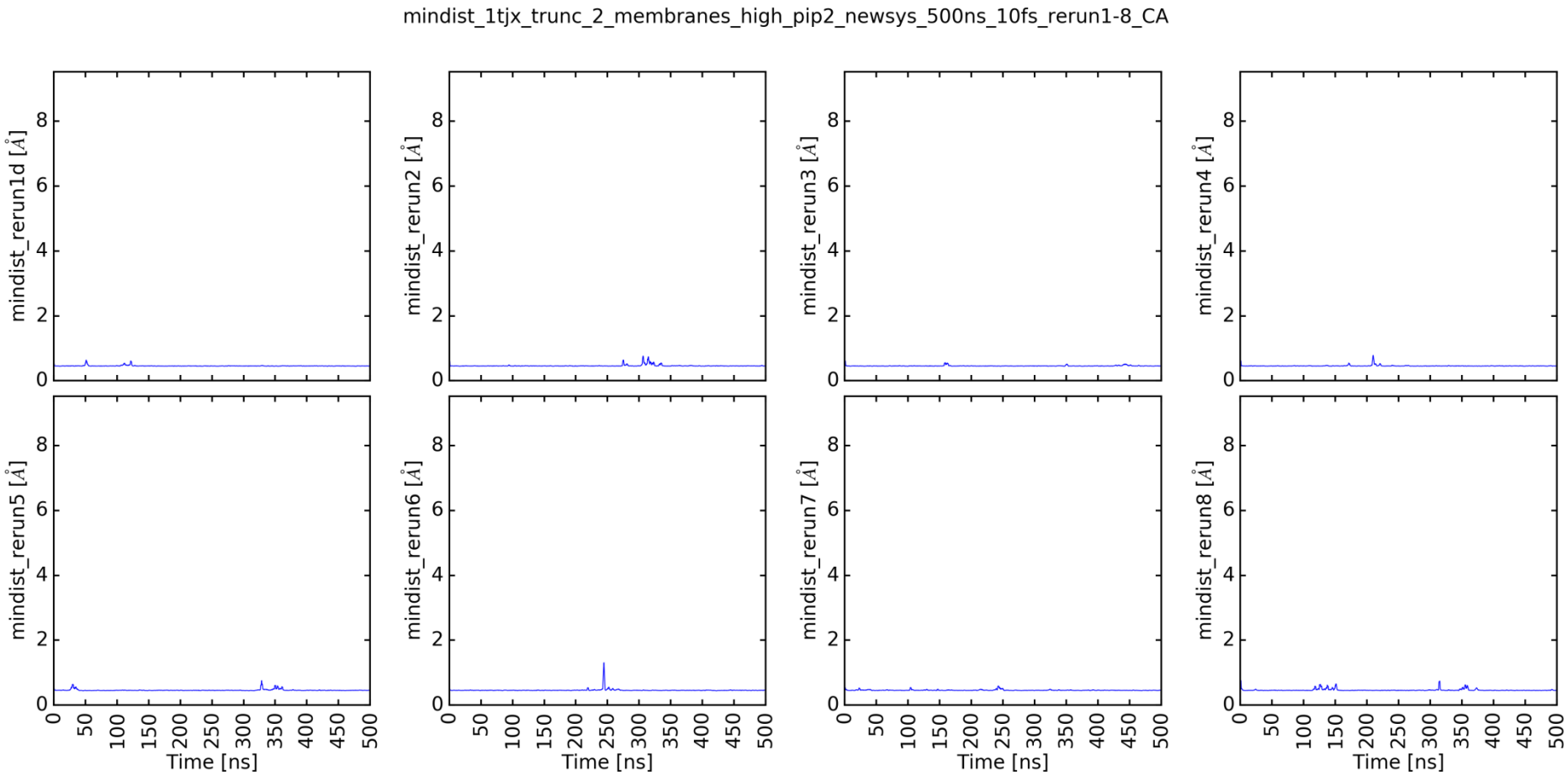

6.6 Distance between Ca^{2+} and the five Aspartic acids (D303, D309, D363, D365, D371) in the binding pocket of 1tjx_trunc over the runtime of 500ns in system High PIP2 (eight runs), calculated with g_mindist (see Chapter 2.3.1.2)

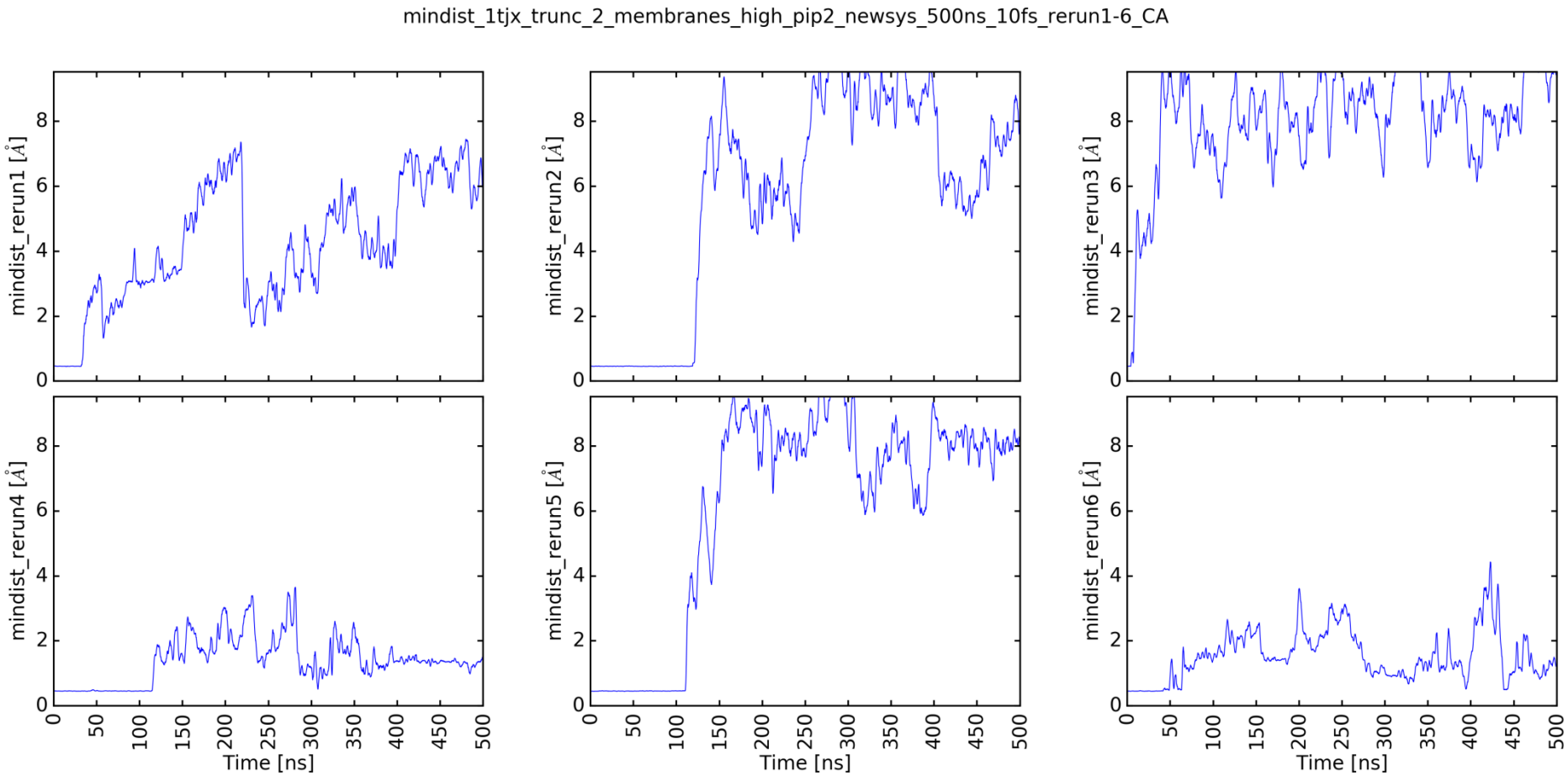

6.7 Distance between Ca^{2+} and the five Aspartic acids (D303, D309, D363, D365, D371) in the binding pocket of 1tjx_trunc over the runtime of 500ns in system High PIP2 Low Ca^{2+} (six runs), calculated with g_mindist (see Chapter 2.3.1.2)

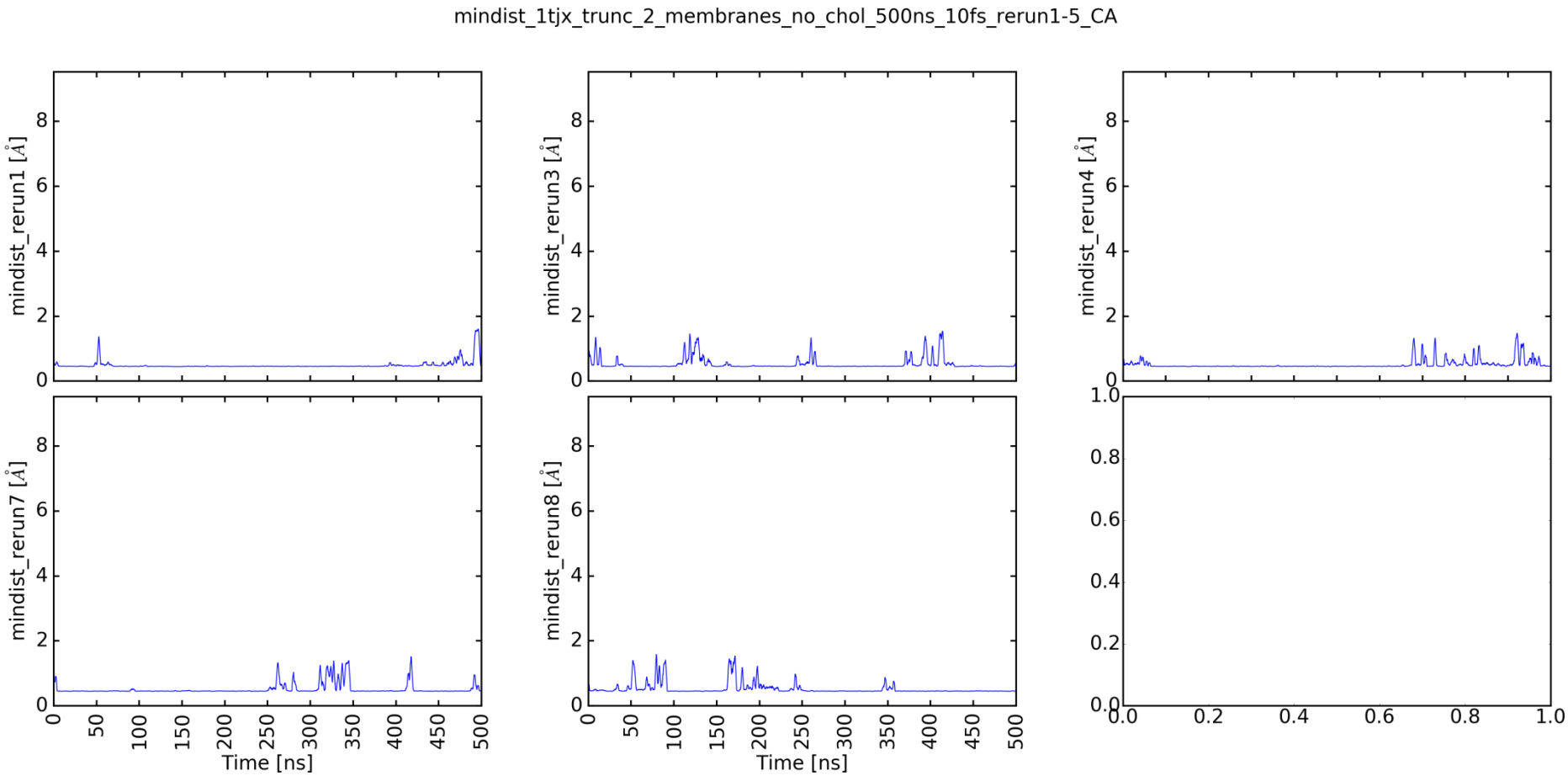

6.8 Distance between Ca^{2+} and the five Aspartic acids (D303, D309, D363, D365, D371) in the binding pocket of 1tjx_trunc over the runtime of 500ns in system No Chol (five runs), calculated with g_mindist (see Chapter 2.3.1.2)

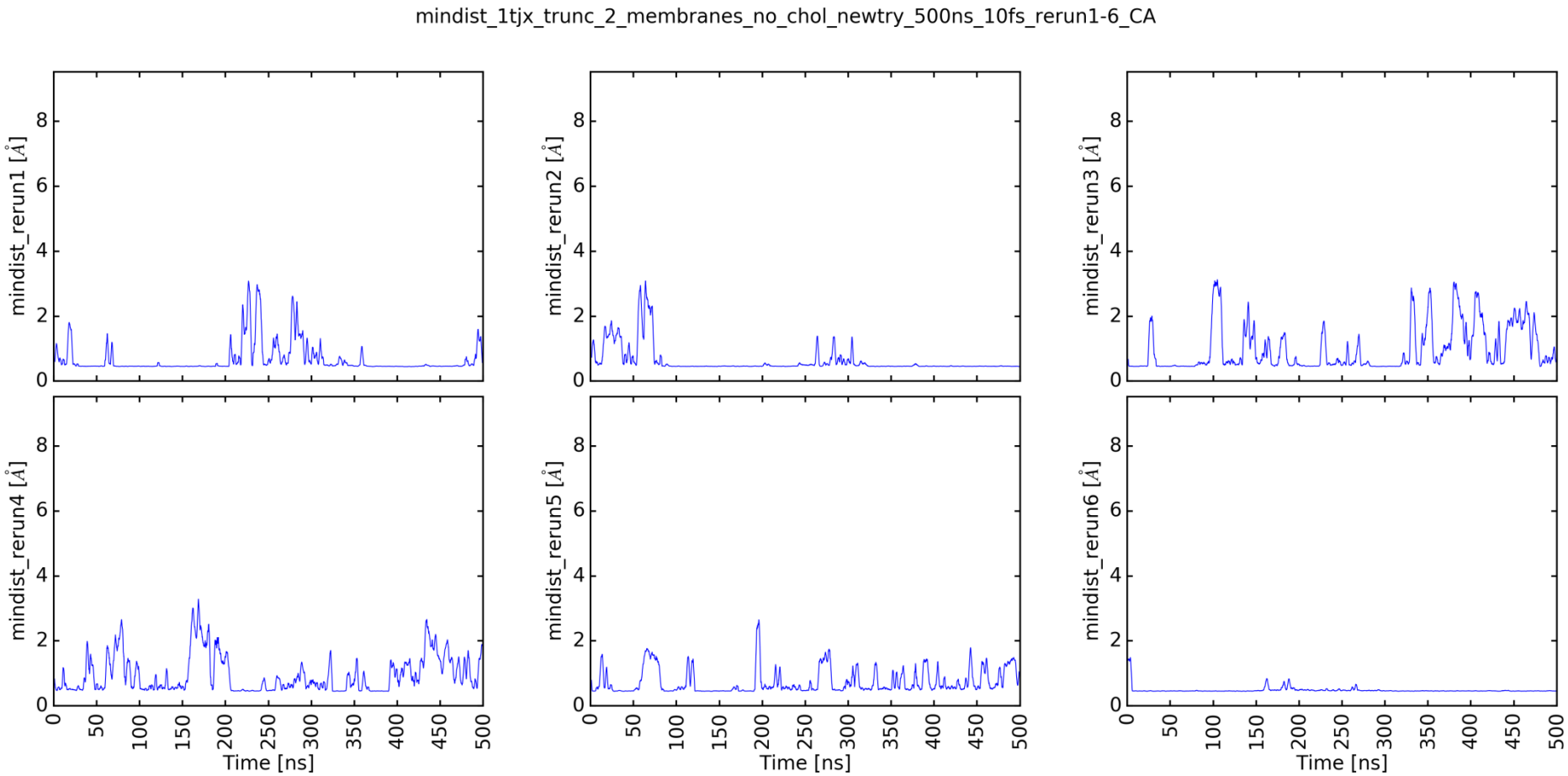

6.9 Distance between Ca^{2+} and the five Aspartic acids (D303, D309, D363, D365, D371) in the binding pocket of 1tjx_trunc over the runtime of 500ns in system No Chol Low Ca^{2+} (five runs), calculated with g_mindist (see Chapter 2.3.1.2)

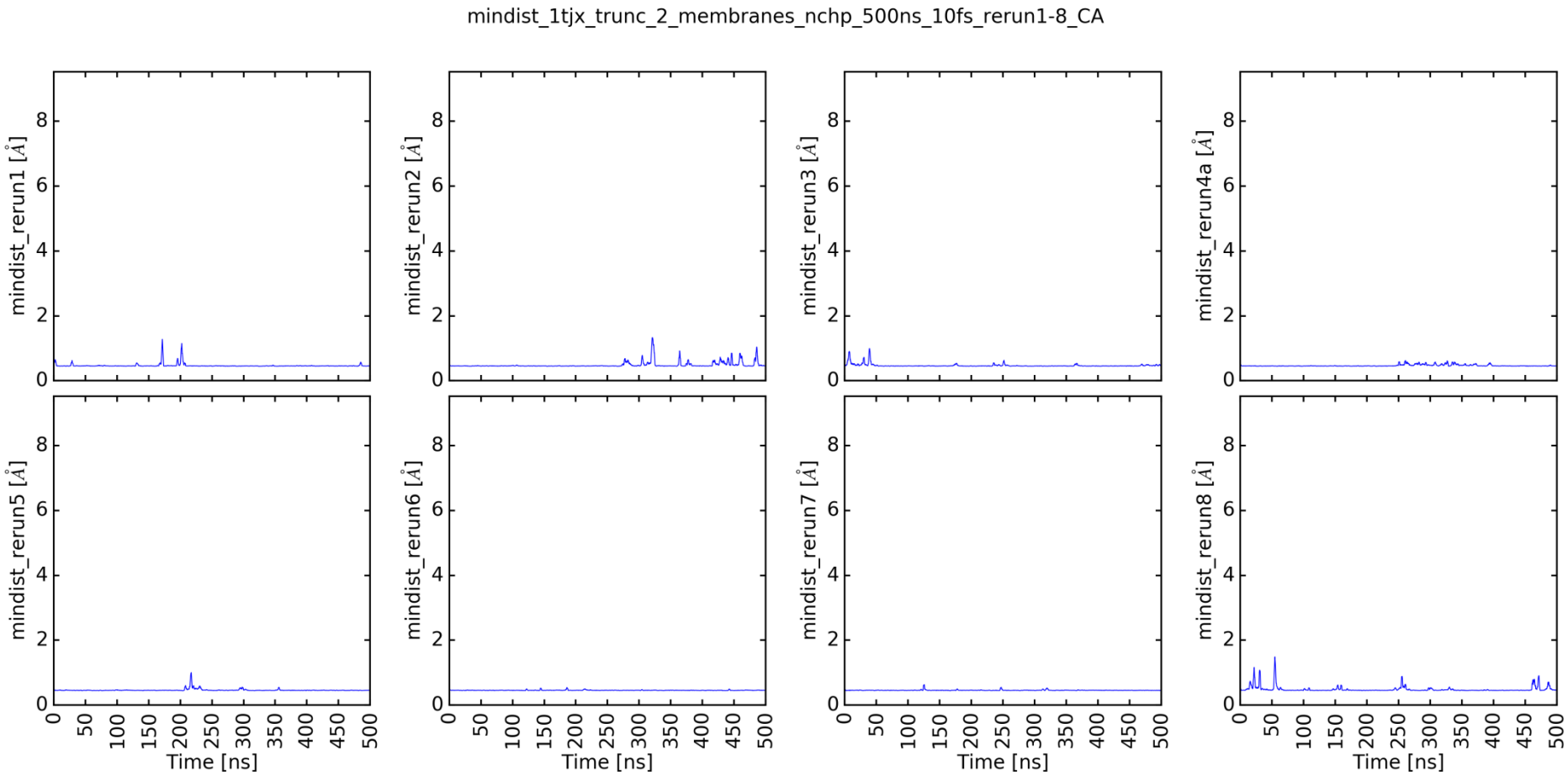

6.10 Distance between Ca^{2+} and the five Aspartic acids (D303, D309, D363, D365, D371) in the binding pocket of 1tjx_trunc over the runtime of 500ns in system NCHP (eight runs), calculated with g_mindist (see Chapter 2.3.1.2)

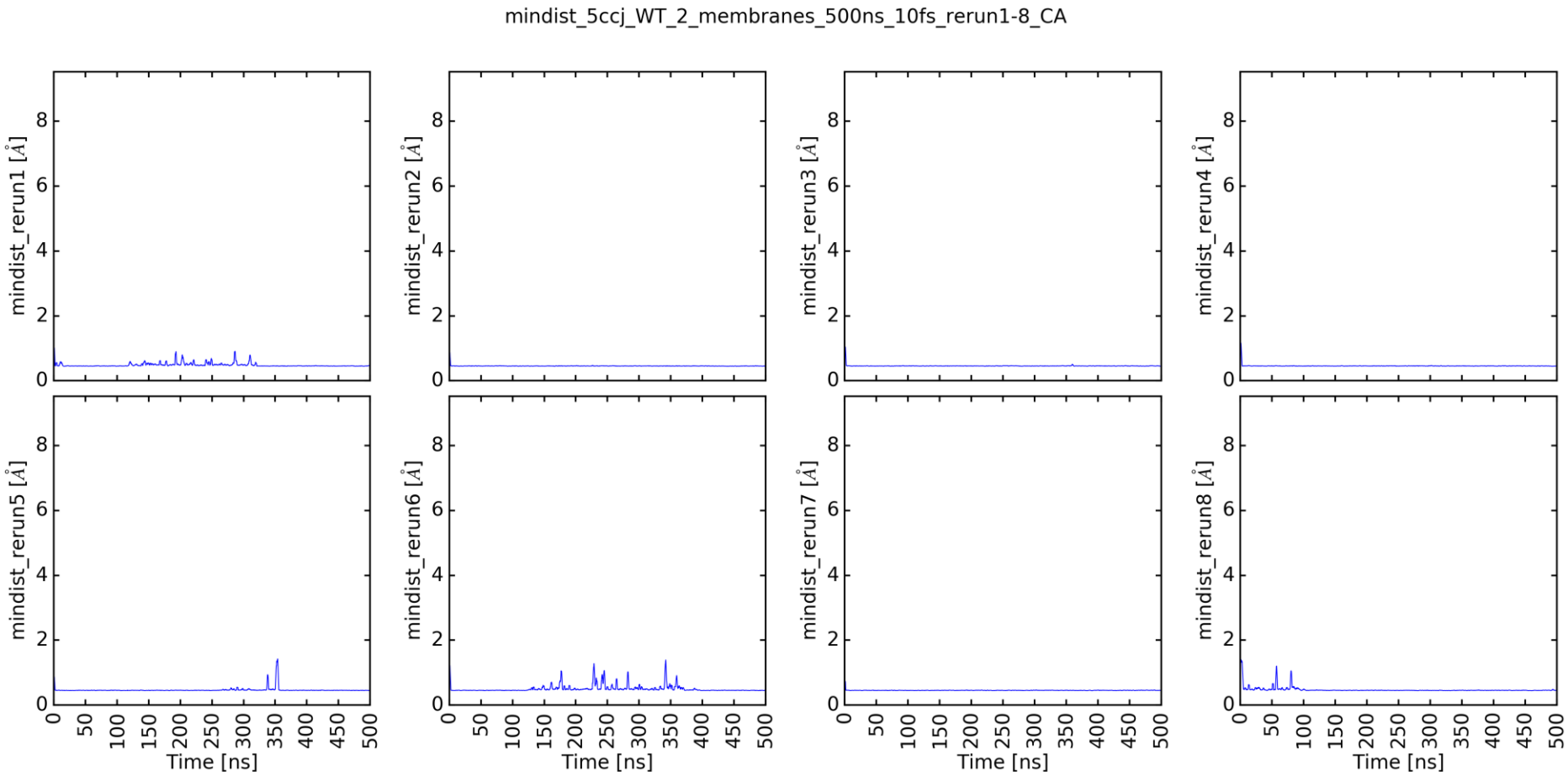

6.11 Distance between Ca^{2+} and the five Aspartic acids (D303, D309, D363, D365, D371) in the binding pocket of 5ccj_WT over the runtime of 500ns in system Standard 895 (eight runs), calculated with g_mindist (see Chapter 2.3.1.2)

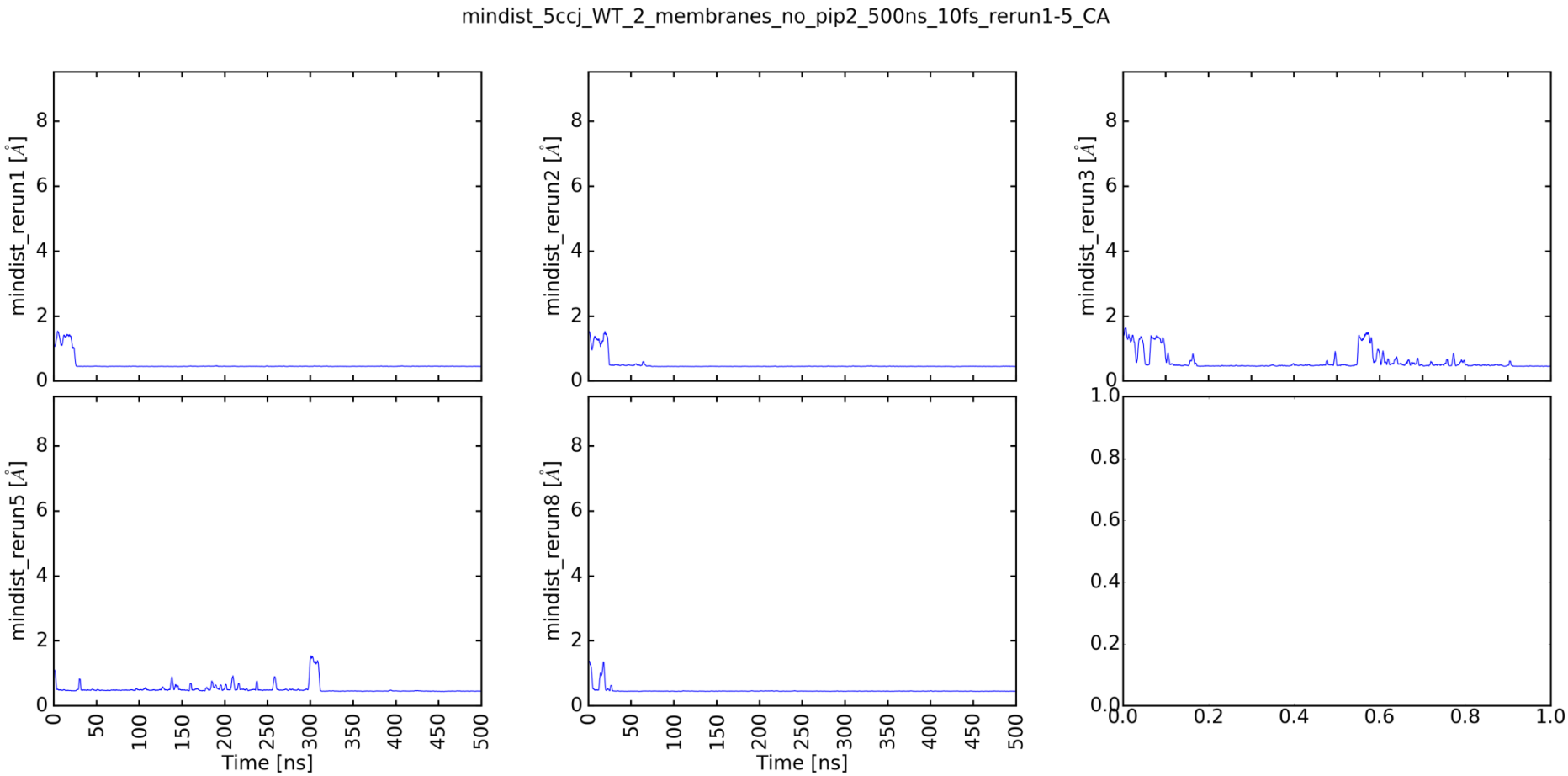

6.12 Distance between Ca^{2+} and the five Aspartic acids (D303, D309, D363, D365, D371) in the binding pocket of 5ccj_WT over the runtime of 500ns in system No PIP2 (five runs), calculated with g_mindist (see Chapter 2.3.1.2)

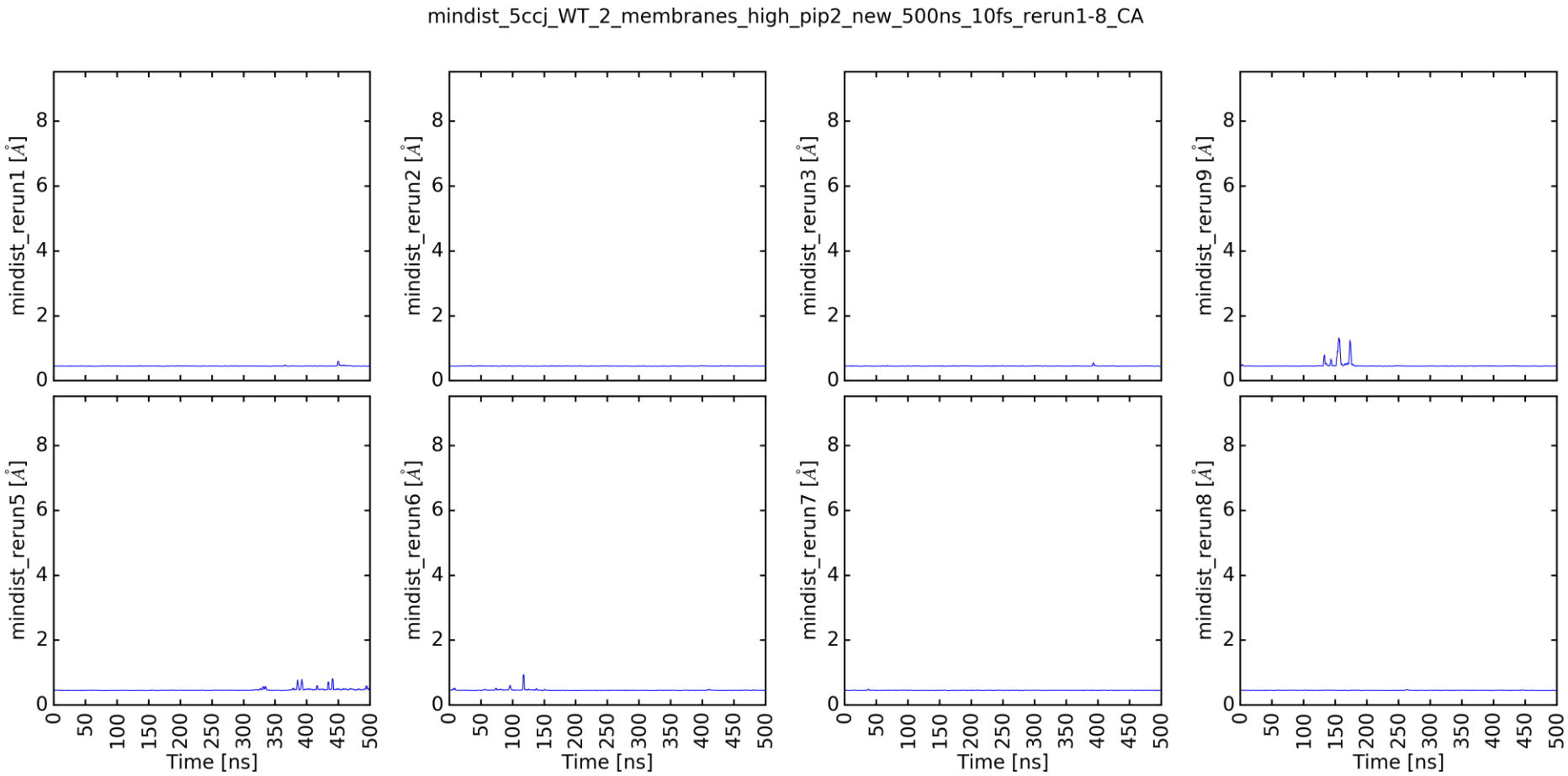

6.13 Distance between Ca^{2+} and the five Aspartic acids (D303, D309, D363, D365, D371) in the binding pocket of 5ccj_WT over the runtime of 500ns in system High PIP2 (eight runs), calculated with g_mindist (see Chapter 2.3.1.2)

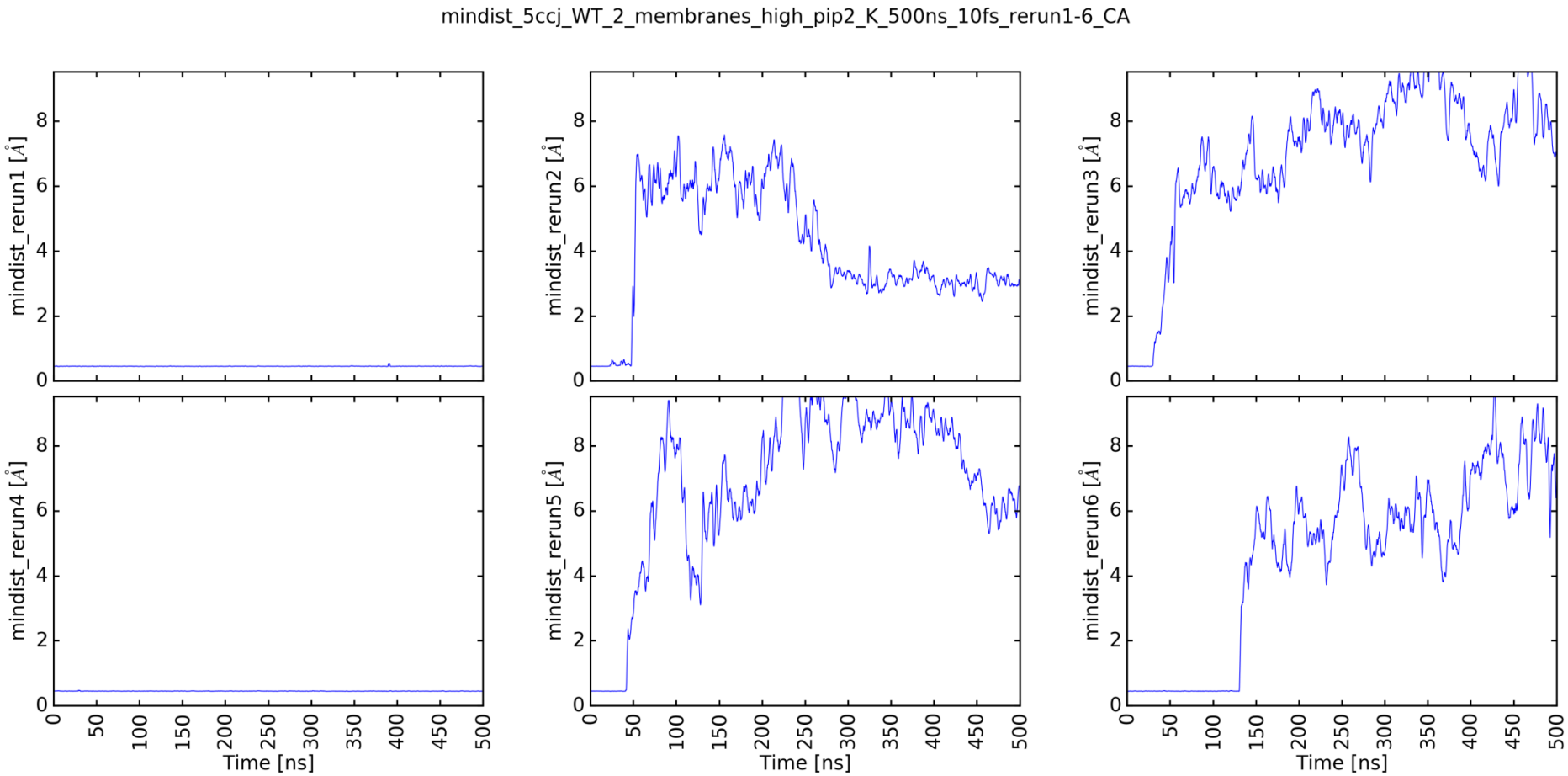

6.14 Distance between Ca^{2+} and the five Aspartic acids (D303, D309, D363, D365, D371) in the binding pocket of 5ccj_WT over the runtime of 500ns in system High PIP2 Low Ca^{2+} (six runs), calculated with g_mindist (see Chapter 2.3.1.2)

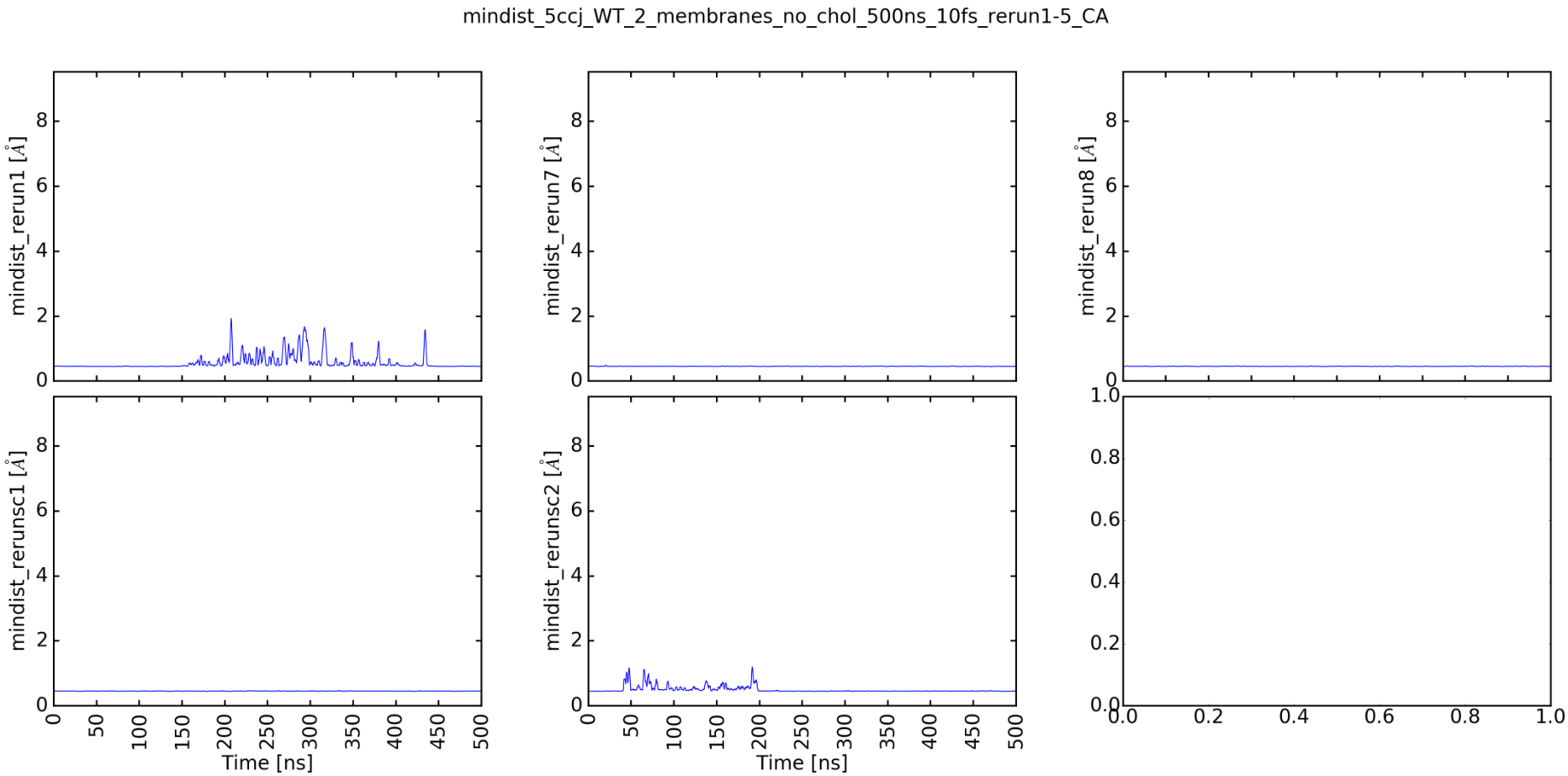

6.15 Distance between Ca^{2+} and the five Aspartic acids (D303, D309, D363, D365, D371) in the binding pocket of 5ccj_WT over the runtime of 500ns in system No Chol (five runs), calculated with g_mindist (see Chapter 2.3.1.2)

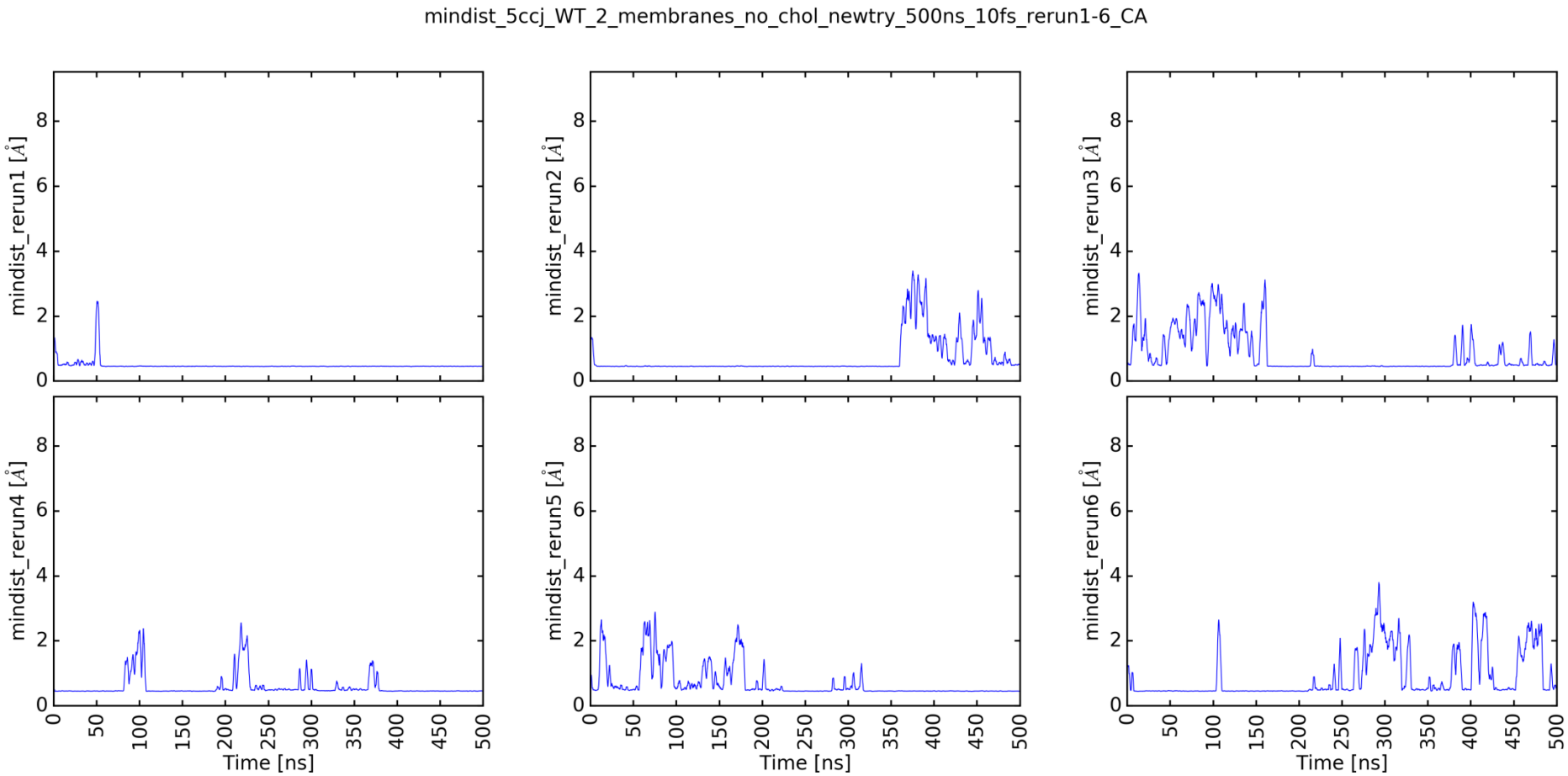

6.16 Distance between Ca^{2+} and the five Aspartic acids (D303, D309, D363, D365, D371) in the binding pocket of 5ccj_WT over the runtime of 500ns in system No Chol Low Ca^{2+} (six runs), calculated with g_mindist (see Chapter 2.3.1.2)

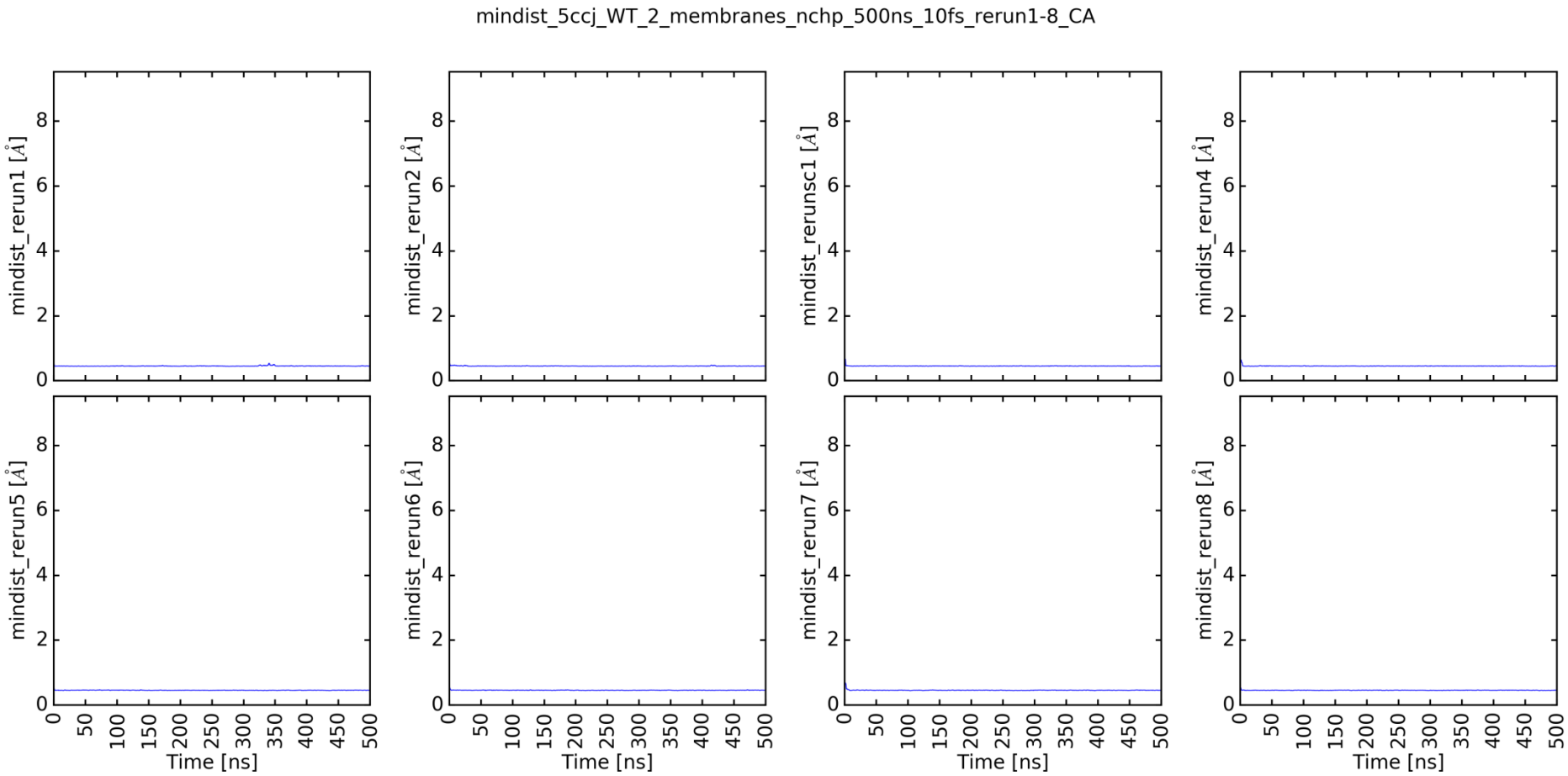

6.17 Distance between Ca^{2+} and the five Aspartic acids (D303, D309, D363, D365, D371) in the binding pocket of 5ccj_WT over the runtime of 500ns in system NCHP (eight runs), calculated with g_mindist (see Chapter 2.3.1.2)

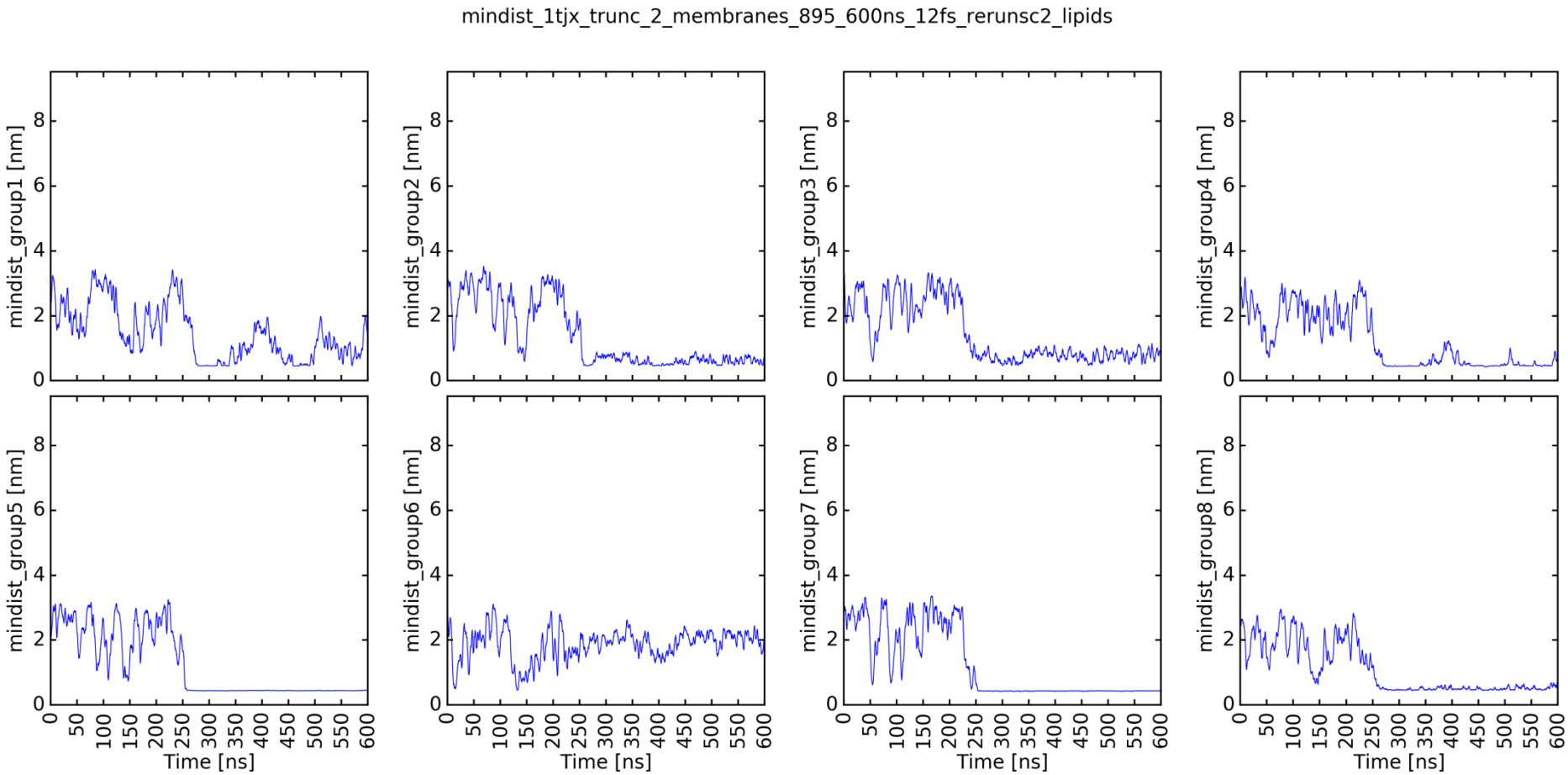

6.18 Distance between groups and membrane lipids. System 1tjx_trunc / Standard 895, Rerunsc2; Group1: Linker, Group2: Lateral1, Group3: Lysinestretch, Group4: Lateral2, Group5: ARG, Group6: Loops, Group7: oppARG, Group8: Rest; see Chapter 3.12.3

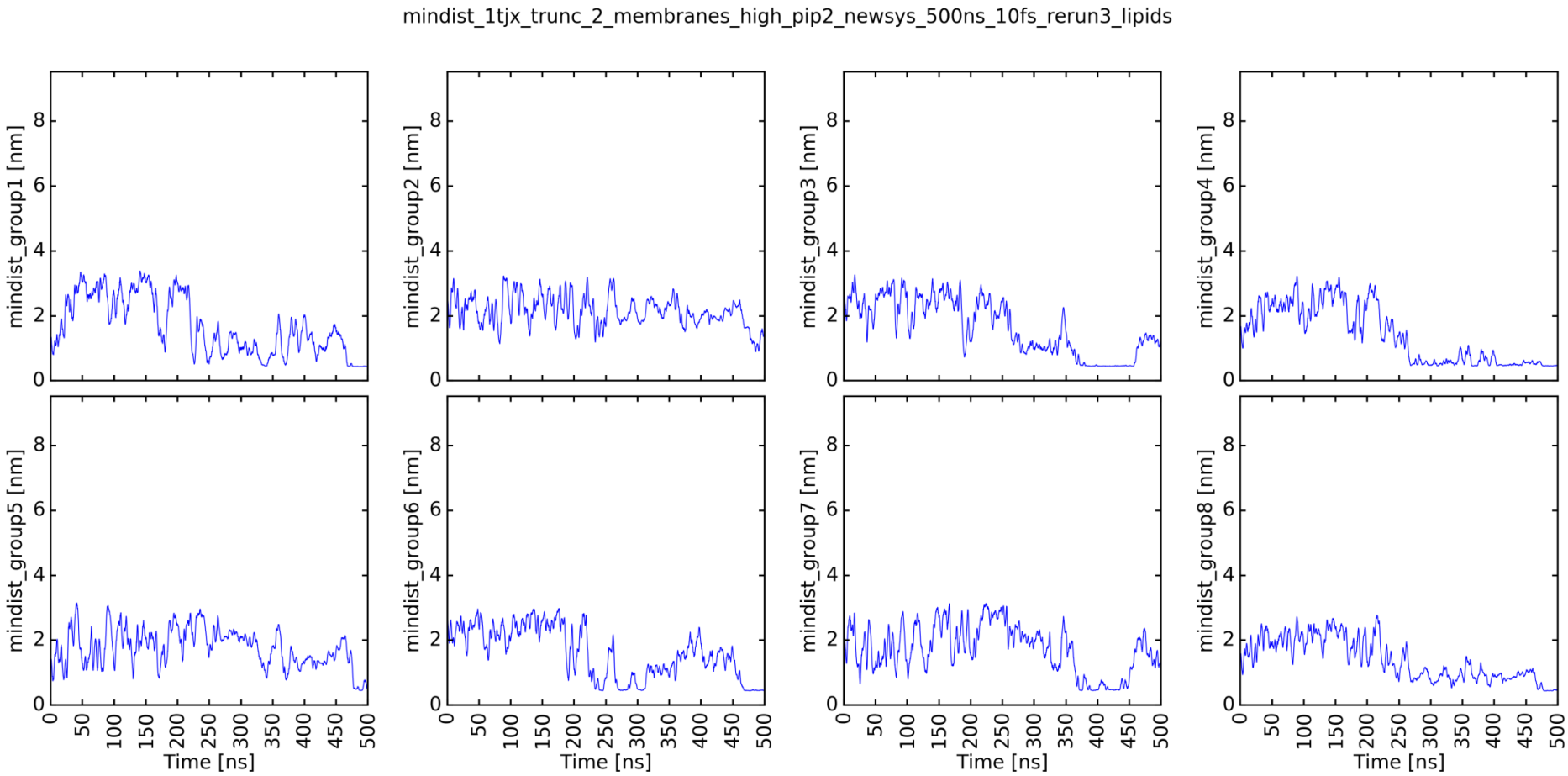

6.19 Distance between groups and membrane lipids. System 1tjx_trunc / HighPIP2, Rerun3; Group1: Linker, Group2: Lateral1, Group3: Lysinestretch, Group4: Lateral2, Group5: ARG, Group6: Loops, Group7: oppARG, Group8: Rest; see Chapter 3.12.3

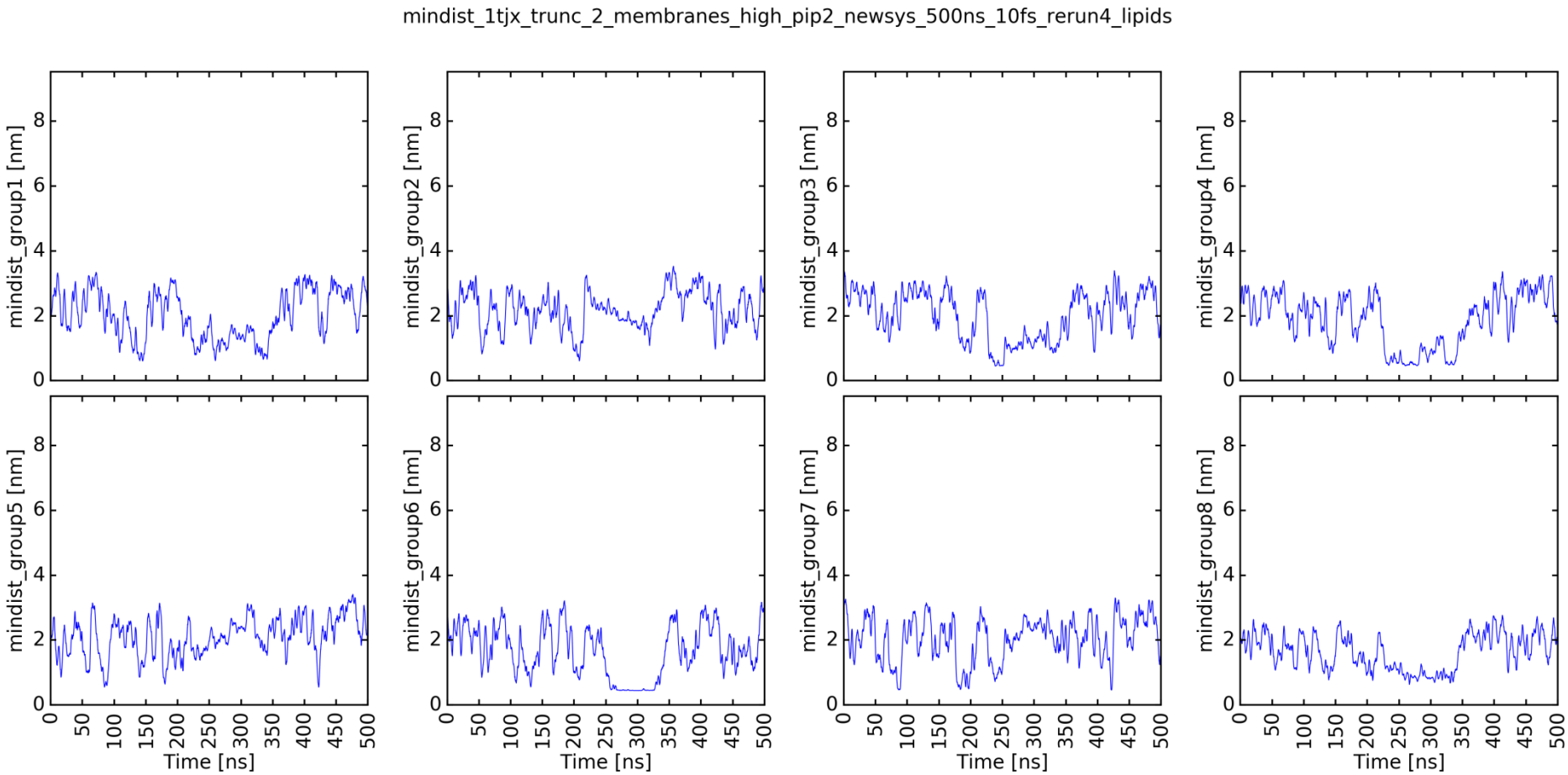

6.20 Distance between groups and membrane lipids. System 1tjx_trunc / HighPIP2, Rerun4; Group1: Linker, Group2: Lateral1, Group3: Lysinestretch, Group4: Lateral2, Group5: ARG, Group6: Loops, Group7: oppARG, Group8: Rest; see Chapter 3.12.3

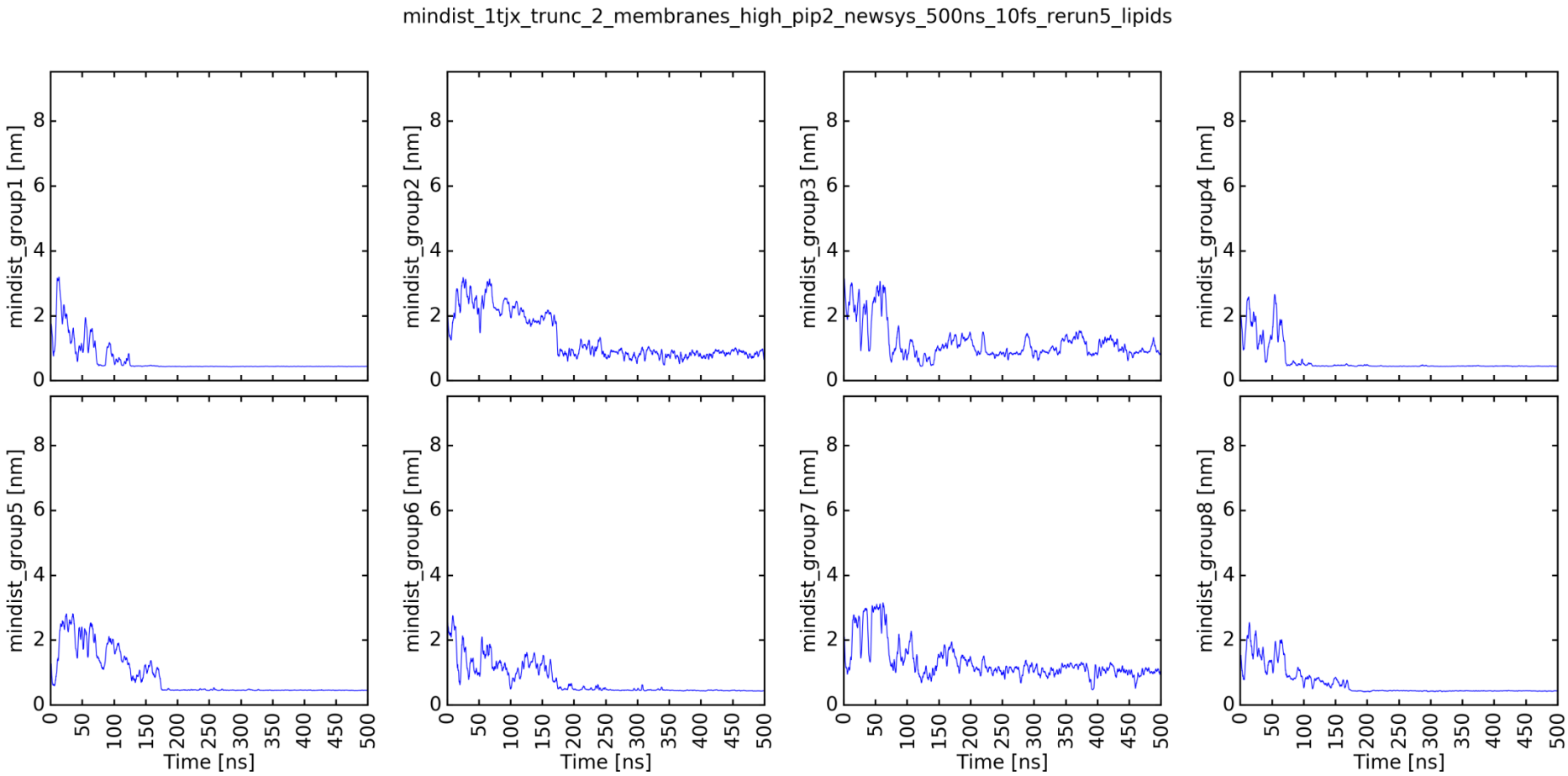

6.21 Distance between groups and membrane lipids. System 1tjx_trunc / HighPIP2, Rerun5; Group1: Linker, Group2: Lateral1, Group3: Lysinestretch, Group4: Lateral2, Group5: ARG, Group6: Loops, Group7: oppARG, Group8: Rest; see Chapter 3.12.3

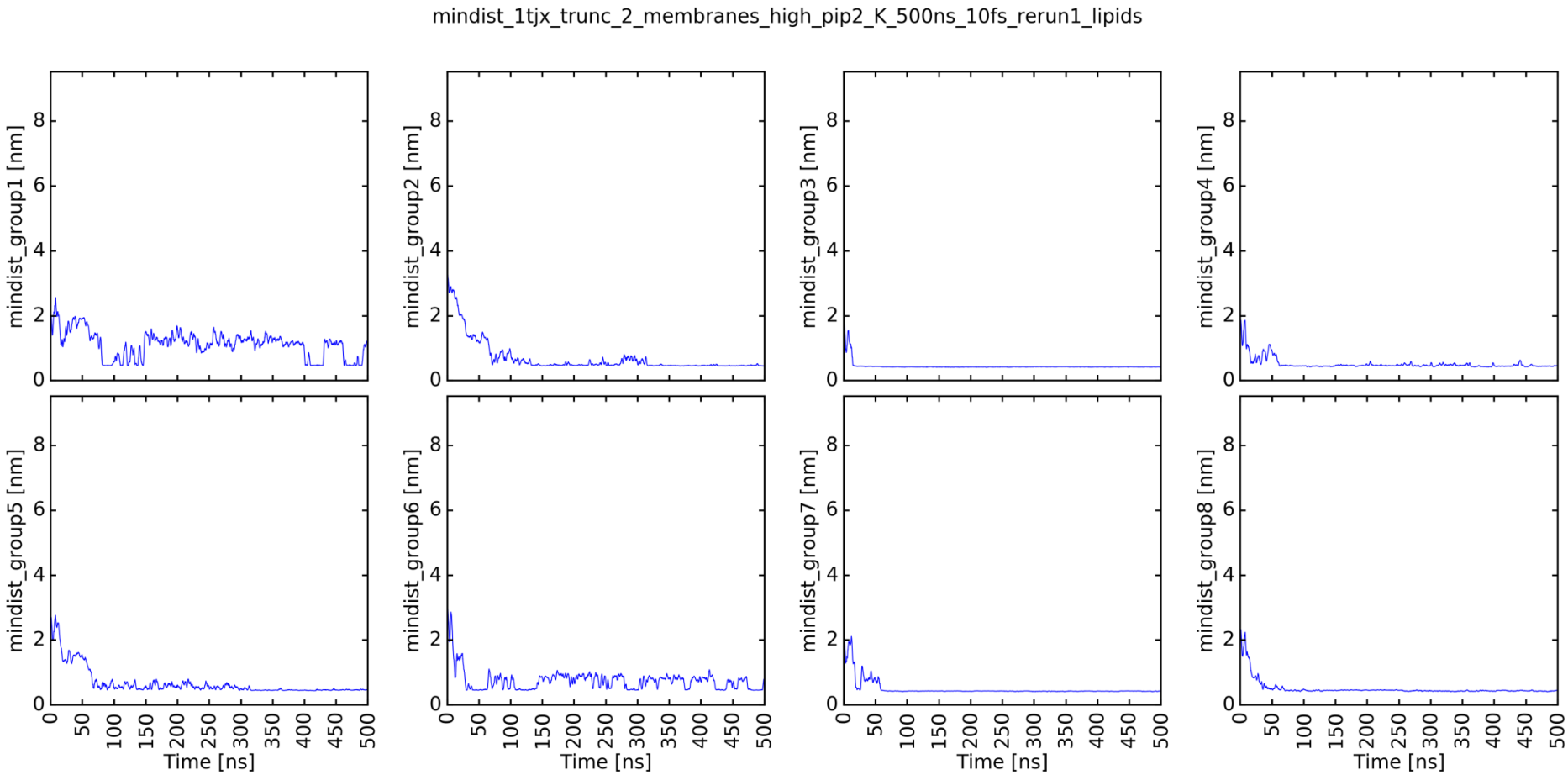

6.22 Distance between groups and membrane lipids. System 1tjx_trunc / HighPIP2 Low CA, Rerun1; Group1: Linker, Group2: Lateral1, Group3: Lysinestretch, Group4: Lateral2, Group5: ARG, Group6: Loops, Group7: oppARG, Group8: Rest; see Chapter 3.12.3

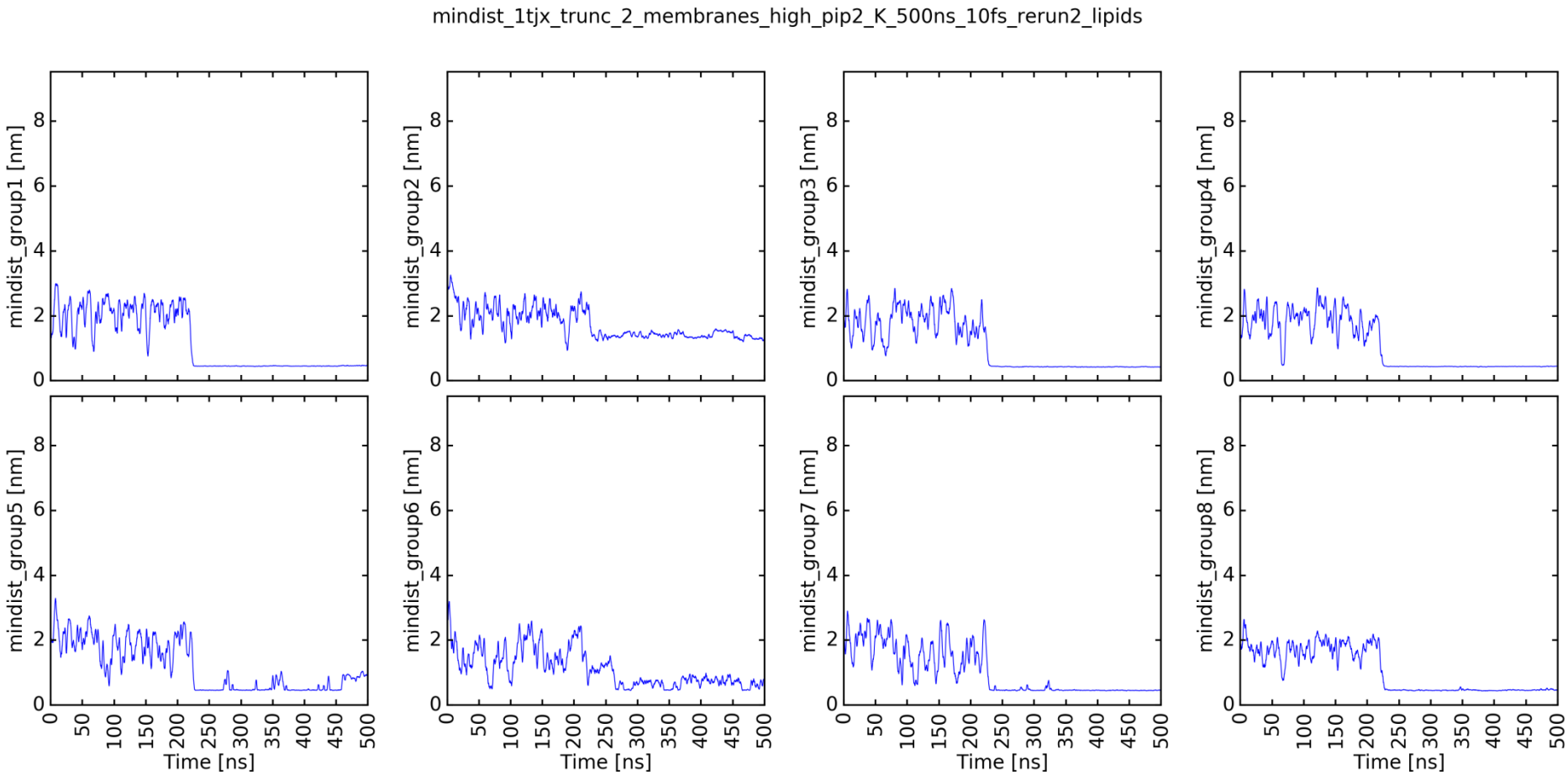

6.23 Distance between groups and membrane lipids. System 1tjx_trunc / HighPIP2 Low CA, Rerun2; Group1: Linker, Group2: Lateral1, Group3: Lysinestretch, Group4: Lateral2, Group5: ARG, Group6: Loops, Group7: oppARG, Group8: Rest; see Chapter 3.12.3

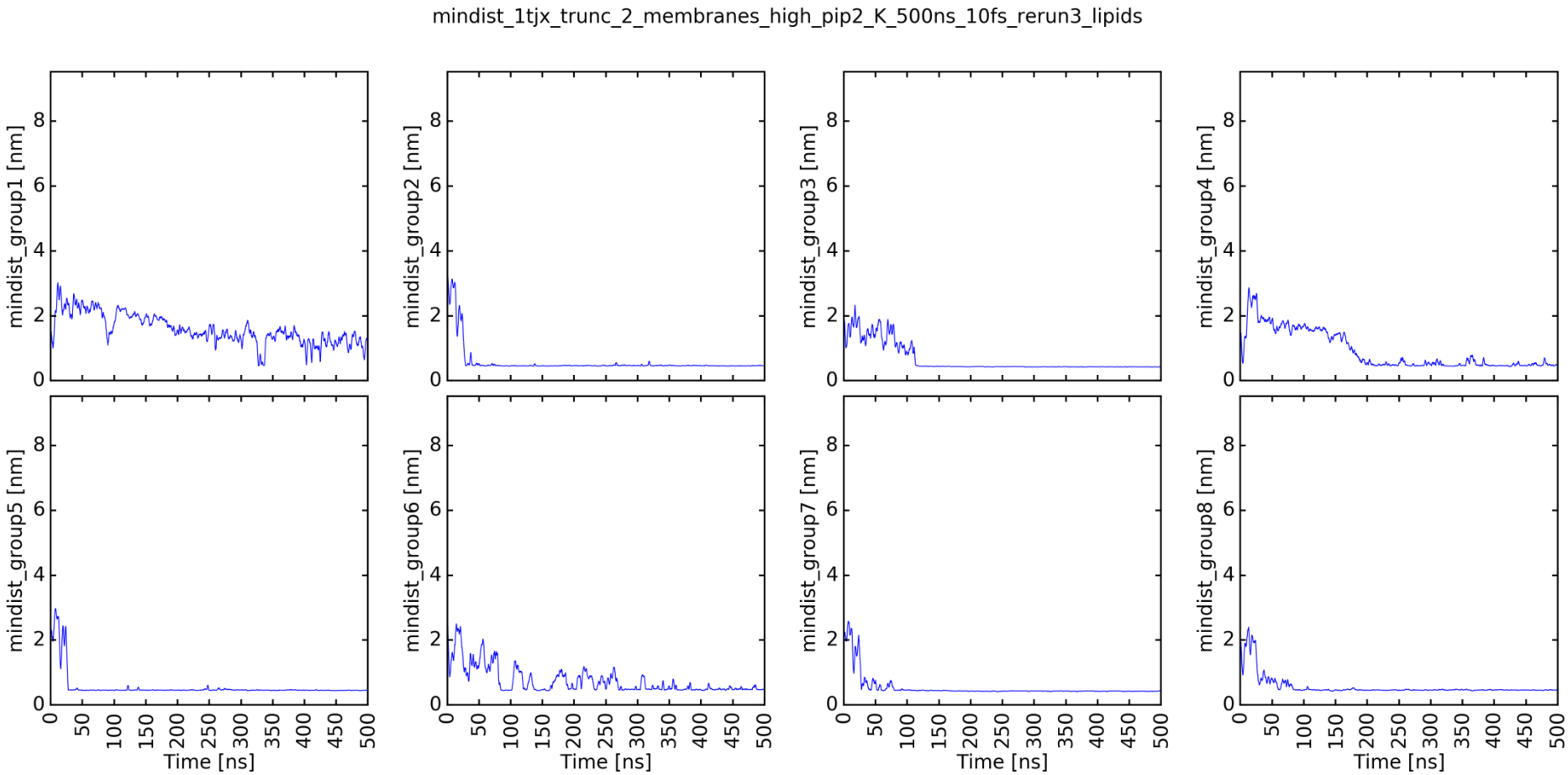

6.24 Distance between groups and membrane lipids. System 1tjx_trunc / HighPIP2 Low CA, Rerun3; Group1: Linker, Group2: Lateral1, Group3: Lysinestretch, Group4: Lateral2, Group5: ARG, Group6: Loops, Group7: oppARG, Group8: Rest; see Chapter 3.12.3

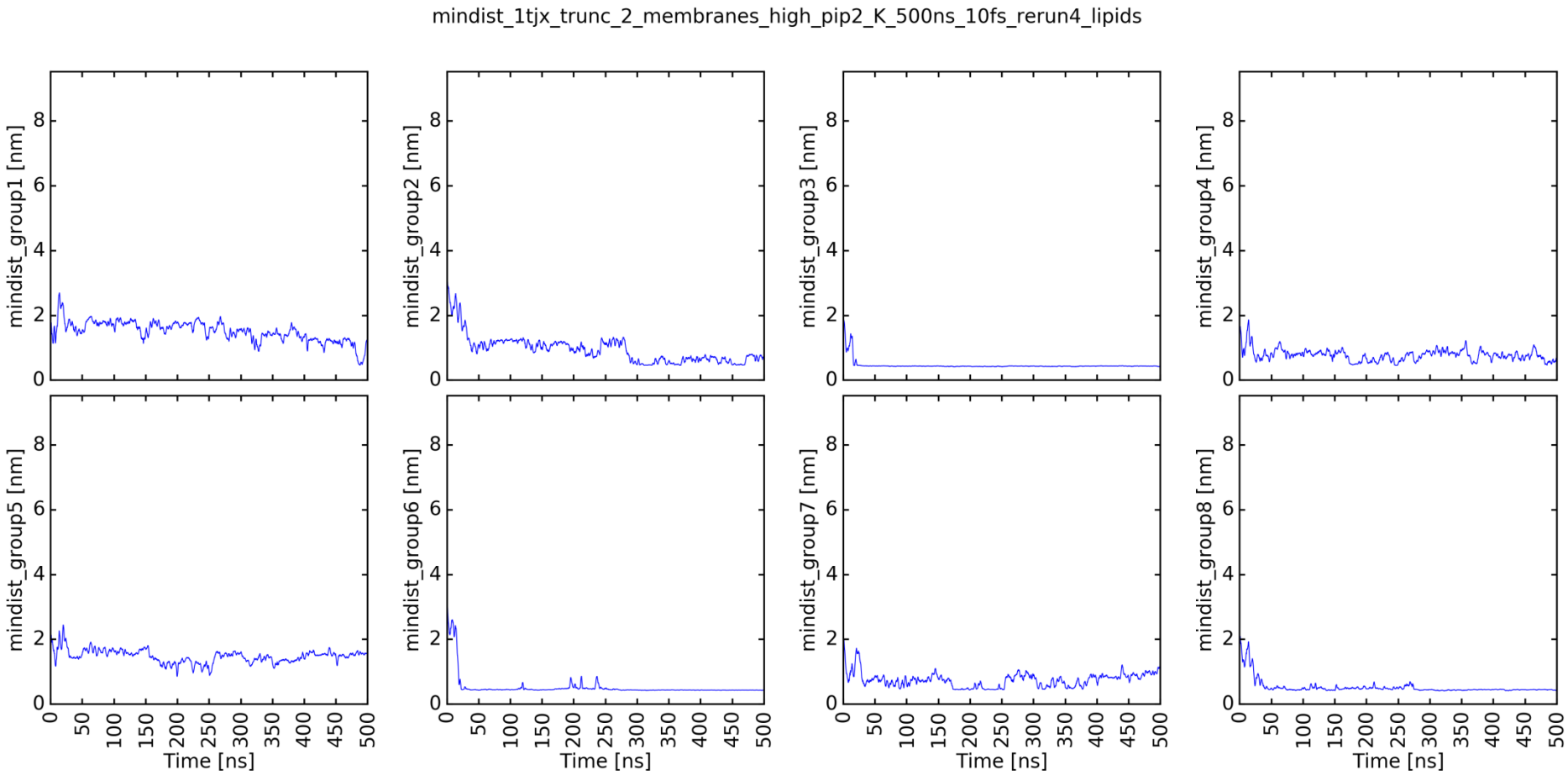

6.25 Distance between groups and membrane lipids. System 1tjx_trunc / HighPIP2 Low CA, Rerun4; Group1: Linker, Group2: Lateral1, Group3: Lysinestretch, Group4: Lateral2, Group5: ARG, Group6: Loops, Group7: oppARG, Group8: Rest; see Chapter 3.12.3

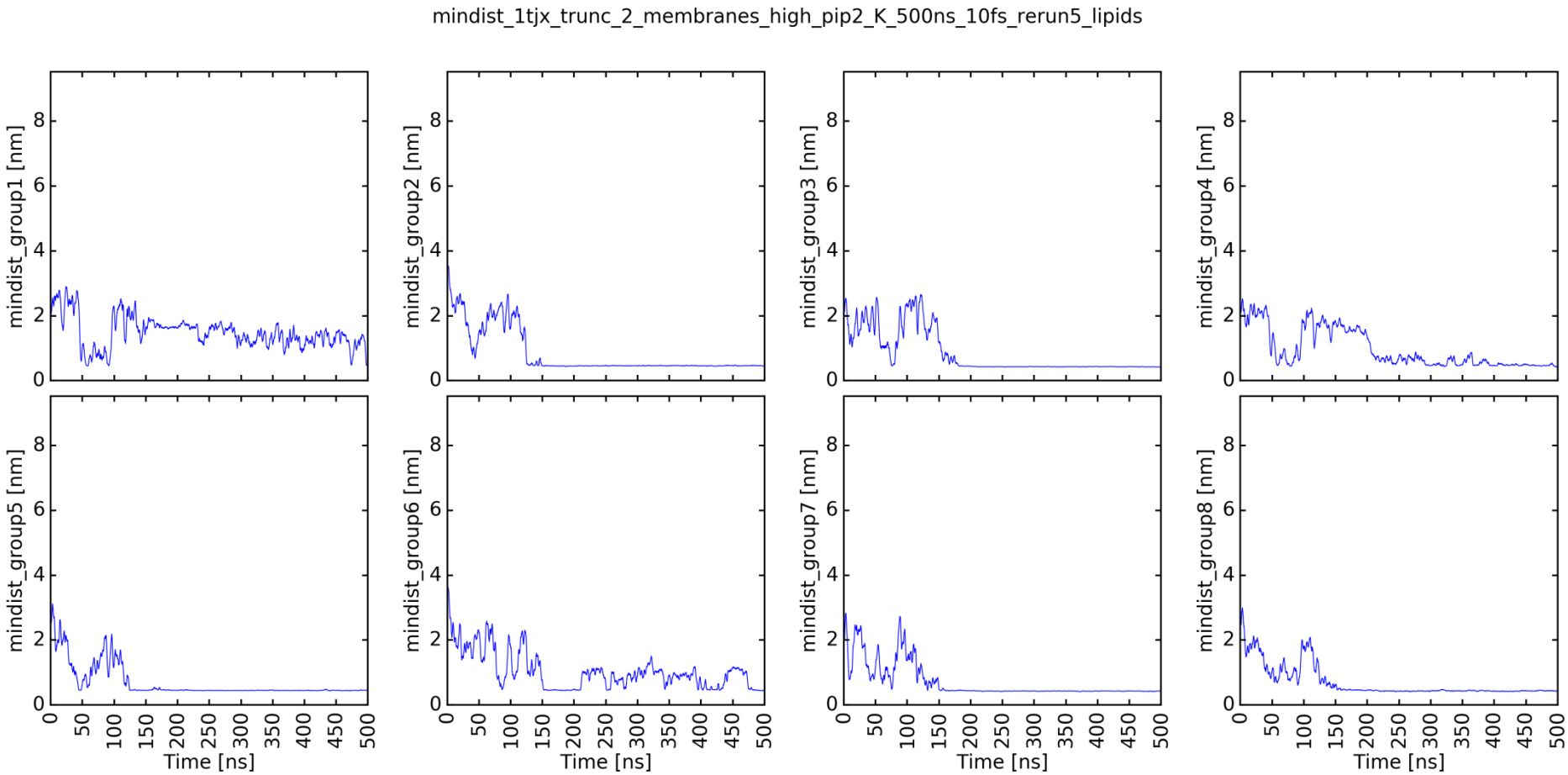

6.26 Distance between groups and membrane lipids. System 1tjx_trunc / HighPIP2 Low CA, Rerun5; Group1: Linker, Group2: Lateral1, Group3: Lysinestretch, Group4: Lateral2, Group5: ARG, Group6: Loops, Group7: oppARG, Group8: Rest; see Chapter 3.12.3

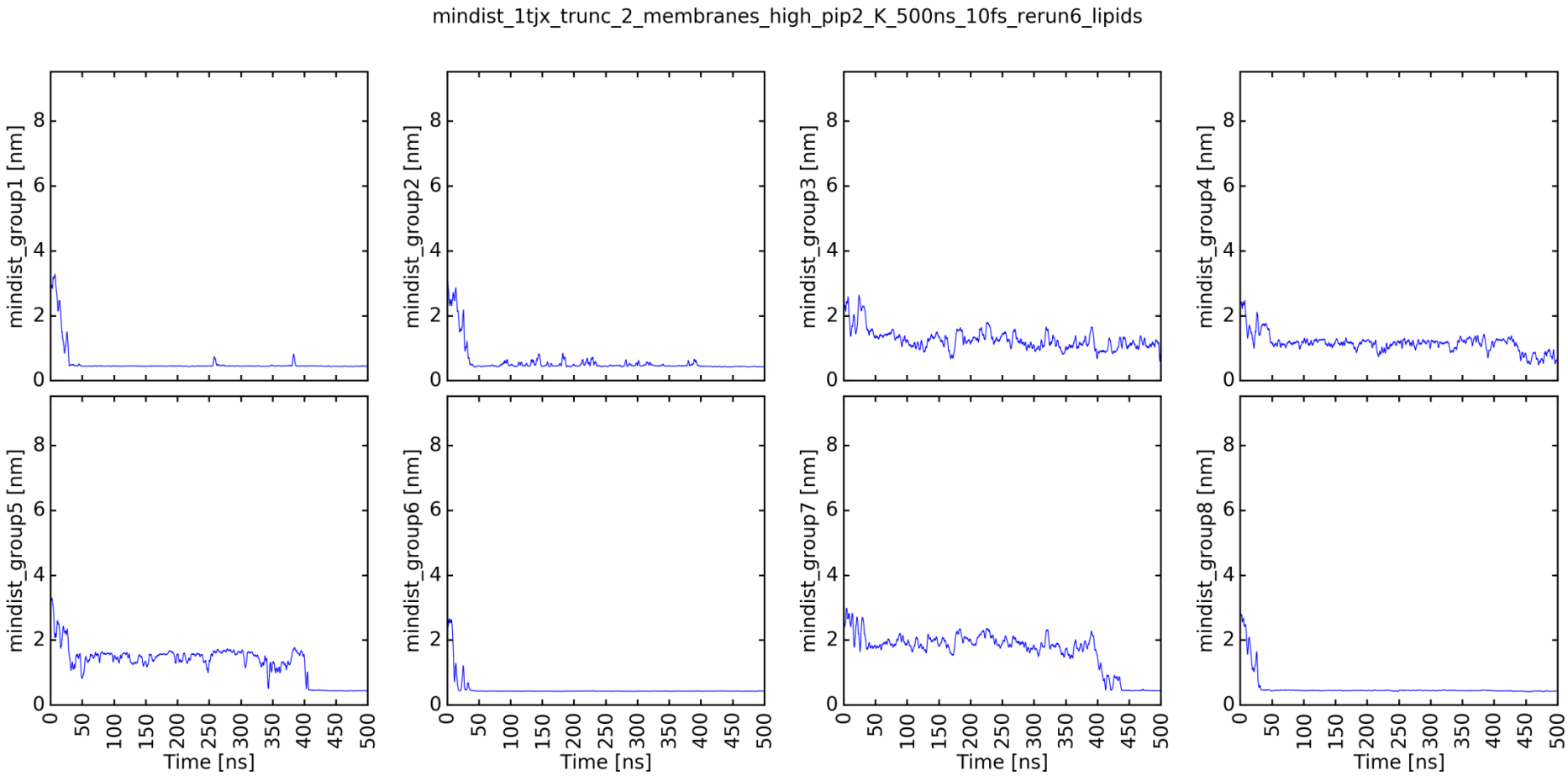

6.27 Distance between groups and membrane lipids. System 1tjx_trunc / HighPIP2 Low CA, Rerun6; Group1: Linker, Group2: Lateral1, Group3: Lysinestretch, Group4: Lateral2, Group5: ARG, Group6: Loops, Group7: oppARG, Group8: Rest; see Chapter 3.12.3

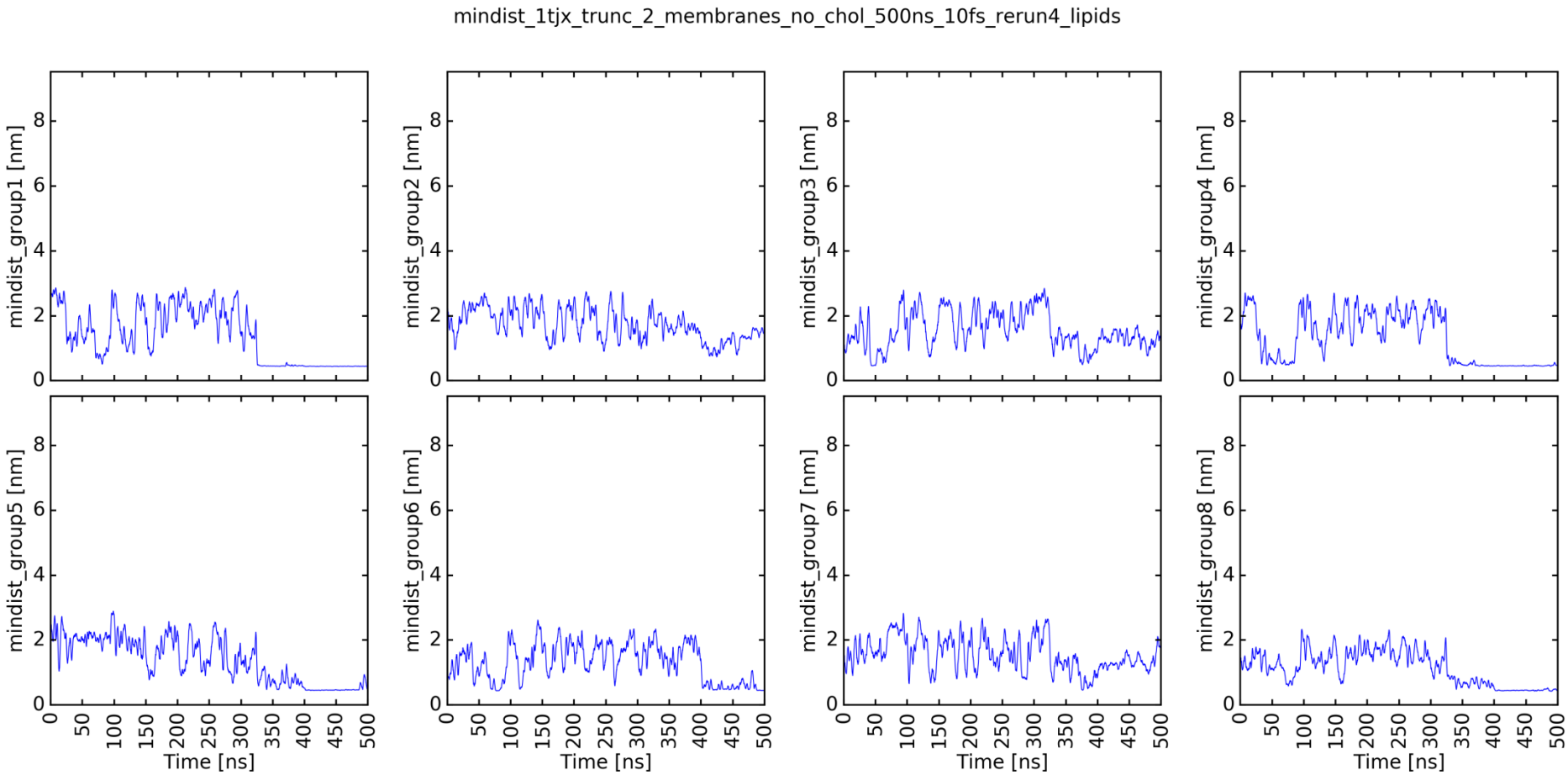

6.28 Distance between groups and membrane lipids. System 1tjx_trunc / NoChol, Rerun4; Group1: Linker, Group2: Lateral1, Group3: Lysinestretch, Group4: Lateral2, Group5: ARG, Group6: Loops, Group7: oppARG, Group8: Rest; see Chapter 3.12.3

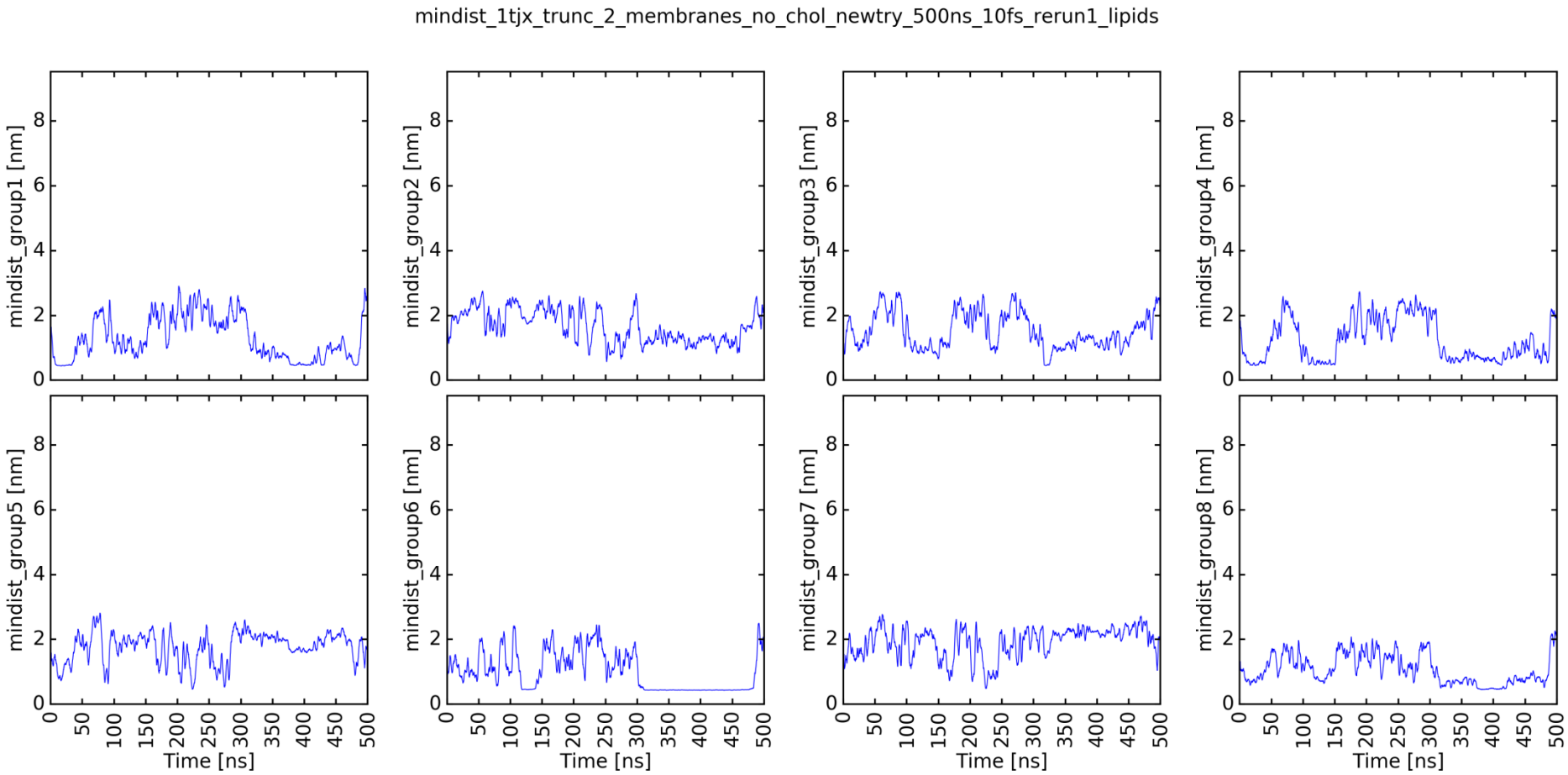

6.29 Distance between groups and membrane lipids. System 1tjx_trunc / NoChol Low CA, Rerun1; Group1: Linker, Group2: Lateral1, Group3: Lysinestretch, Group4: Lateral2, Group5: ARG, Group6: Loops, Group7: oppARG, Group8: Rest; see Chapter 3.12.3

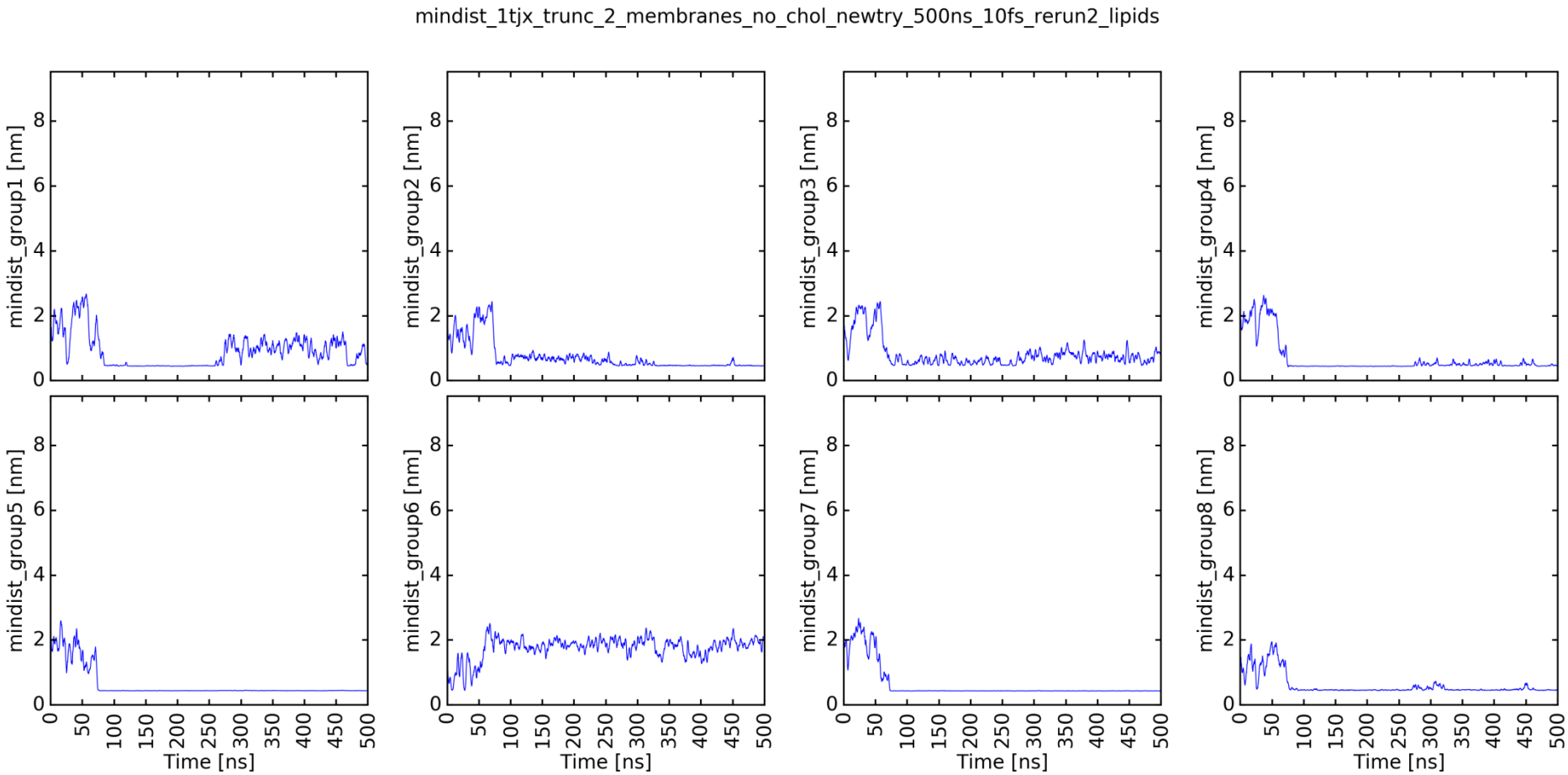

6.30 Distance between groups and membrane lipids. System 1tjx_trunc / NoChol Low CA, Rerun2; Group1: Linker, Group2: Lateral1, Group3: Lysinestretch, Group4: Lateral2, Group5: ARG, Group6: Loops, Group7: oppARG, Group8: Rest; see Chapter 3.12.3

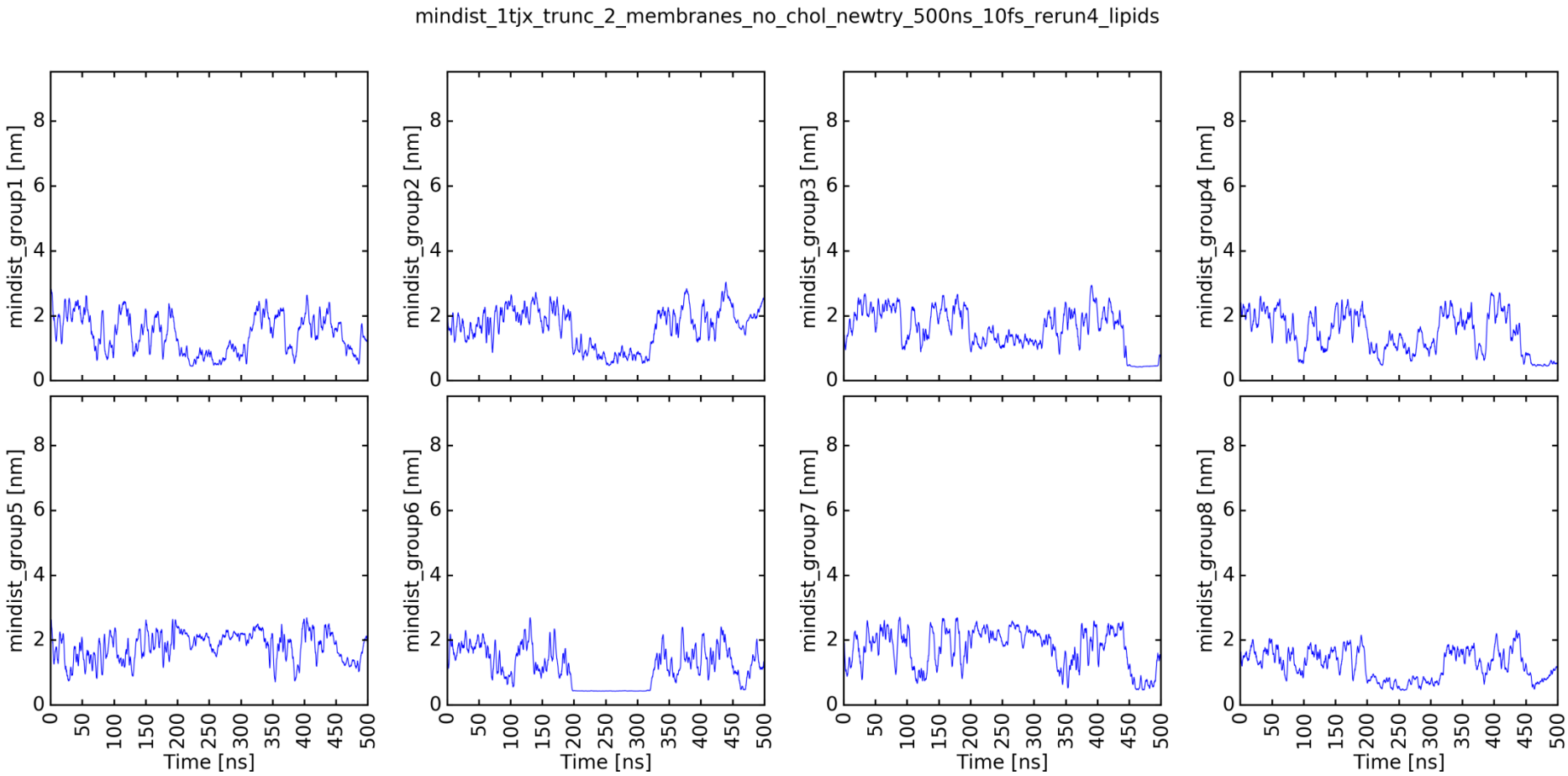

6.31 Distance between groups and membrane lipids. System 1tjx_trunc / NoChol Low CA, Rerun4; Group1: Linker, Group2: Lateral1, Group3: Lysinestretch, Group4: Lateral2, Group5: ARG, Group6: Loops, Group7: oppARG, Group8: Rest; see Chapter 3.12.3

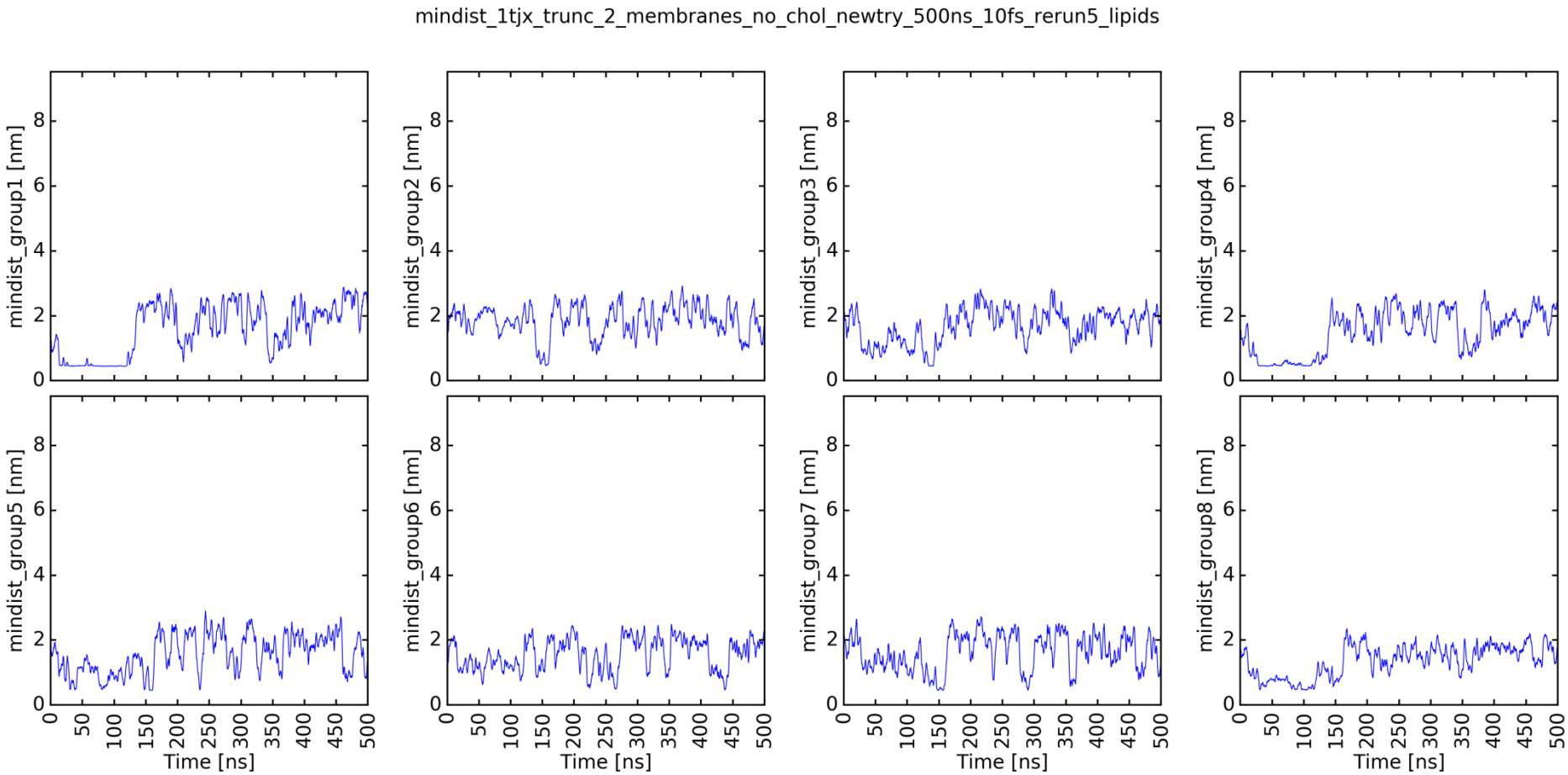

6.32 Distance between groups and membrane lipids. System 1tjx_trunc / NoChol Low CA, Rerun5; Group1: Linker, Group2: Lateral1, Group3: Lysinestretch, Group4: Lateral2, Group5: ARG, Group6: Loops, Group7: oppARG, Group8: Rest; see Chapter 3.12.3

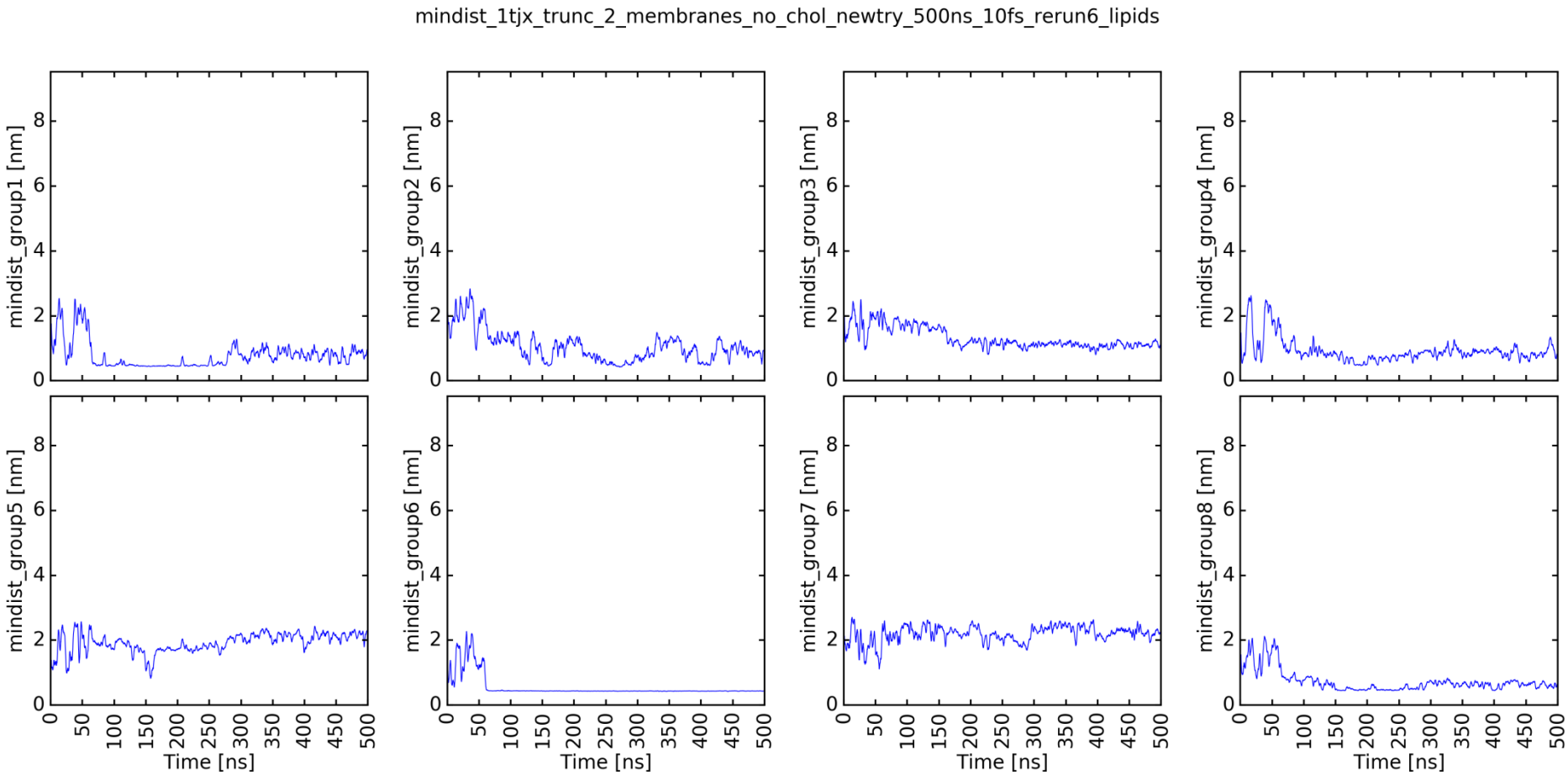

6.33 Distance between groups and membrane lipids. System 1tjx_trunc / NoChol Low CA, Rerun6; Group1: Linker, Group2: Lateral1, Group3: Lysinestretch, Group4: Lateral2, Group5: ARG, Group6: Loops, Group7: oppARG, Group8: Rest; see Chapter 3.12.3

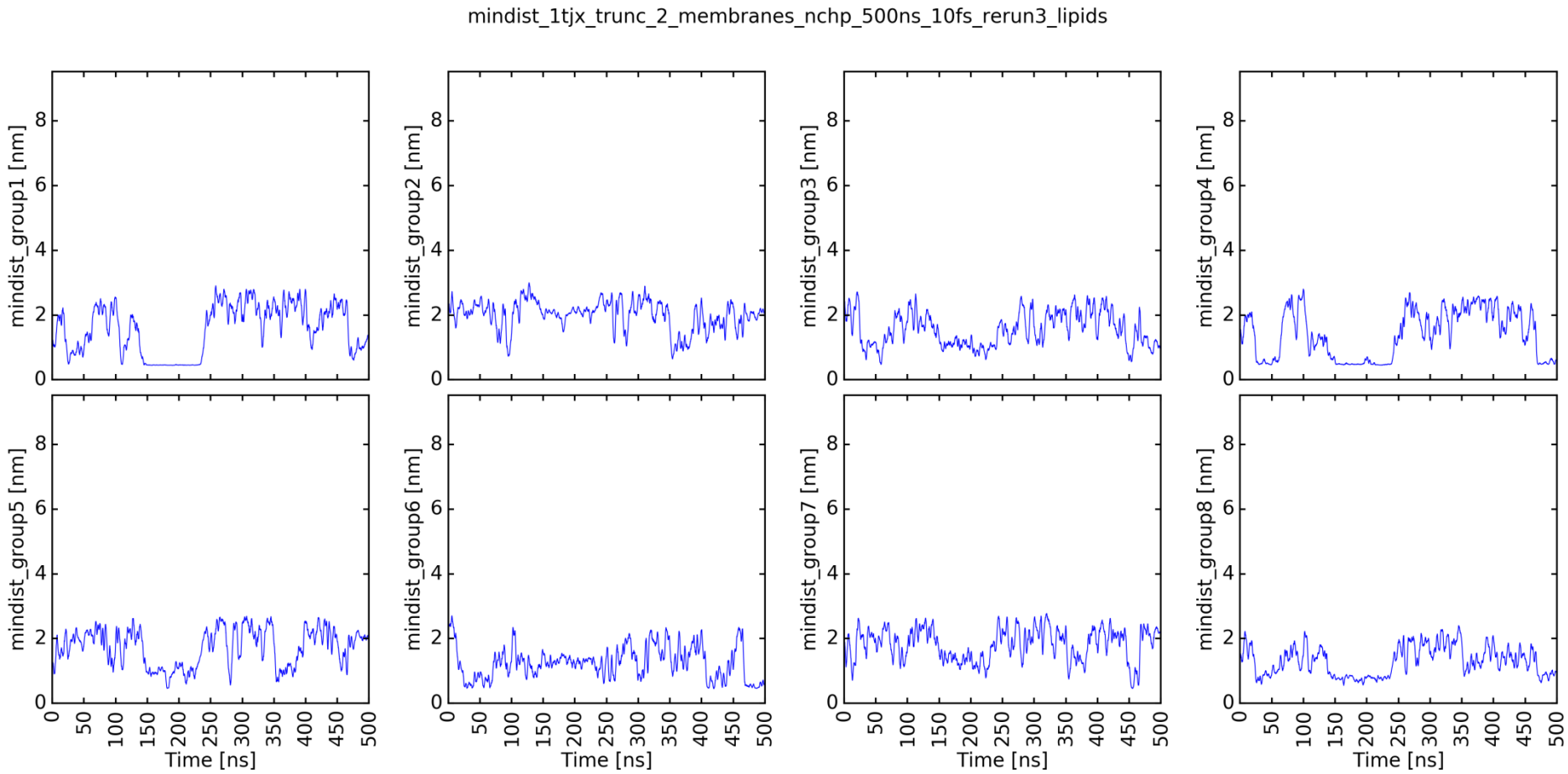

6.34 Distance between groups and membrane lipids. System 1tjx_trunc / NCHP, Rerun3; Group1: Linker, Group2: Lateral1, Group3: Lysinestretch, Group4: Lateral2, Group5: ARG, Group6: Loops, Group7: oppARG, Group8: Rest; see Chapter 3.12.3

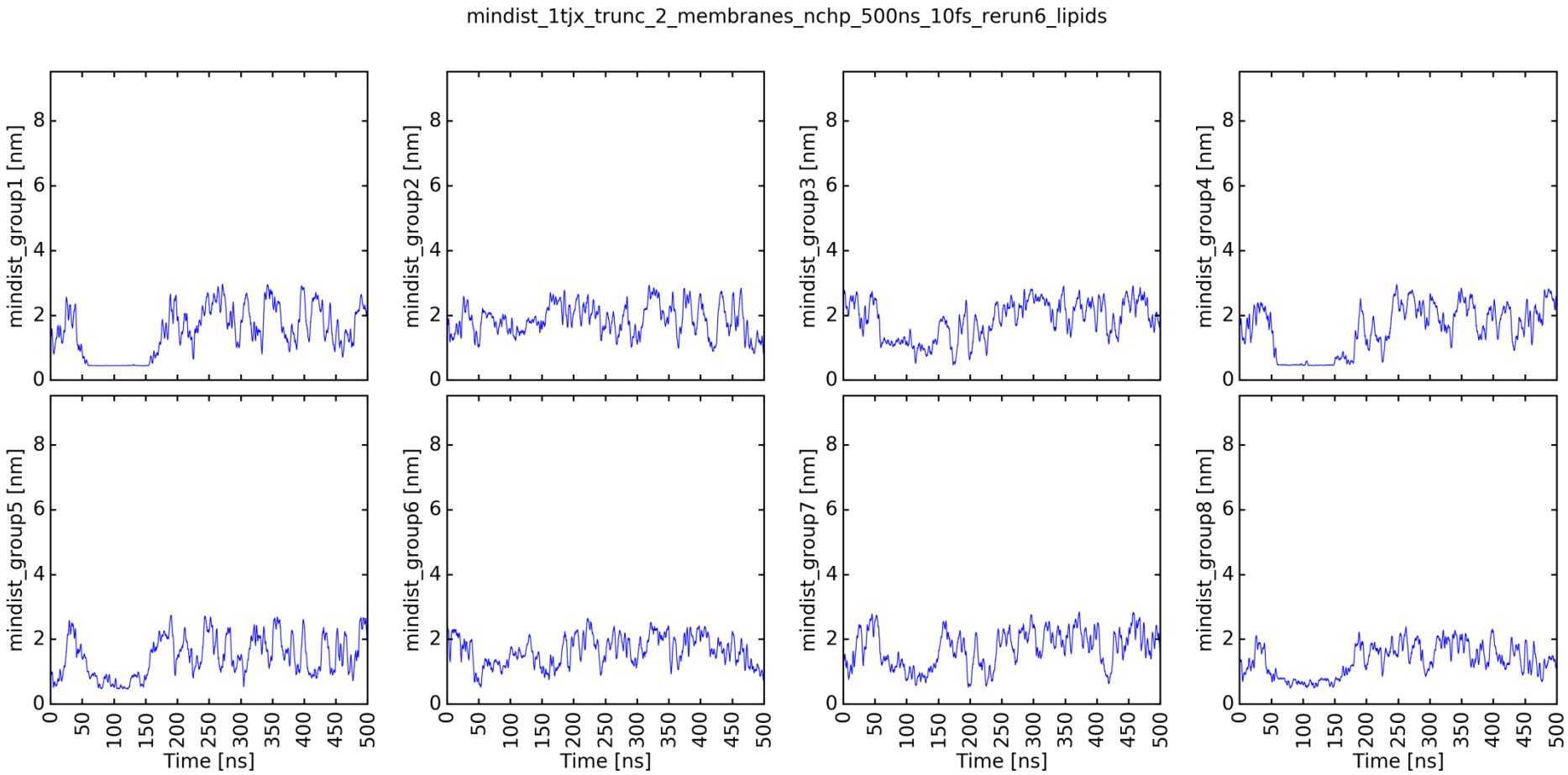

6.35 Distance between groups and membrane lipids. System 1tjx_trunc / NCHP, Rerun6; Group1: Linker, Group2: Lateral1, Group3: Lysinestretch, Group4: Lateral2, Group5: ARG, Group6: Loops, Group7: oppARG, Group8: Rest; see Chapter 3.12.3

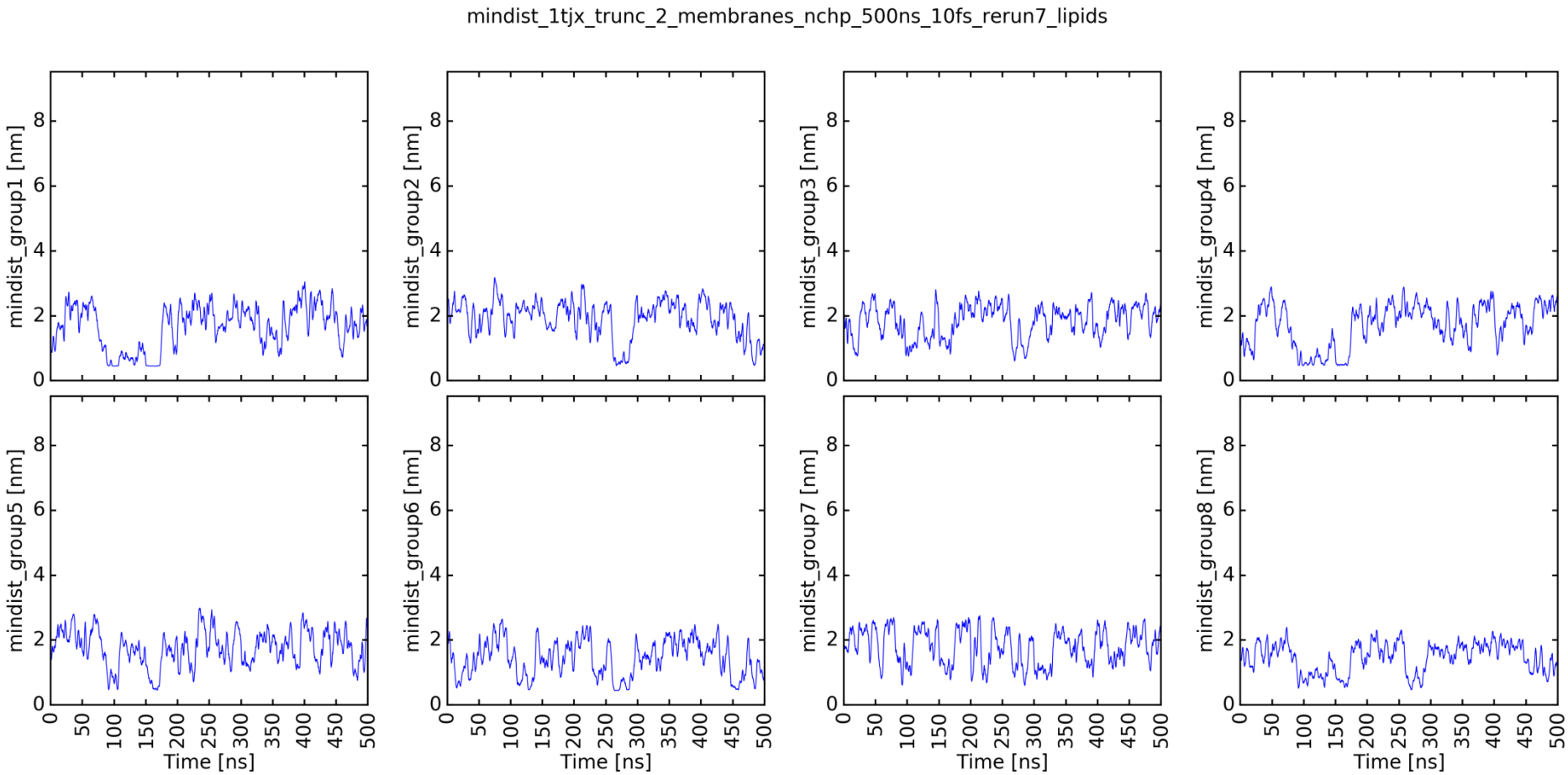

6.36 Distance between groups and membrane lipids. System 1tjx_trunc / NCHP, Rerun7; Group1: Linker, Group2: Lateral1, Group3: Lysinestretch, Group4: Lateral2, Group5: ARG, Group6: Loops, Group7: oppARG, Group8: Rest; see Chapter 3.12.3

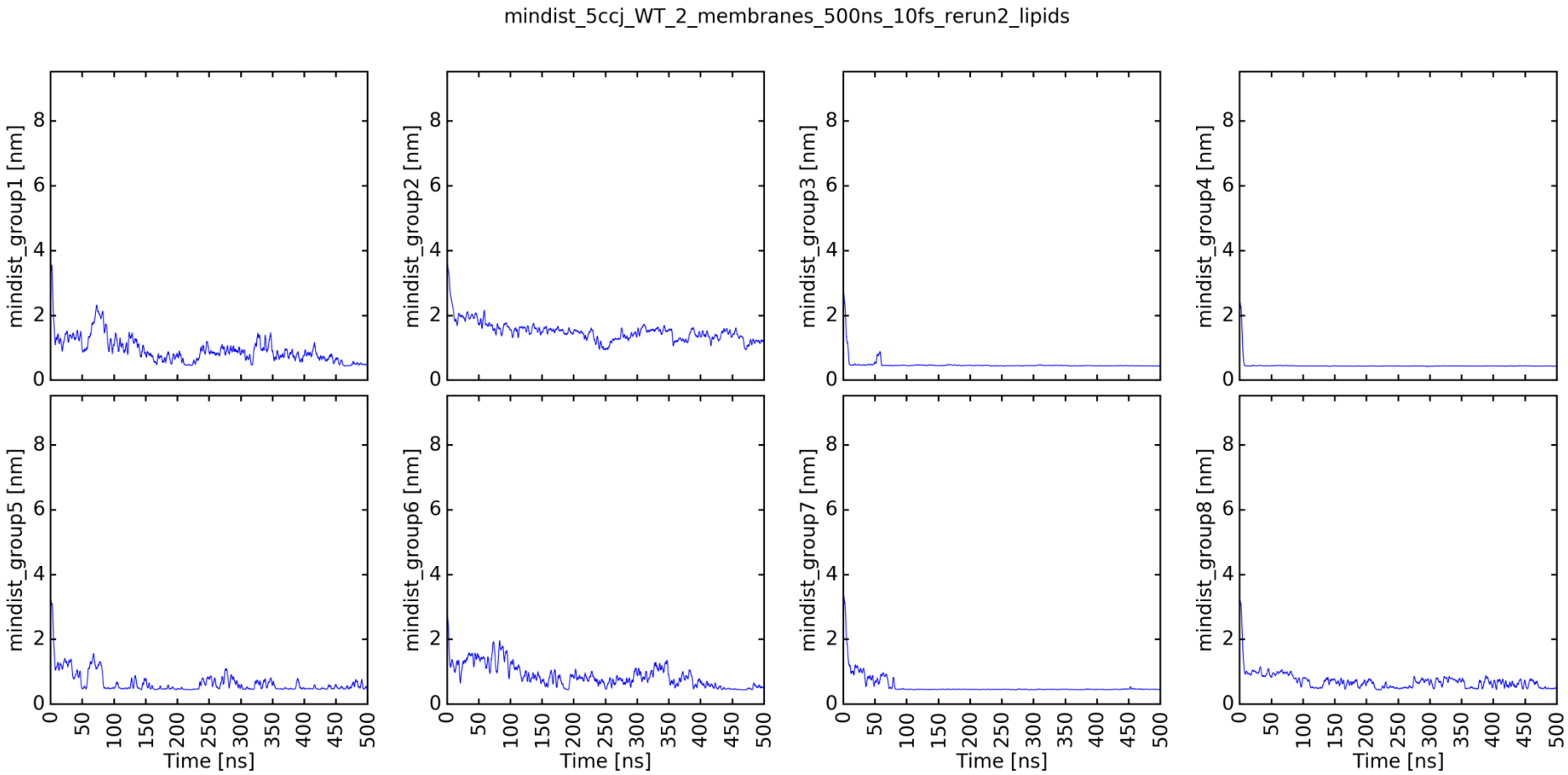

6.37 Distance between groups and membrane lipids. System 5ccj_WT /Standard 895, Rerun2; Group1: Linker, Group2: Lateral1, Group3: Lysinestretch, Group4: Lateral2, Group5: ARG, Group6: Loops, Group7: oppARG, Group8: Rest; see Chapter 3.12.3

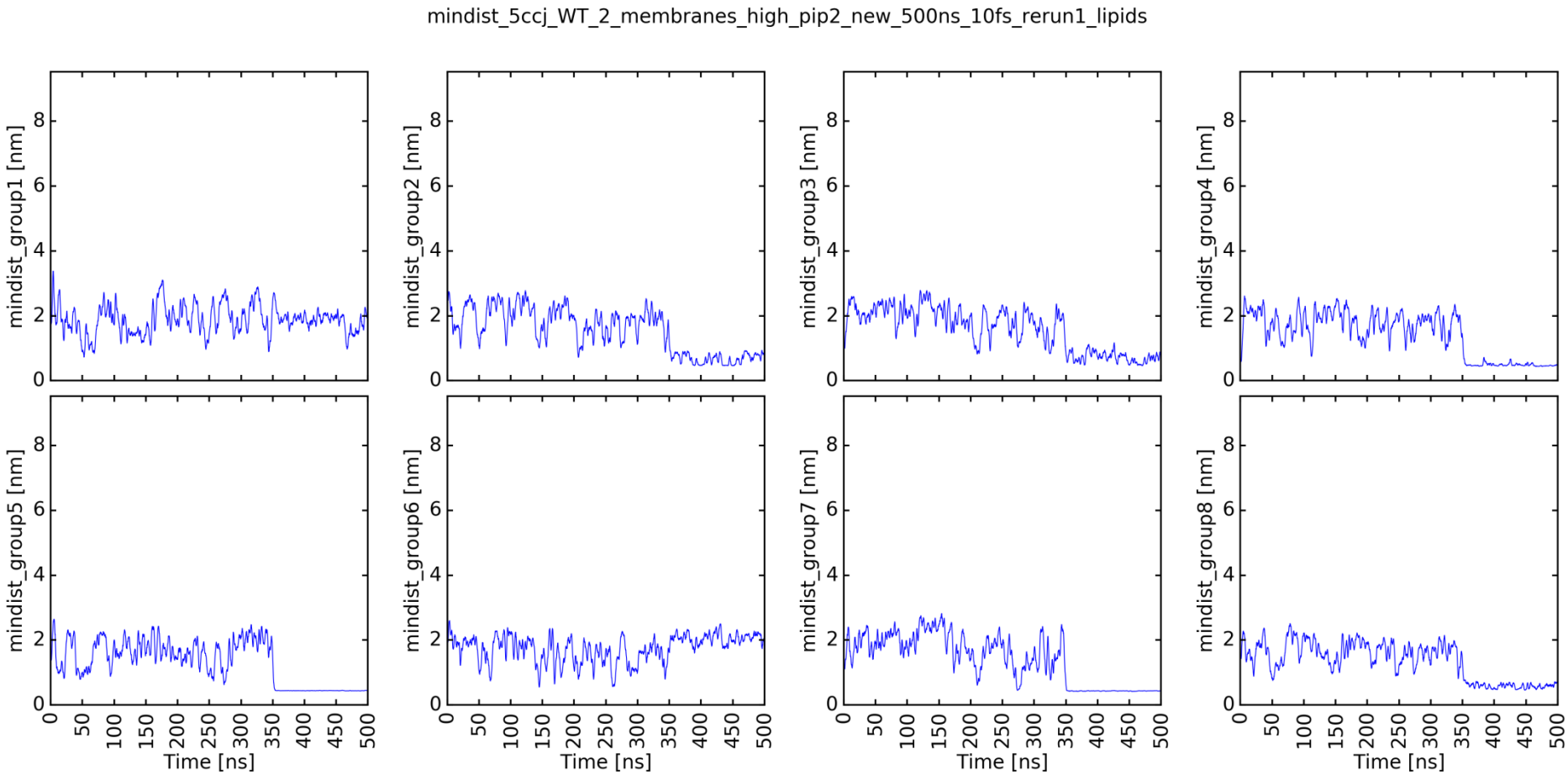

6.38 Distance between groups and membrane lipids. System 5ccj_WT /High PIP2, Rerun1; Group1: Linker, Group2: Lateral1, Group3: Lysinestretch, Group4: Lateral2, Group5: ARG, Group6: Loops, Group7: oppARG, Group8: Rest; see Chapter 3.12.3

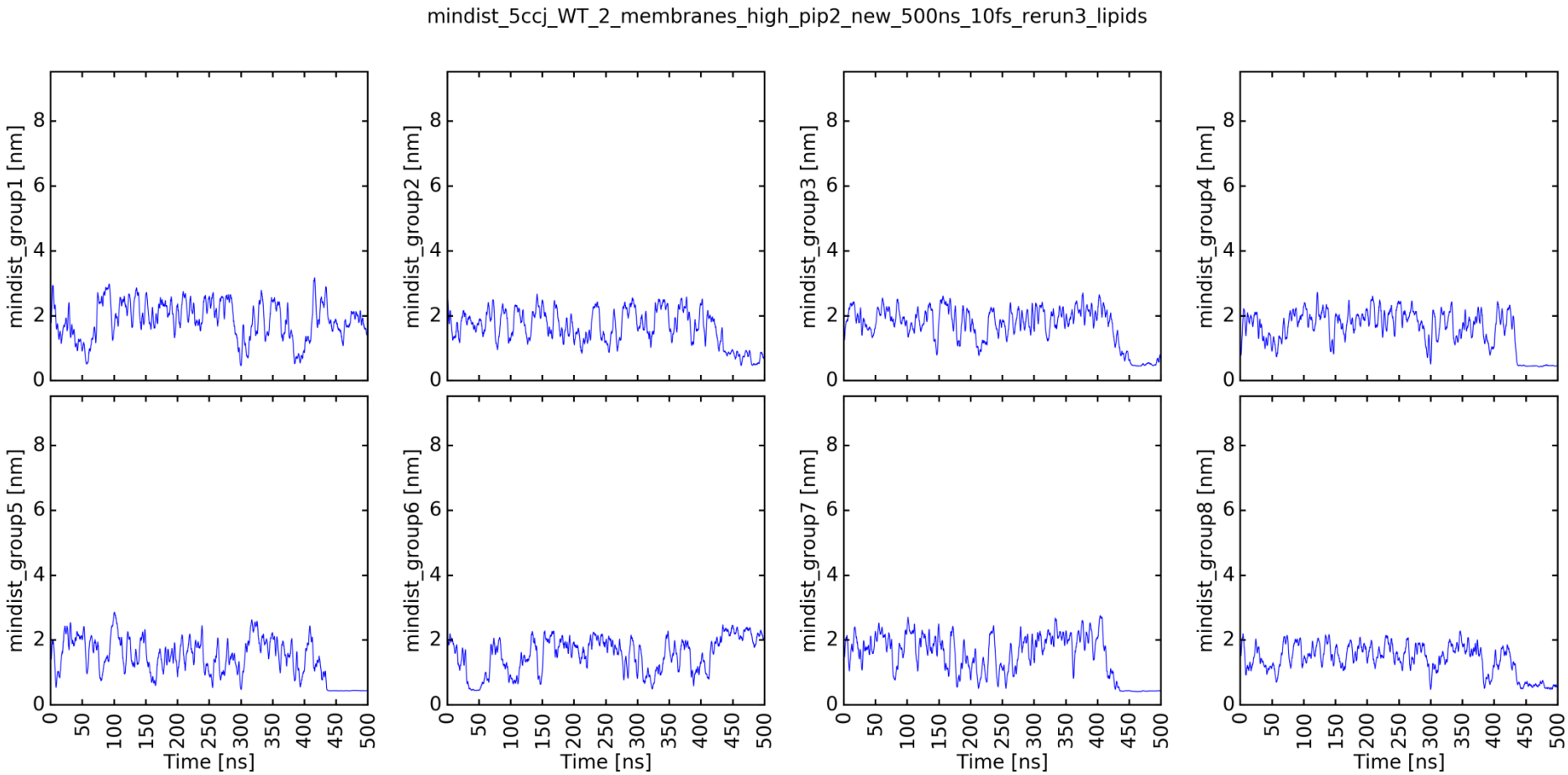

6.39 Distance between groups and membrane lipids. System 5ccj_WT /High PIP2, Rerun3; Group1: Linker, Group2: Lateral1, Group3: Lysinestretch, Group4: Lateral2, Group5: ARG, Group6: Loops, Group7: oppARG, Group8: Rest; see Chapter 3.12.3

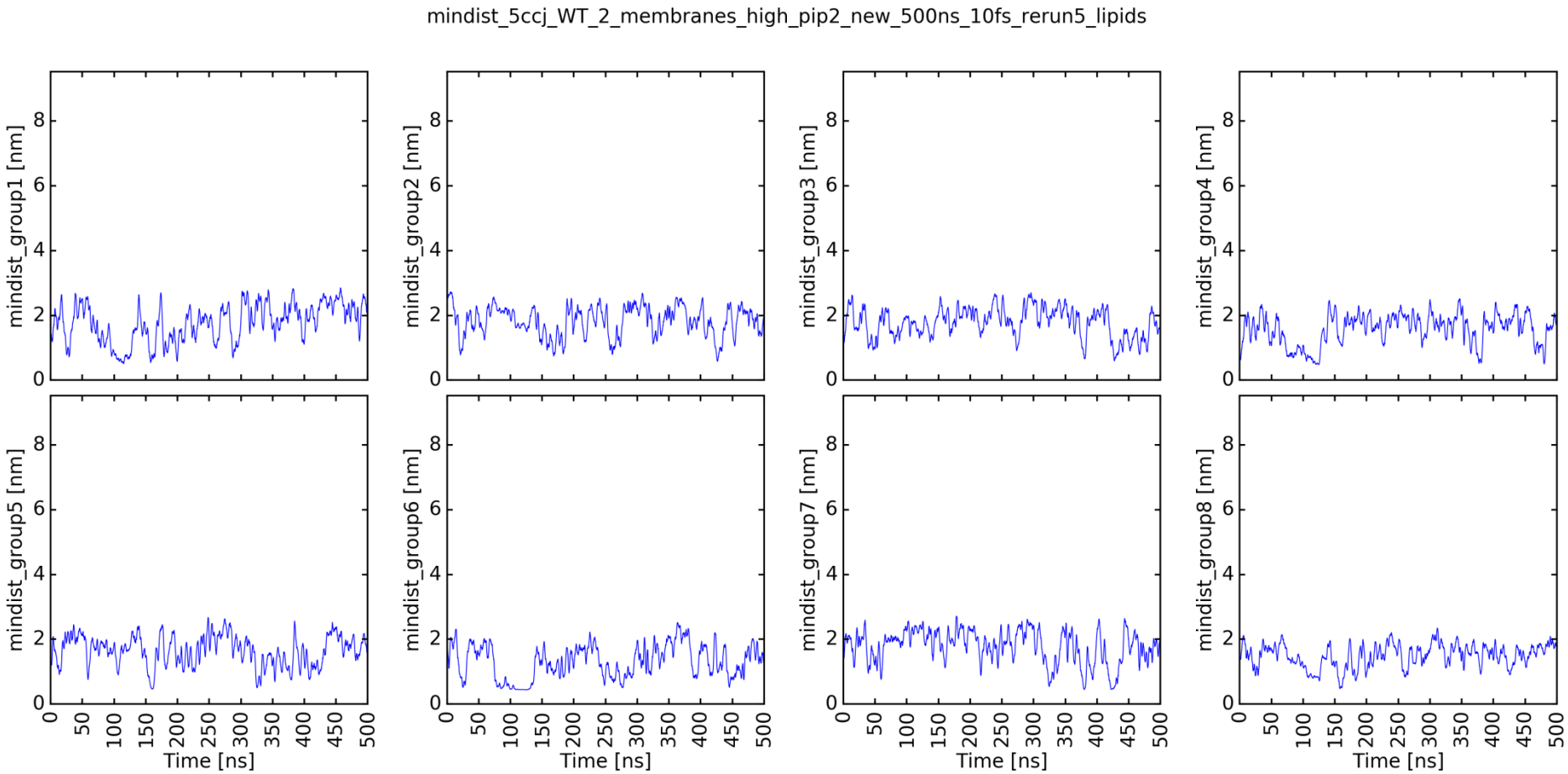

6.40 Distance between groups and membrane lipids. System 5ccj_WT /High PIP2, Rerun5; Group1: Linker, Group2: Lateral1, Group3: Lysinestretch, Group4: Lateral2, Group5: ARG, Group6: Loops, Group7: oppARG, Group8: Rest; see Chapter 3.12.3

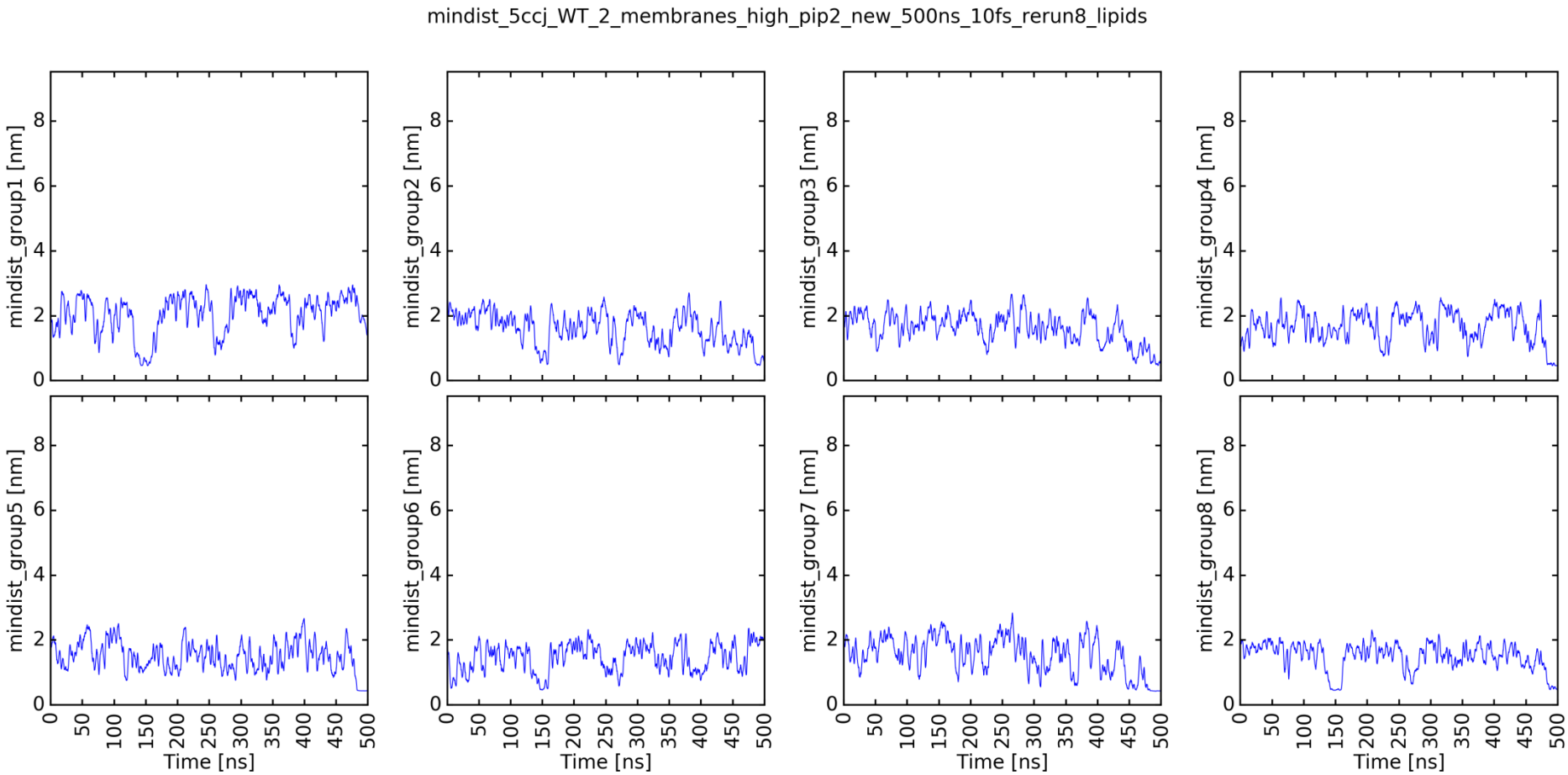

6.41 Distance between groups and membrane lipids. System 5ccj_WT /High PIP2, Rerun8; Group1: Linker, Group2: Lateral1, Group3: Lysinestretch, Group4: Lateral2, Group5: ARG, Group6: Loops, Group7: oppARG, Group8: Rest; see Chapter 3.12.3

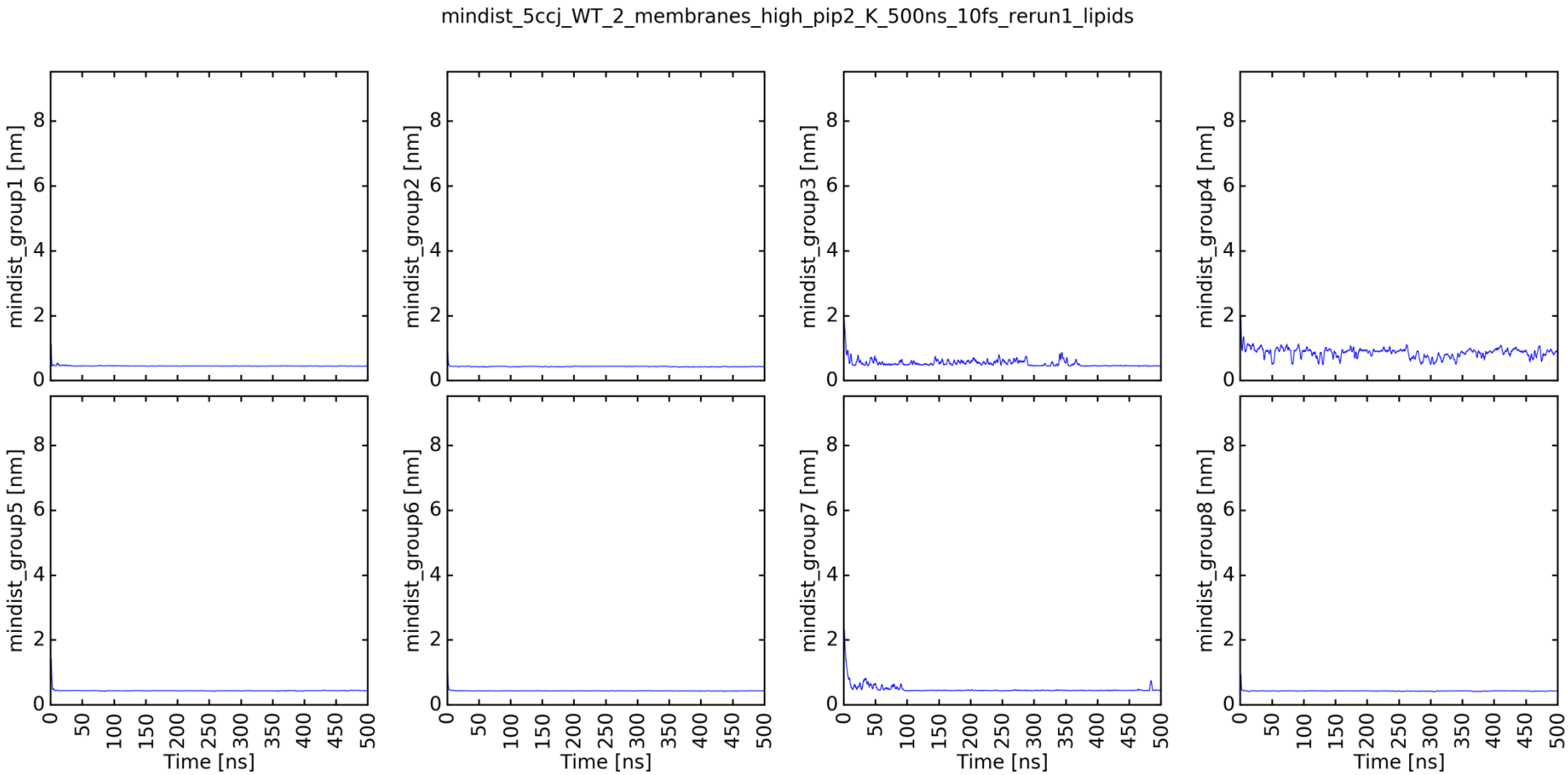

6.42 Distance between groups and membrane lipids. System 5ccj_WT /High PIP2 Low CA, Rerun1; Group1: Linker, Group2: Lateral1, Group3: Lysinestretch, Group4: Lateral2, Group5: ARG, Group6: Loops, Group7: oppARG, Group8: Rest; see Chapter 3.12.3

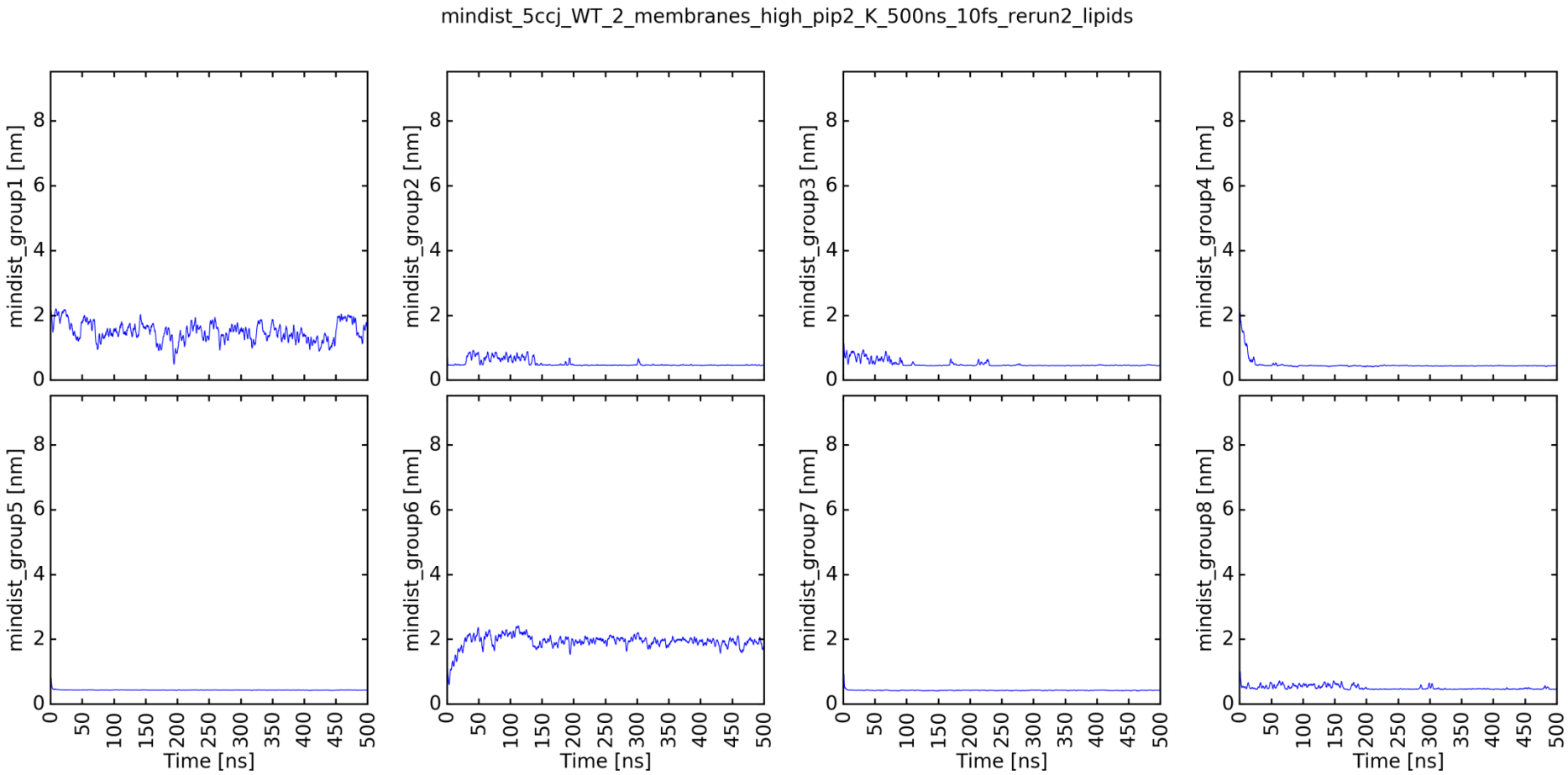

6.43 Distance between groups and membrane lipids. System 5ccj_WT /High PIP2 Low CA, Rerun2; Group1: Linker, Group2: Lateral1, Group3: Lysinestretch, Group4: Lateral2, Group5: ARG, Group6: Loops, Group7: oppARG, Group8: Rest; see Chapter 3.12.3

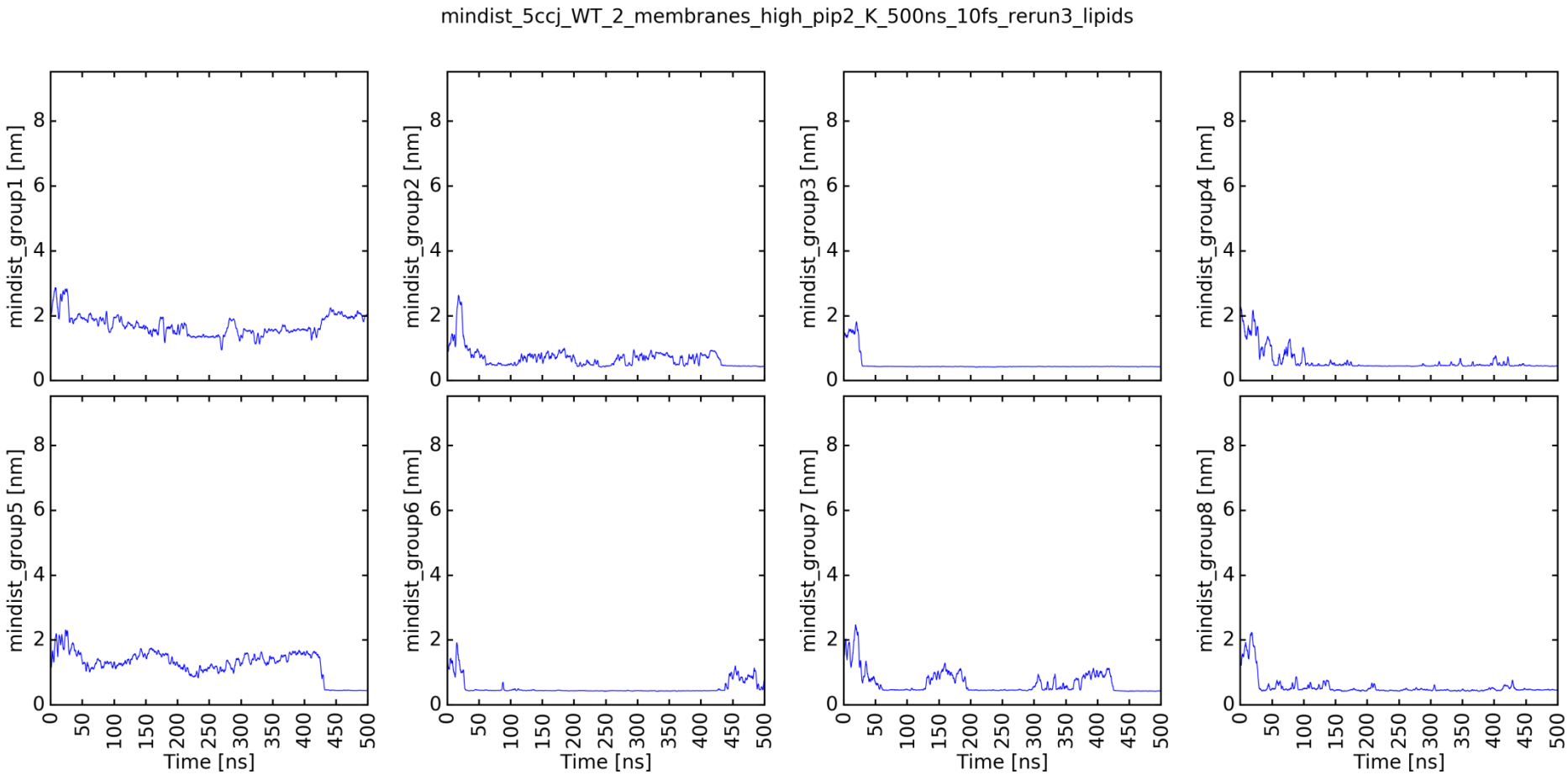

6.44 Distance between groups and membrane lipids. System 5ccj_WT /High PIP2 Low CA, Rerun3; Group1: Linker, Group2: Lateral1, Group3: Lysinestretch, Group4: Lateral2, Group5: ARG, Group6: Loops, Group7: oppARG, Group8: Rest; see Chapter 3.12.3

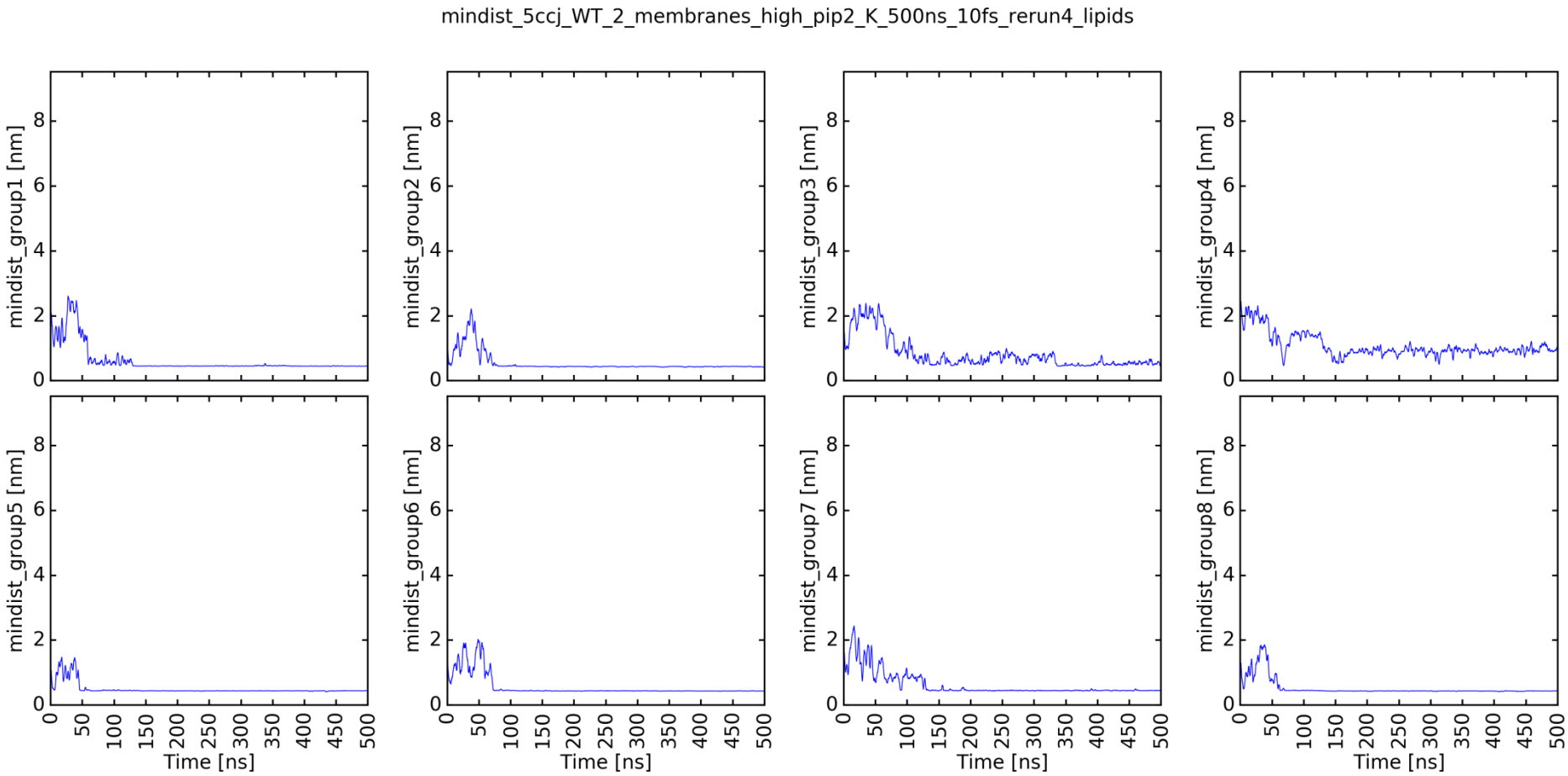

6.45 Distance between groups and membrane lipids. System 5ccj_WT /High PIP2 Low CA, Rerun4; Group1: Linker, Group2: Lateral1, Group3: Lysinestretch, Group4: Lateral2, Group5: ARG, Group6: Loops, Group7: oppARG, Group8: Rest; see Chapter 3.12.3

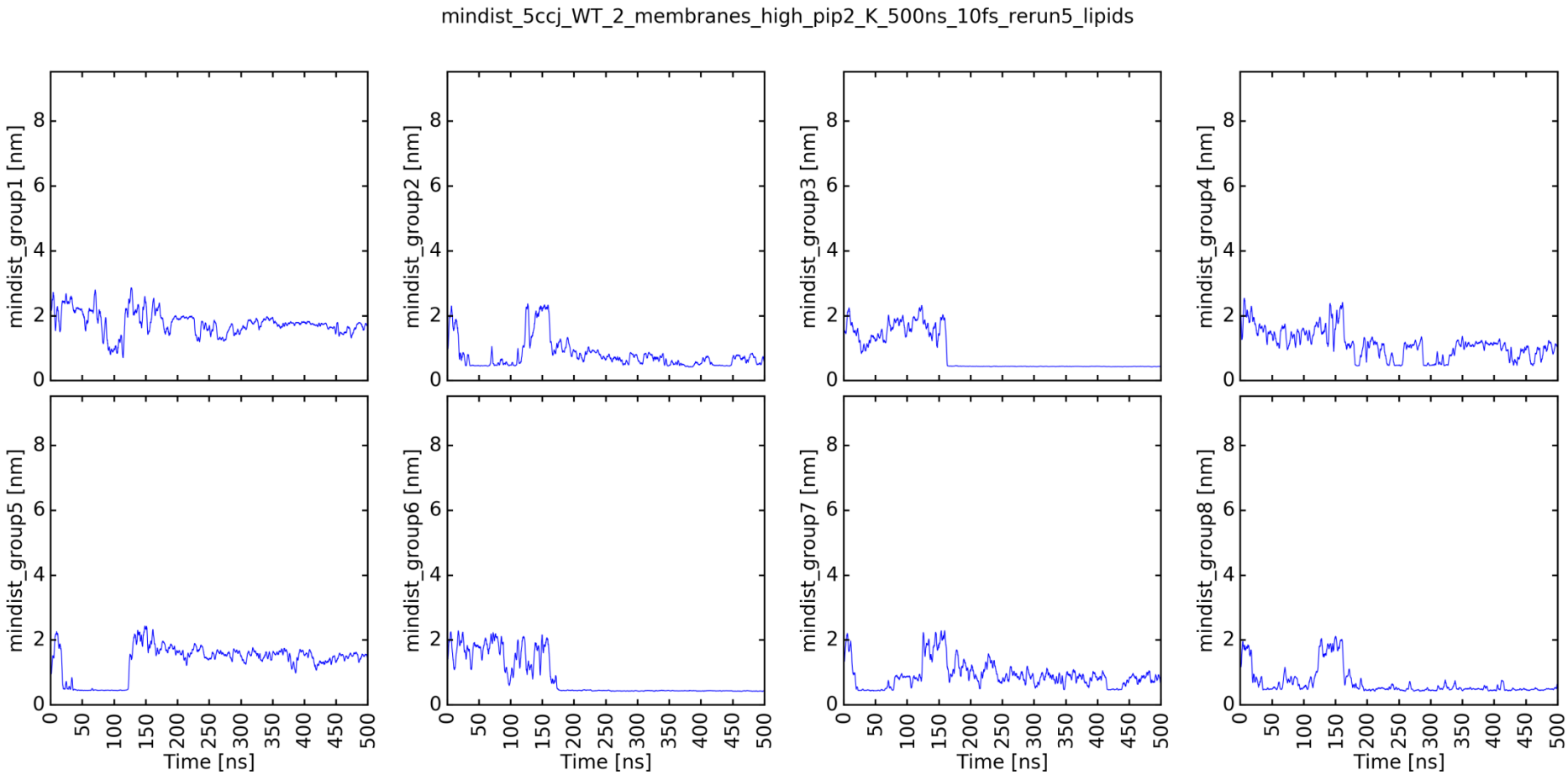

6.46 Distance between groups and membrane lipids. System 5ccj_WT /High PIP2 Low CA, Rerun5; Group1: Linker, Group2: Lateral1, Group3: Lysinestretch, Group4: Lateral2, Group5: ARG, Group6: Loops, Group7: oppARG, Group8: Rest; see Chapter 3.12.3

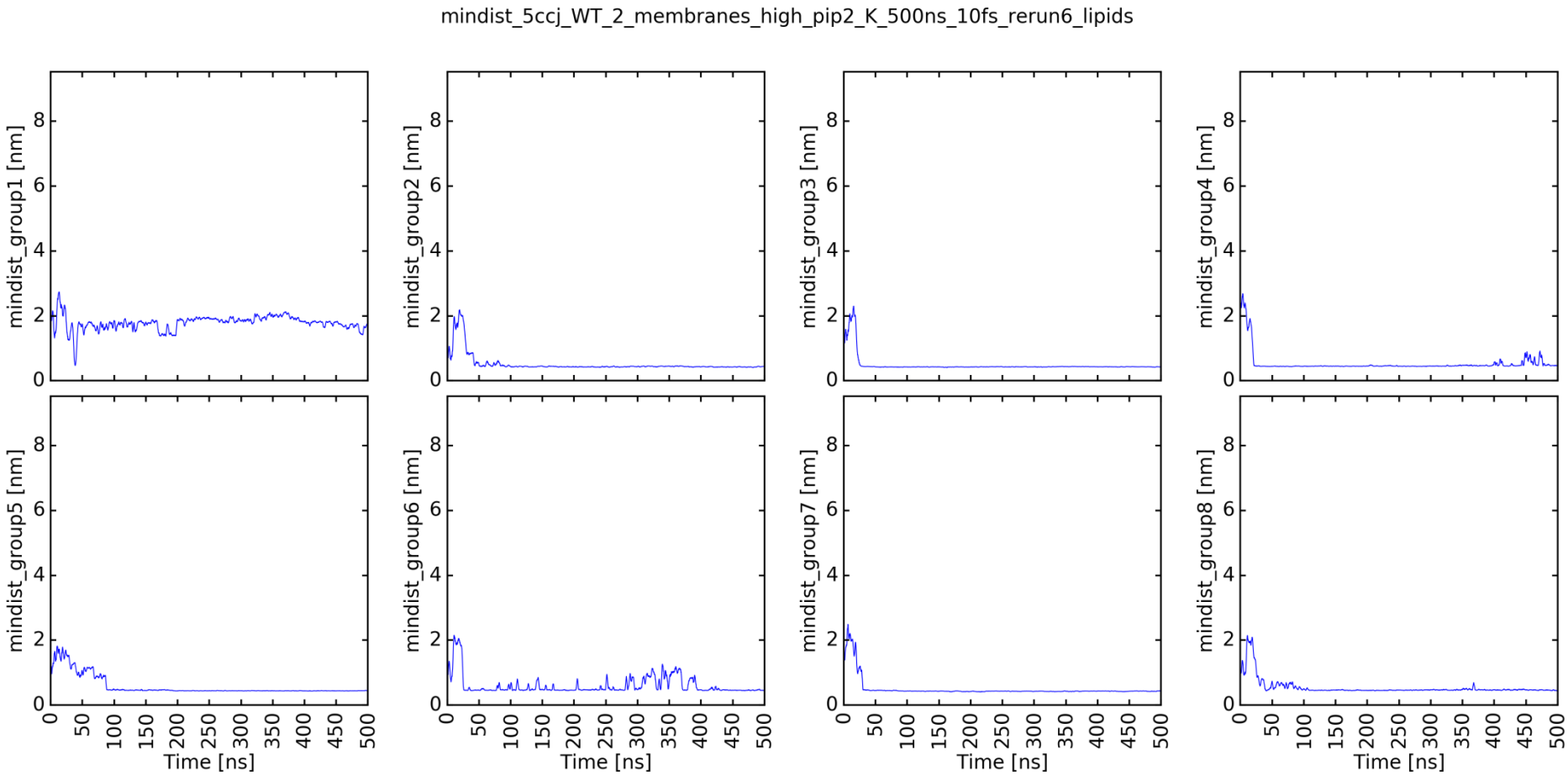

6.47 Distance between groups and membrane lipids. System 5ccj_WT /High PIP2 Low CA, Rerun6; Group1: Linker, Group2: Lateral1, Group3: Lysinestretch, Group4: Lateral2, Group5: ARG, Group6: Loops, Group7: oppARG, Group8: Rest; see Chapter 3.12.3

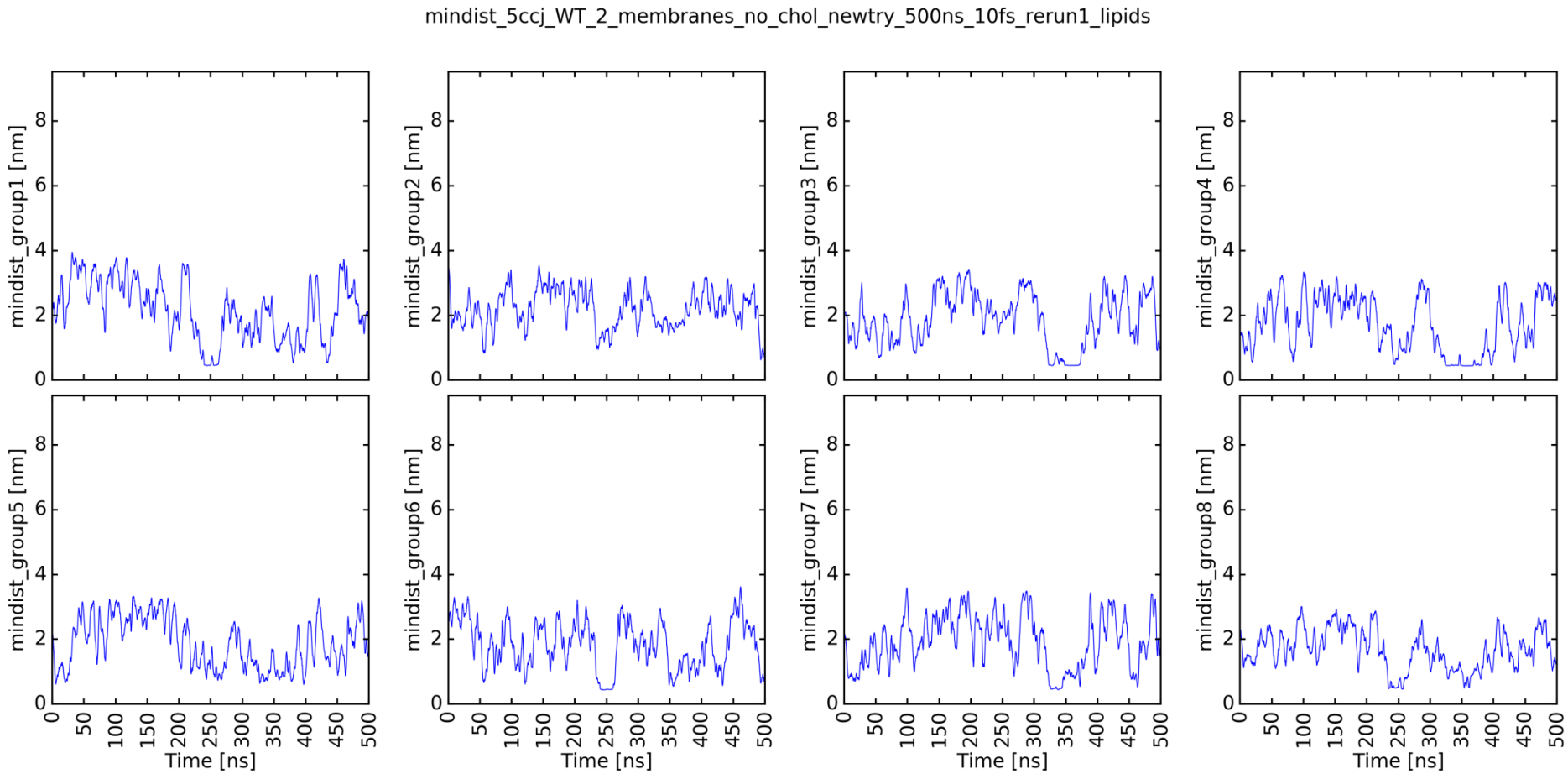

6.48 Distance between groups and membrane lipids. System 5ccj_WT /NoChol Low CA, Rerun1; Group1: Linker, Group2: Lateral1, Group3: Lysinestretch, Group4: Lateral2, Group5: ARG, Group6: Loops, Group7: oppARG, Group8: Rest; see Chapter 3.12.3

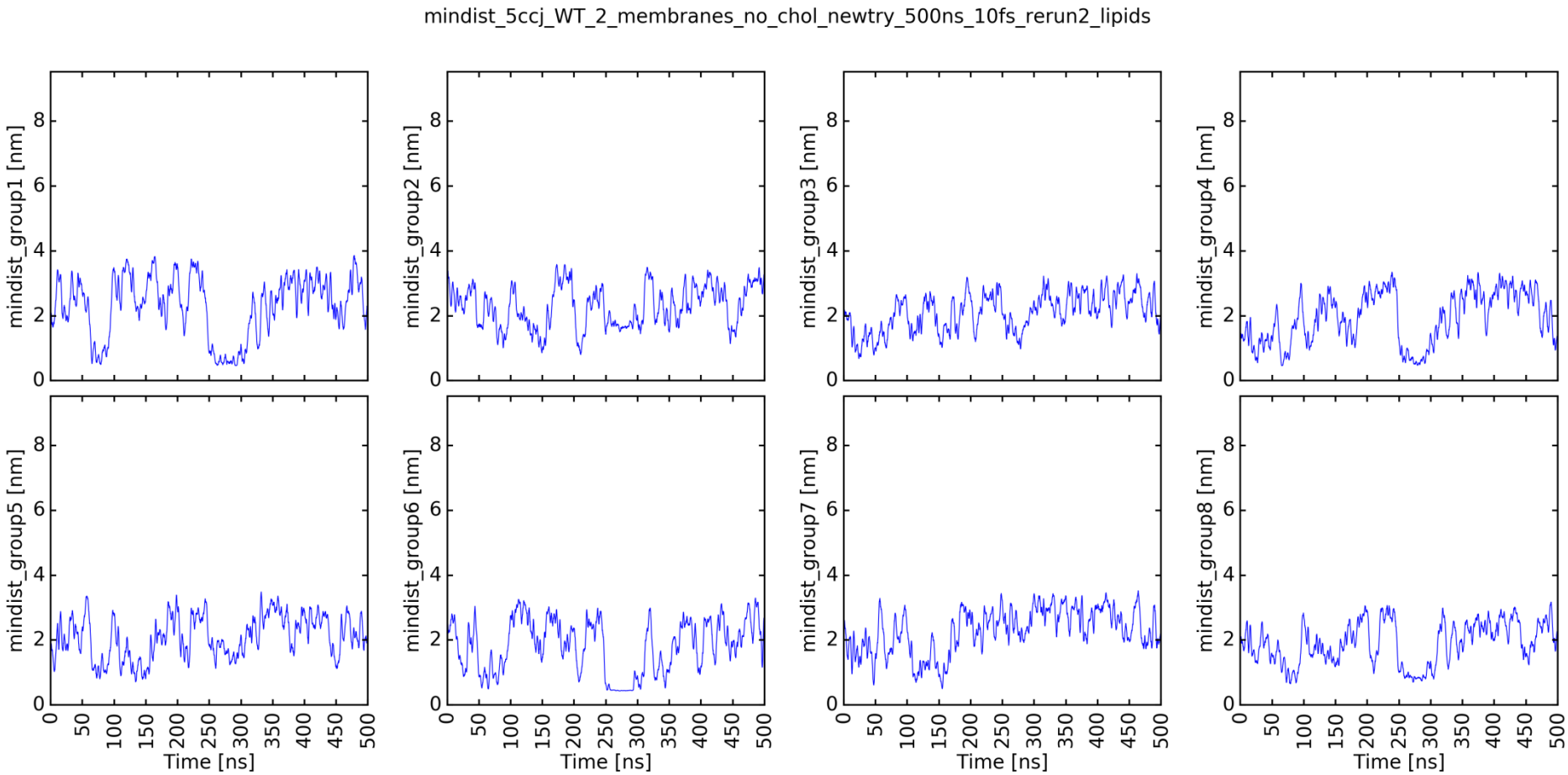

6.49 Distance between groups and membrane lipids. System 5ccj_WT /NoChol Low CA, Rerun2; Group1: Linker, Group2: Lateral1, Group3: Lysinestretch, Group4: Lateral2, Group5: ARG, Group6: Loops, Group7: oppARG, Group8: Rest; see Chapter 3.12.3

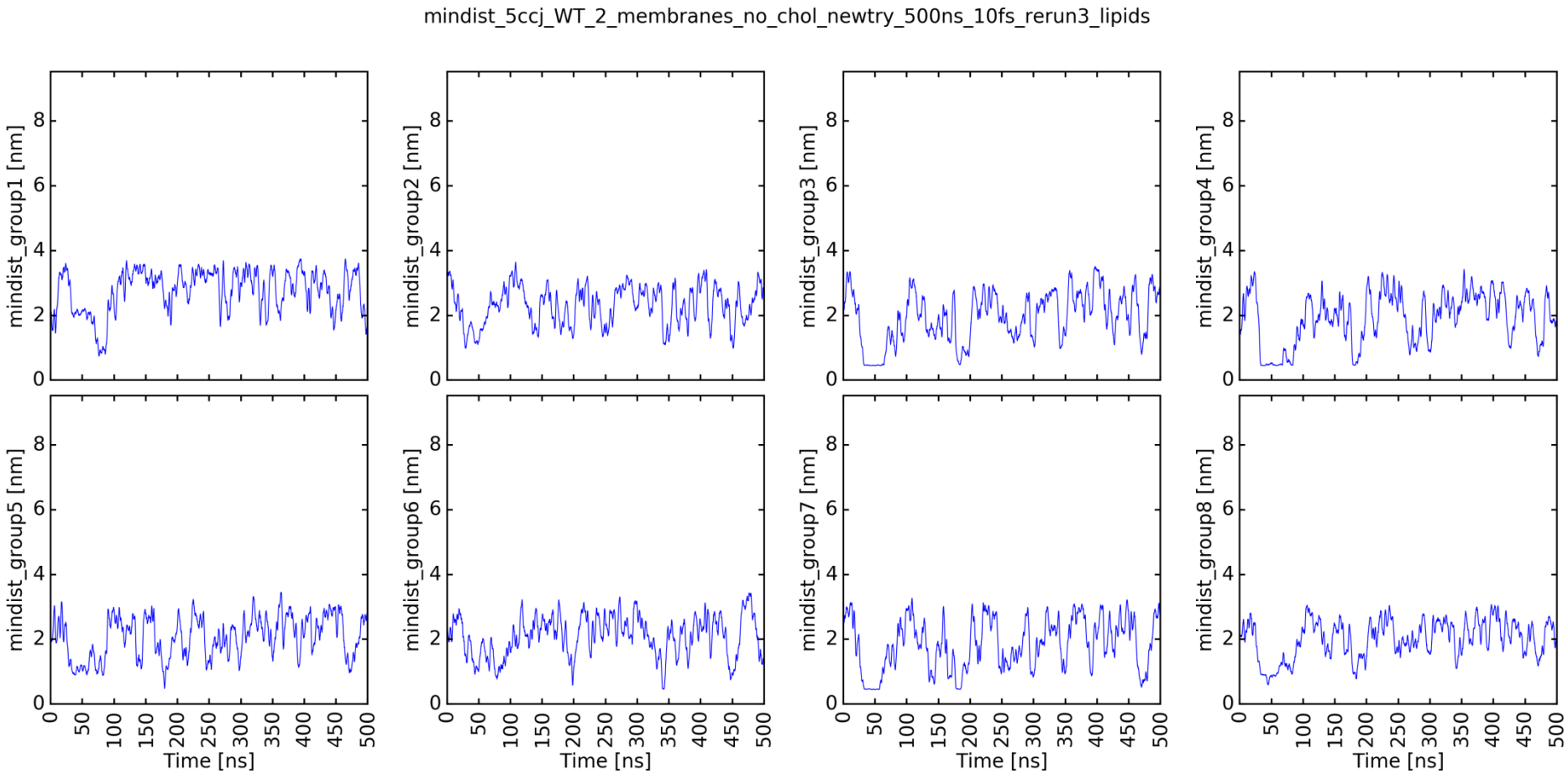

6.50 Distance between groups and membrane lipids. System 5ccj_WT /NoChol Low CA, Rerun3; Group1: Linker, Group2: Lateral1, Group3: Lysinestretch, Group4: Lateral2, Group5: ARG, Group6: Loops, Group7: oppARG, Group8: Rest; see Chapter 3.12.3

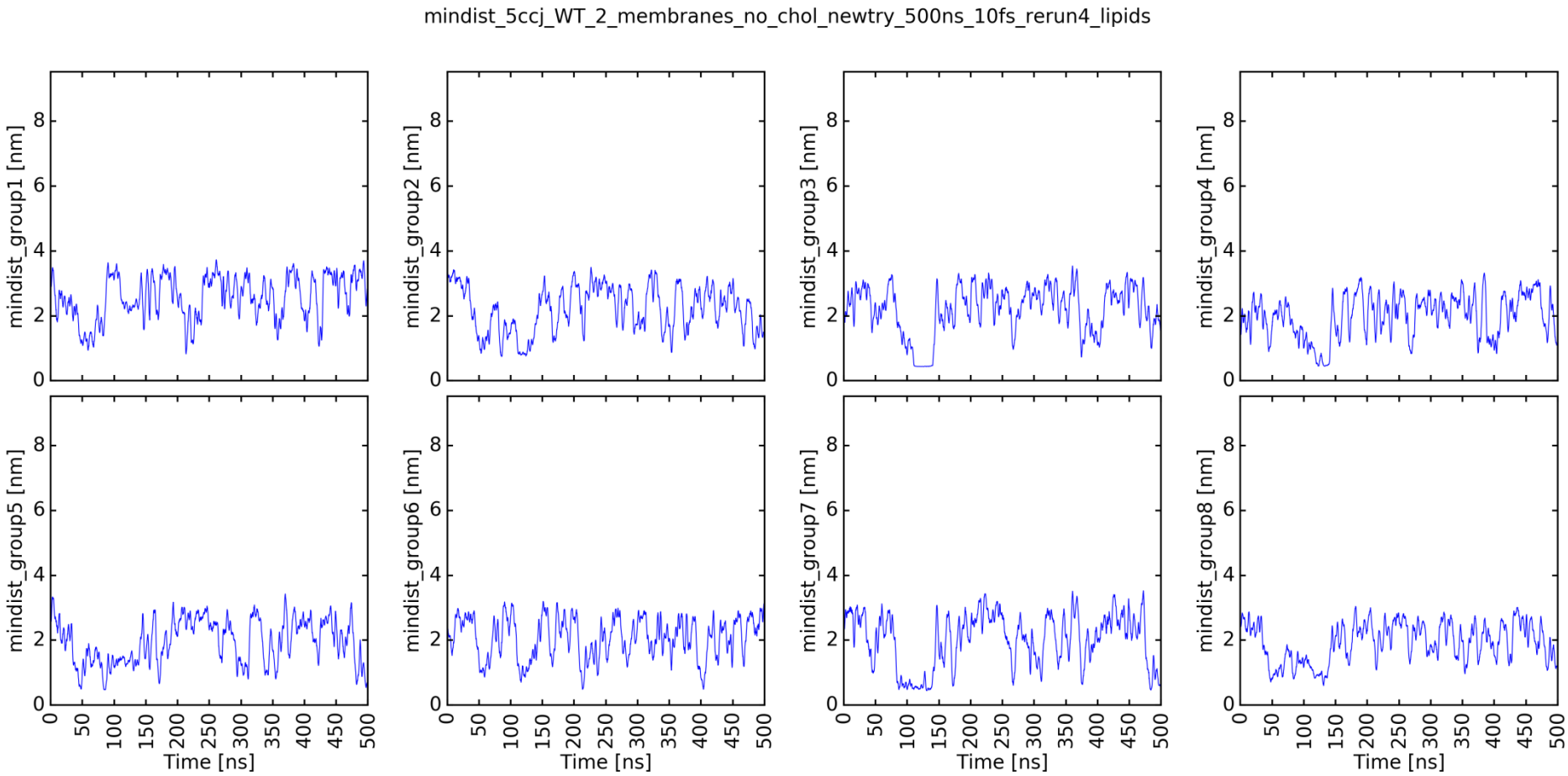

6.51 Distance between groups and membrane lipids. System 5ccj_WT /NoChol Low CA, Rerun4; Group1: Linker, Group2: Lateral1, Group3: Lysinestretch, Group4: Lateral2, Group5: ARG, Group6: Loops, Group7: oppARG, Group8: Rest; see Chapter 3.12.3

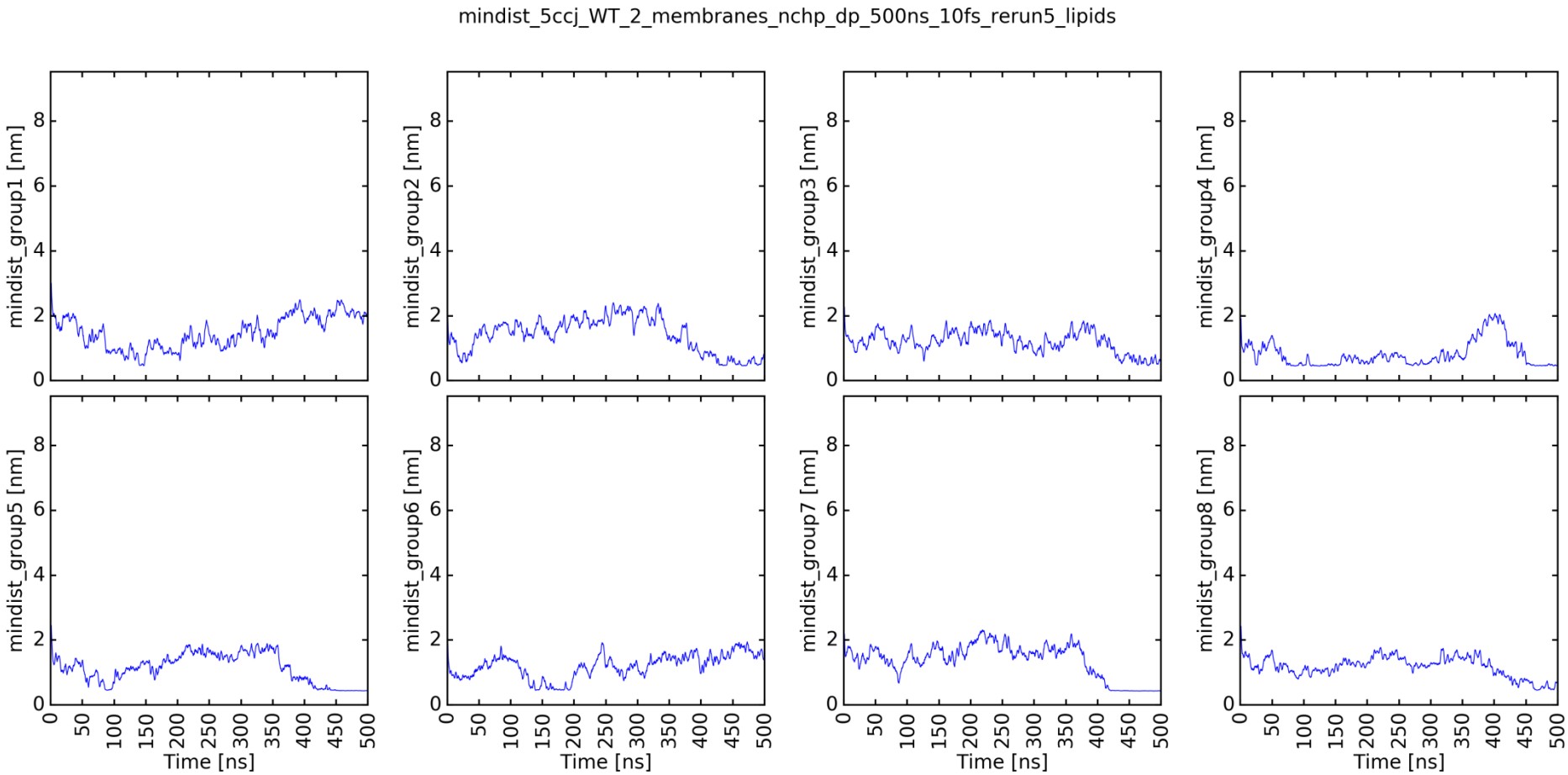

6.52 Distance between groups and membrane lipids. System 5ccj_WT /NCHP, Rerun5; Group1: Linker, Group2: Lateral1, Group3: Lysinestretch, Group4: Lateral2, Group5: ARG, Group6: Loops, Group7: oppARG, Group8: Rest; see Chapter 3.12.3

7. Bibliography

[1] Müller-Esterl, W., *Biochemie* 2. Auflage 2011; S. 35, S. 456ff

[2] Ramirez, D.M., Kavalali, E.T., Differential regulation of spontaneous and evoked neurotransmitter release at central synapses, *Current Opinion in Neurobiology* **21**, 275-282 (2011)

[3] Science News for Students, [Online], Available: https://www.sciencenewsforstudents.org/article/explainer-what-neurotransmission, [Accessed: 21-Aug-2017]

[4] Wasser, C.R. & Kavalali, E.T. Leaky synapses: regulation of spontaneous neurotransmission in central synapses, *Neuroscience* **158** 177-188 (2009)

[5] Südhof, T.C. Calcium control of neurotransmitter release; Cold Spring Harbor Perspectives in Biology (2012) 4(1):a011353.10.1101/cshperspect.a011353

[6] Maximov, A. & Sudhof, T. C., Autonomous function of synaptotagmin 1 in triggering synchronous release independent of asynchronous release, *Neuron* 48, 547–554 (2005)

[7] Sara, Y., Virmani, T., Deák, F., Liu, X., Kavalali, E.T., An isolated pool of synaptic vesicles recycles at rest and drives spontaneous neurotransmission, *Neuron* **45**, 563-573 (2005)

[8] Waters, J. & Smith, S.J., Phorbol esters potentiate evoked and spontaneous release by different presynaptic mechanisms, *The Journal of Neuroscience* 20, 7863–7870 (2000)

[9] Li, Y. C., Chanaday, N. L., Xu, W., and Kavalali, E. T., Synaptotagmin-1- and synaptotagmin-7-dependent fusion mechanisms target synaptic vesicles to kinetically distinct endocytic pathways*, Neuron **93**, 616.e3–631.e3. (2017) doi: 10.1016/j.neuron.2016.12.010*

[10] McMahon Homepage, [Online], Available: http://www.endocytosis.org/Synaptotagmin/index.html, [Accessed: 04-Sep-2017]

[11] Chapman, E.R. How Does Synaptotagmin Trigger Neurotransmitter Release?, *Annual Review of Biochemistry* **77**. 615-641 (2008)

[12] Südhof, T. C. A molecular machine for neurotransmitter release: synaptotagmin and beyond, *Nature Medicine* **19**, 1227–1231 (2013)

[13] Katz B., The Release of Neural Transmitter Substances, Liverpool: Liverpool Univ. Press (1969)

[14] Matthew, W.D., Tsavaler, L., Reichardt, L.F., Identification of a synaptic vesicle-specific membrane protein with a wide distribution in neuronal and neurosecretory tissue, *The Journal of Cell Biology* 91 (1), 257 (1981)

[15] Perin, M.S., Fried, V.A., Mignery, G.A., Jahn, R., Südhof, T.C., Phospholipid binding by a synaptic vesicle protein homologous to the regulatory region of protein kinase, *Nature* **345,** 260-263 (1990)

[16] Perin, M.S., Brose, N., Jahn, R., Südhof, T.C., Domain structure of synaptotagmin (p65), *Journal of Biological Chemistry* **266**, 623-29 (1991)

[17] *Cooper G. M., The Cell - A Molecule Approach, 2nd edition (Sunderland MA: Sinauer Associates) (2000)*

[18] UniProt, [Online], Available: http://www.uniprot.org/uniprot/P21579, [Accessed: 04-Sep-2017]

[19] Lin, C.-C. *et al.* Control of membrane gaps by synaptotagmin-Ca^{2+} measured with a novel membrane distance ruler, *Nature Communications* 5:5859 (2014), doi: 10.1038/ncomms6859

[20] Zhou, Q., Lai, Y., Bacaj, T., Zhao, M., Lyubimov, A. Y., Uervirojnangkoorn, M., et al. Architecture of the synaptotagmin-SNARE machinery for neuronal exocytosis, *Nature* **525**, 62–67 (2015) doi: 10.1038/nature14975

[21] Bykhovskaia, M. Calcium Binding Promotes Conformational Flexibility of the Neuronal Ca^{2+} Sensor Synaptotagmin, *Biophysical Journal* **108**, 2507-2520 (2015)

[22] Wu, Z. & Schulten, K. Synaptotagmin's Role in Neurotransmitter Release Likely Involves Ca^{2+}-induced Conformational Transition, *Biophysical Journal* 107, 1156-1166 (2014)

[23] Honigmann, A., van den Bogaart, G., Iraheta, E., Risselada, H.J., Milovanovic, D., Mueller, V., Müllar, S., Diederichsen, U., Fasshauer, D., Grubmüller, H., Hell, S.W., Eggeling, C., Kühnel, K. & Jahn, R. Phosphatidylinositol 4,5-bisphosphate clusters act as molecular beacons for vesicle recruitment, *Nature Structural & Molecular Biology* **20**, 679–686 (2013)

[24] Geppert, M., Goda, Y., Hammer, R.E., Li, C., Rosahl, T.W., Stevens, C.F., Südhof, T.C., Synaptotagmin I: A major Ca^{2+} sensor for transmitter release at a central synapse, *Cell* 79, 717-727 (1994)

[25] Lou, X. & Shin, Y.K. SNARE zippering, *Bioscience Reports* **36**, e00327 (2016), doi: 10.1042/BSR20160004

[26] McMahon, H. T., Kozlov, M. M. & Martens, S., *Membrane curvature in synaptic vesicle fusion and beyond. Cell* **140**, 601–605 (2010)

[27] Max Planck Institute for Biophysical Chemistry, [Online], Available: http://www.mpibpc.mpg.de/14795307/pr_1440, [Accessed: 22-Aug-2017]

[28] Trimbuch, T., & Rosenmund, C. (2016). Should I stop or should I go? The role of complexin in neurotransmitter release, *Nature Reviews Neuroscience* **17** (2), 118–125 (2016), doi:10.1038/nrn.2015.16

[29] Giraudo, C.G., Eng, W.S., Melia, T.J. & Rothman, J.E., A clamping mechanism involved in SNARE-dependent exocytosis, *Science* **313**, 676–680 (2006)

[30] Lee, H.K. *et al.* Dynamic Ca^{2+}-dependent stimulation of vesicle fusion by membrane-anchored synaptotagmin 1, *Science* **328**, 760–763 (2010)

[31] Martens, S., Kozlov, M.M. & McMahon, H.T. *How synaptotagmin promotes membrane fusion, Science* **316**, 1205–1208 (2007)

[32] Lynch, K.L., Gerona, R.R., Kielar, D.M., Martens, S., McMahon, H.T., Martin, T.F., Synaptotagmin-1 utilizes membrane bending and SNARE binding to drive fusion pore expansion, *Molecular Biololgy of the Cell* **19**, 5093-5103 (2008)

[33] Park, Y. et al., Synaptotagmin-1 binds to PIP_2-containing membrane but not to SNAREs at physiological ionic strength*, Nature Structural and Molecular Biology* **22**, 815–823 (2015)

[34] Zhou, Q., Zhou, P., Wang, A.L., Wu, D., Zhao, M., Südhof, T.C., Brunger, A.T., The primed SNARE-complexin-synaptotagmin complex for neuronal exocytosis, *Nature* **548**, 420-425 (2017)

[35] Xu, J., Pang, Z.P., Shin, O.H., Südhof, T.C., Synaptotagmin-1 functions as a Ca^{2+} sensor for spontaneous release, *Nature Neuroscience* **12**, 759-766 (2009)

[36] HGNC, [Online], Available: http://www.genenames.org/cgi-bin/genefamilies/set/765, [Accessed: 22-Aug-2017]

[37] Xu, J., Mashimo, T., Südhof, T.C., Synaptotagmin-1, -2, and -9: Ca^{2+} Sensors for Fast Release that Specify Distinct Presynaptic Properties in Subsets of Neurons, *Neuron* 54, 567-581 (2007)

[38] Chen, C., Arai, I., Satterfield, R., Young Jr., S.M., Jonas, P., Synaptotagmin 2 is the fast Ca^{2+} sensor at a central inhibitory synapse*, Cell Reports **18**, 723-736 (2017)*

[39] Vermaas, J.V., & Tajkhorshid, E., Differential Membrane Binding Mechanics of Synaptotagmin Isoforms Observed in Atomic Detail, *Biochemistry* 56 (1), 281–293 (2017)

[40] Jackman, S. L., Turecek, J., Belinsky, J. E. & Regehr, W. G. The calcium sensor synaptotagmin 7 is required for synaptic facilitation*, Nature* **529**, 88–91 (2016)

[41] Liu, H. et al., Synaptotagmin 7 functions as a Ca^{2+}-sensor for synaptic vesicle replenishment*, eLife* **3**, e01524 (2014)

[42] Südhof, T.C., Synaptotagmins: why so many?, *Journal of Biological Chemistry* **277**, 7629–7632 (2002)

[43] Alberts, B.J.A., Johnson, A., Lewis, J., Raff, M., Roberts, K., Walter, P., The lipid bilayer, *Molecular biology of the cell* (4th ed), Garland Science, New York (2002) Available from: http://www.ncbi.nlm.nih.gov/books/NBK26871/

[44] Lipowsky, R., Sackmann, E., Structure and dynamics of membranes: From cells to vesicles, Elsevier, Amsterdam (1995)

[45] Hammond, G.R.V., Does PtdIns (4,5) P_2 concentrate so it can multi-task?, *Biochemical Society Transactions* **44** (1) 228-233 (2016) doi: 10.1042/BST20150211

[46] Thapa, N., Anderson, R.A., PIP2 signaling, an integrator of cell polarity and vesicle trafficking in directionally migrating cells, *Cell Adhesion & Migration* **6** 409-412 (2012)

[47] Eberhard, D.A., Cooper, C.L., Low, M.G., Holz, R.W., Evidence that the inositol phospholipids are necessary for exocytosis. Loss of inositol phospholipids and inhibition of secretion in permeabilized cells caused by a bacterial phospholipase C and removal of ATP*, Biochemical Journal **268**, 15-25 (1990)*

[48] Hamilton, J.A., Fast flip-flop of cholesterol and fatty acids in membranes: implications for membrane transport proteins, *Current Opinion in Lipidology* **14**, 263-271 (2003)

[49] Pfrieger F.W. Role of cholesterol in synapse formation and function*, Biochimica et Biophysica Acta* **1610***, 271–280 (2003)*

[50] Wood, G.W., Schroeder, F., Audolov, N.A., Chochina, S.V., Igbavboa, U., Recent advances in brain cholesterol dynamics: Transport, domains and Alzheimer's disease, *Lipids* **4**, 225-234 (1999)

[51] Lang, T., Bruns, D., Wenzel, D., Riedel, D., Holroyd, P., Thiele, C., Jahn, R., SNAREs are concentrated in cholesterol-dependent clusters that define docking and fusion sites for exocytosis, *The Embo Journal* **20,** 2202-2213 (2001)

[52] Wasser, C.R.*,* Ertunc M.*,* Liu X. *&* Kavalali E.T. Cholesterol-dependent balance between evoked and spontaneous synaptic vesicle recycling*, The Journal of Physiology* **579***,* 413–429 (2007)

[53] Kmiecik, S., Gront, D., Kolinski, M., Wieteska, L., Dawid, A.E. and Kolinski, A., Coarse-Grained Protein Models and Their Applications, *Chemical Reviews* 116 (14), 7898-7936 (2016)

[54] Alder, B.J. & Wainwright, T.E., Studies in Molecular Dynamics. I. General Method, *The Journal of Chemical Physics* 31, 459 (1959), https://doi.org/10.1063/1.1730376

[55] Hansson*,* T., Oostenbrink*,* C., van Gunsteren, W.F., Molecular Dynamics Simulations, *Current Opinion in Structural Biology* 12, 190-196 (2002)

[56] McCammon, J., et al., Dynamics of folded Proteins, *Nature* 267, 585-590 (1977)

[57] NIH Center for Macromolecular Modeling & Bioinformatics University of Illinois at Urbana-Champaign, “Coarse-Grained Molecular Dynamics”, [Online], Available: http://www.ks.uiuc.edu/Research/CG/, [Accessed: 18-Sep-2017]

[58] Bond, P.J., Holyoake, J., Ivetac, A., Khalid, S., Sansom, M.S.P., Coarse-grained molecular dynamics simulations of membrane proteins and peptides, *Journal of Structural Biology* 157, 593-605 (2007)

[59] Leong, S.W., Lim, T.S. and Choong Y.S., Bioinformatics for Membrane Lipid Simulations: Models, Computational Methods, and Web Server Tools, *Bioinformatics - Updated Features and Applications, InTech*, (2016) doi: 10.5772/62576

[60] NIH Center for Macromolecular Modeling & Bioinformatics University of Illinois at Urbana-Champaign, "NAMD." [Online], Available: http://www.ks.uiuc.edu/Research/namd/, [Accessed: 18-Aug-2017]

[61] "GROMACS." [Online], Available: http://www.gromacs.org/About_Gromacs, [Accessed: 18-Aug-2017]

[62] "GROMACS." [Online], Available: http://www.gromacs.org/About_Gromacs/People, [Accessed: 18-Aug-2017]

[63] Official Gromacs Manual, [Online], Available: http://manual.gromacs.org/archive/4.6.7/online.html, [Accessed: 14-Sep-2017]

[64] Gromacs Tutorial by Justin Lemkuhl, [Online], Available: http://www.bevanlab.biochem.vt.edu/Pages/Personal/justin/gmx-tutorials/, [Accessed 14-Sep-2017]

[65] de Groot, B., Practical 2: Introduction to protein simulation, [Online], Available: http://www3.mpibpc.mpg.de/groups/de_groot/compbio1/p2/, [Accessed 02-Oct-2017]

[66] Protein Data Bank, [Online], Available: https://www.rcsb.org/pdb/home/home.do, [Accessed: 18-Sep-2017]

[67] PyMol, [Online], Available: https://pymol.org/, [Accessed: 18-Sep-2017]

[68] Python, [Online], Available: https://www.python.org/, [Accessed: 18-Sep-2017]

[69] Swiss Pdb-Viewer / DeepView, [Online], Available: http://spdbv.vital-it.ch/, [Accessed: 18-Sep-2017]

[70] Vi, [Online], Available: pubs.opengroup.org/onlinepubs/9699919799/utilities/vi.html, [Accessed: 18-Sep-2017]

[71] VMD, [Online], Available: www.ks.uiuc.edu/Research/vmd/, [Accessed: 18-Sep-2017]

[72] xxdiff, [Online], Available: furius.ca/xxdiff/, [Accessed: 18-Sep-2017]

[73] XmGrace / Grace, [Online], Available: plasma-gate.weizmann.ac.il/Grace/, [Accessed: 18-Sep-2017]

[74] NIH Center for Macromolecular Modeling & Bioinformatics University of Illinois at Urbana-Champaign, "Force Fields for MD Simulations", [Online], Available: http://www.ks.uiuc.edu/Training/Workshop/SanFrancisco/lectures/Wednesday-ForceFields.pdf, [Accessed 02-Oct-2017]

[75] González, M.A., Force fields and molecular dynamics simulations, *Collection SFN* **12**, 169-200 (2011)

[76] Marchi, M., Akasaka, K., Simulation of hydrated BPTI at high pressure: changes in hydrogen bonding and its relation with NMR experiments, *The Journal of Physical Chemistry*, **B 105**, 711-714 (2001)

[77] Guvench O., MacKerell A.D. Comparison of Protein Force Fields for Molecular Dynamics Simulations, In: Kukol A. (eds) *Molecular Modeling of Proteins, Methods Molecular Biology™*l **443**, Humana Press (2008)

[78] Martini Force Field, [Online], Available: http://cgmartini.nl/index.php/about, [Accessed: 02-Oct-2017]

[79] Wikipedia, [Online], Available: https://en.wikipedia.org/wiki/CUDA, [Accessed: 21-Aug-2017]

[80] Cheng, Y. et al., Crystallographic identification of Ca^{2+} and Sr^{2+} coordination sites in synaptotagmin I C2B domain, *Protein Science* **13**, 2665–2672 (2004)